THESIS FOR THE DEGREE OF DOCTOR OF PHILOSOPHY

Polyelectrolyte Brush Electrodes for Protein Capture and Release

GUSTAV FERRAND-DRAKE DEL CASTILLO

Department of Chemistry and Chemical Engineering
CHALMERS UNIVERSITY OF TECHNOLOGY
Gothenburg, Sweden 2020

Polyelectrolyte Brush Electrodes for Protein Capture and Release
GUSTAV FERRAND-DRAKE DEL CASTILLO

ISBN 978-91-7905-414-4

© GUSTAV FERRAND-DRAKE DEL CASTILLO, 2020

Doktorsavhandlingar vid Chalmers Tekniska Högskola
Ny serie nr 4881
ISSN 0346-718X

Department of Chemistry and Chemical Engineering
Chalmers University of Technology
SE-412 96 Gothenburg
Telephone +46 31 772 1000

Cover:
Illustration of selective protein release from polymer brush electrodes by application of an electrical signal.

Printed by Chalmers Reproservice
Gothenburg, Sweden 2020

Till morfar, för att du uppmuntrade mig till att studera fåglar och naturvetenskap.

Polyelectrolyte Brush Electrodes for Protein Capture and Release

GUSTAV FERRAND-DRAKE DEL CASTILLO
Department of Chemistry and Chemical Engineering
Chalmers University of Technology

ABSTRACT

Stimuli-responsive polyelectrolyte brushes switch as a function of pH between a charged and neutral state that affects their electrostatic interactions with other charged molecules like proteins. Adjustment of the pH results in the binding of large quantities of proteins making polyelectrolyte brushes widely used as biointerfaces. However, the interaction between proteins and polyelectrolyte brushes remains poorly understood. Protein binding to brushes despite net repulsion indicate that the mechanism is determined by more than electrostatic effects. In this thesis polyelectrolyte brushes, and protein-polyelectrolyte interactions were characterized using new methods. The results show that non-electrostatic interactions play an important role in protein binding to pH-responsive polyelectrolyte brushes.

Active switching of polyelectrolyte brushes requires control of the pH. However, controlled pH switching that is convenient and non-invasive has proven difficult to achieve. In this thesis electrochemistry was used to generate local pH gradients, that resulted in reversible switches of polyelectrolyte brushes, even in highly buffered liquids and in biological solutions like serum. Reversible electrochemical switching of polyelectrolyte brushes was accomplished by employing diazonium salt surface functionalization. Electrochemical switching was used to control protein-polyelectrolyte interactions to create polyelectrolyte brush electrodes that captured and released high quantities of proteins on-demand. Our method for electronic control of protein immobilization should increase the utility of pH-stimuli-responsive polymer brushes in applications such as bioanalytics, protein purification, and protein drug-delivery.

Keywords: Polyelectrolyte brushes, stimuli-responsive polymers, protein immobilization, electrochemistry.

LIST OF PUBLICATIONS

This thesis is based on the following appended papers:

I, Quantitative Analysis of Thickness and pH-Actuation of Weak Polyelectrolyte Brushes
Gustav Ferrand-Drake del Castillo, Gustav Emilsson and Andreas B. Dahlin,
Journal of Physical Chemistry C, 2018, 122, 27516–27527

II, Large Changes in Protonation of Weak Polyelectrolyte Brushes with Salt Concentration - Implications for Protein Immobilization
Gustav Ferrand-Drake del Castillo, Rebekah L. N. Hailes and Andreas Dahlin
Journal of Physical Chemistry Letters, 2020, 11, 5212–5218

III, Enzyme Immobilization in Polyelectrolyte Brushes: High Loading and Enhanced Activity Compared to Monolayers
Gustav Ferrand-Drake del Castillo, Meike Koenig, Gustav Emilsson, Martin Müller, Klaus-Jochen Eichhorn, Manfred Stamm, Petra Uhlmann and Andreas B. Dahlin,
Langmuir, 2019, 35, 3479–3489

IV, Generic High-Capacity Protein Capture and Release by pH Control
Gustav Ferrand-Drake del Castillo, Zeynep Adali, Rebekah L. N. Hailes, Timothy Robson and Andreas Dahlin
Chemical Communications, 2020,56, 5889–5892

V, Generic High-Capacity Electrochemical Capture and Release of Proteins by Polyelectrolyte Brushes
Gustav Ferrand-Drake del Castillo, Zeynep Adali, Rebekah L. N. Hailes, Kunli Xiong and Andreas Dahlin
Preprint ChemRxiv

CONTRIBUTION REPORT

Paper I

Performed all experimental work with guidance of G.E. I wrote the first version of the manuscript and participated in the editing of the final version.

Paper II

Conceived the idea for the research project. Conducted all experiments together with R.H. Co-wrote the first version of the manuscript together with R.H. and participated in the editing of the final version.

Paper III

Performed the majority of the experimental work; grafting-from polymer brush synthesis, SPR experimental work, and the enzyme kinetics experiments. I wrote the first version of the manuscript and participated in the editing of the final version of the manuscript.

Paper IV

Performed all experimental work in collaboration with co-authors Z.A. R.H. and T.R. I wrote the first version of the manuscript and participated in the editing of the final version.

Paper V

Performed all experimental work in collaboration with co-authors and I wrote the preprint manuscript in collaboration with R.H. and A.D.

PAPERS NOT INCLUDED

The following paper was excluded from the thesis:

Detecting selective protein binding inside plasmonic nanopores: Toward a mimic of the nuclear pore complex
Bita Malekian, Rafael L. Schoch, Timothy Robson, Gustav Ferrand-Drake del Castillo, Kunli Xiong, Gustav Emilsson, Larisa E. Kapinos, Roderick Y.H. Lim and Andreas Dahlin
Frontiers in Chemistry, 2018, 6, 637

Nomenclature

Physics

$\delta n/\delta c$	Refractive index increment,	$cm^3\ g^{-1}$
δ	Decay length,	m
ϵ	Dielectric constant	
ϵ_0	Vacuum permittivity	$F\ m^{-1}$
ω	Frequency,	s^{-1}
θ_0	Angle of incidence	
θ_c	Critical angle of incidence, TIR	
c	Speed of light	$m\ s^{-1}$
k	Wave vector, momentum,	m^{-1}
n	Refractive index	
n_b	Bulk refractive index	
n_f	Film refractive index	

Polymer physics

α	Degree of charging	
χ	Interaction parameter	
Γ	Surface density,	$g\ m^{-2}$
σ	Grafting density	
a	Monomer length	m
b	Kuhn length	m
k_B	Boltzman constant	$m^2\ kg\ s^{-2}\ K^{-1}$

N	Degree of polymerization	
pK_a	Dissociation constant for acid	
pK_a		
PDI	Polydispersity index	
R_{coil}	Radius of solvated polymer coil	m
T	Temperature	K

Chemistry

ABTS (2,2'-azino-bis(3-ethylbenzothiazoline-6-sulfonic acid))

APTES (3-Aminopropyl)triethoxysilane

ARGET Activator Regeneration Electron Transfer

ATRP Atom Transfer Radical Polymerization

CNF Carboxynaphtofluorescein

DCM Dichloromethane

EDC 1-ethyl-3-(3-dimethylaminopropyl) carbodiimide hydrochloride

LbL Layer-by-Layer

NHS N-hydroxysulfosuccinimide

PAA poly(acrylic acid)

PAH polyallylamine chloride

PDAMAC polydiallyldimethylammonium chloride

PDEA poly(2-(diethylamino)ethyl methacrylate)

PDMS poly(dimethylsiloxane)

PEG poly(ethylene glycol)

PHEA poly(2-hydroxyethyl methacrylate)

PMAA poly(methacrylic acid)

PNIPAAM poly(N-isopropylacrylamide)

PTBA poly(tert-butyl acrylate)

PTBMA poly(tert-butyl methacrylate)

SAM Self-assembled monolayer

SVA Succinimidyl valerate

TFP Tetrafluorophenyl

Biology

BSA Bovine serum albumin

Cyt-C Cytochrome-C

GAL Galactosidase

GOX Glucose oxidase

HRP Horse radish peroxidase

pI Isoelectric point

Other

F Fresnel coefficient

IR-RAS Infra-red Reflective absorption spectroscopy

MALDI Matrix assisted laser desorption/ionization

QCM-D Quartz crystal microbalance with dissipation monitoring

SEC Size exclusion chromatography

SPR Surface plasmon resonance

TIRF Total internal reflection fluoresence

Contents

1 Background **1**

2 Introduction **5**

3 Theory **11**

3.1 Polymers 11

3.1.1 Polymers 12

3.1.2 Polymer brushes 14

3.1.3 Polyelectrolytes 16

3.1.4 Polyelectrolyte brushes 19

3.1.5 Protonation behavior of polyelectrolyte brushes 23

3.1.6 Locally displaced pH within polyelectrolyte brushes 24

3.1.7 Preparation of polymer brushes 26

3.2 Molecular interactions 30

3.2.1 Electrostatic repulsion and attraction 31

3.2.2 Hydrogen bonds 34

3.2.3 Hydrophobic interactions 37

3.2.4 The combined picture 38

3.3 Enzymes 39

3.3.1 Biocatalysis 39

3.3.2 Enzyme Immobilization 42

3.3.3 Glucose Oxidase 45

3.3.4 Enzyme kinetics 47

3.4 Surface Plasmon Resonance 49

3.4.1 Conditions for Surface Plasmon Resonance 49

3.4.2 Prism coupling and evanescent field 51

3.4.3 The SPR spectra 52
3.4.4 Fresnel models of the SPR spectra 54
3.4.5 Non-interacting Probe Method 56
3.4.6 Alternative methods 59
3.5 Quartz Crystal Microbalance 61
3.6 Electrochemistry 63
3.6.1 Electrochemical cells 63
3.6.2 Oxidation reactions that produce protons 64

4 Experimental 69
4.1 Surface chemistry 69
4.1.1 Thiol self assembly 69
4.1.2 Silanization 71
4.1.3 Diazonium salt 74
4.1.4 Converting monolayers to ARTP initiators 75
4.2 Synthesis of polyelectrolyte brushes 76
4.3 Protein conjugation 77
4.4 Enzyme activity 79
4.5 Electrochemical methods 83
4.6 Spectroscopy 84
4.6.1 Infrared reflective absorption spectroscopy 84
4.6.2 Circular dichroism spectroscopy 87
4.6.3 Fluorescence spectroscopy 88

5 Results and Discussion 93
5.1 Characterization of polyelectrolyte brushes 93
5.1.1 Interpretation of SPR and QCM-D signals 93
5.1.2 Quantification of polyelectrolyte brush heights 96
5.2 Shifts in protonation of brushes by changing salt concentration . 98
5.2.1 Detection of shifted pK_a 98
5.2.2 Implications for protein immobilization 100
5.3 Polymer brushes as soft scaffolds for enzyme catalysis 102
5.3.1 Quantifying enzyme surface coverage to brushes 102
5.3.2 Activity retention on polyelectrolyte brushes 103

5.4 Generic method for protein capture and release by pH control . . 105
5.4.1 Capture of polymers by hydrogen bonds 105
5.4.2 High capacity catch and release of proteins 108
5.5 Electrochemical catch and release of proteins 110
5.5.1 Switch of pH by electrochemical potentials 111
5.5.2 Electrochemical protein catch and release 113
5.5.3 Dynamic protein biochips 114
5.6 Biocatalytic switching of brushes 116
5.6.1 Summary of the concept 119

6 Conclusion 121

7 Outlook 125
7.1 Protein purification 125
7.2 Electrochemical protein drug delivery 128
7.3 Local pH-gradients in brushes: Nanobuffering 129
7.4 Enzyme cascade reactions in brushes 131

Bibliography 136

1

Background

Materials that can capture and release biomolecules like proteins in a controlled way are highly useful for many applications. Proteins are the building stones and chemical catalysts of nature, which enable the chemical reactions that keeps us alive, gives us mobility, and the capacity to think. Fundamental knowledge of how proteins function, and understanding of how we can use them could result in the curing of diseases and creation of technology for resource efficient production of advanced and useful chemicals. However, current materials we make are limited in their capability to handle and use proteins. Advanced use of proteins relies on us to create new material innovations that can control and use proteins with similar efficiency as living cells. The ambition of this thesis is to provide a stepping stone in this direction.

The key to creation of materials which can capture and release proteins with precision, and advanced use of proteins, rely on the use of nanotechnology. Nanotechnology is the manipulation of matter on the scale of molecules and atoms. Similar to the importance of understanding proteins and biomolecules, many current and future societal problems can and will be solved by our steadily improved understanding of nanoscale phenomenon. Examples of such problems include diseases to which we currently have no cure, and rapid destruction of critical ecosystems due to inefficient use of resources. We have only started to explore how including nanoscale features in a material can lead to unique and complex macroscale features. This is evident when comparing with biological systems, where even a slight alteration on the molecular level, e.g. of a protein or the sequence of a DNA molecule, can ultimately determine if the organism will be viable or not. The intersection between human-made and biological made nanomaterials is especially interesting, and where I found much of my inspiration for this thesis. To make synthetic materials that can mimic and interact

with living organisms we must consider two difficult but important questions:

1. Can we create nanoreactors similar to biological cells that produce complex molecules such as proteins?
2. How do we prepare materials that can interface with and operate within biological systems?

The first challenge relate to the desire to develop feasible, high yielding, synthetic routes for making complex molecules. Biological cells are the preferred solution for industrial scale production of many biological molecules used in the production of protein based pharmaceuticals. With nanotechnological developments we will have the possibility to build hybrid pseudo-living human-made constructs that utilize biomolecules but in an artifical cell.[1] However, it will require substantial engineering efforts to develop appropriate interfaces and scaffold materials that can accommodate and organize different enzymatic catalysts with high spatial precision. In addition the enzymes must be handled such that their structure and thereby functions are preserved. The enzymes must be highly accessible to the reactants which also need to travel between different catalysts in a cascade of biochemical reactions resulting in the output product. This thesis investigates how to successfully immobilize enzymes to synthetic surfaces, which is crucial for making successful biomimetic nanoreactors.

The second challenge involves making a surface that can alter its properties rapidly to trigger capture and release of molecules into or out of a biological system. Biological interfaces are highly dynamic out-of-equilibrium systems that constantly undergo reversible changes. Subtle chemical gradients and cues in the surrounding environment give rise to rapid responses. Contrary to biological surfaces, human made surfaces are generally slow, and undergo irreversible change. In many cases the outspoken design criteria of biomaterials and interfaces is for the surface to be inert and static over time. Examples of such materials include ceramics, metal alloys, composites, and plastics, which are used to make implants,[2, 3] cardiovascular stents[4], pacemakers[5], biosensors[6], and neural electrodes[7]. The implants we use today, and biocompatible materials used to make them, are extremely important for the treatment of a diverse range of conditions, and of many patients. However, the design of future

biomedical materials must, in addition to biocompatibility, strive to incorporate dynamic features similar to those of biological surfaces in order to be increasingly useful.[8, 9, 10, 11] One class of material that has the potential to be highly dynamic and changeable as function of the environment are stimuli-responsive polymers.[8] In this thesis I investigated pH-responsive charged polymer interfaces called polyelectrolyte brushes and their interactions with proteins.

2

Introduction

Polymer brushes are polymers attached to surfaces with high coverage that result in strong stretching of the polymer chains to avoid overlap due to intramolecular repulsion.[12, 13] As a result, polymer brushes constitute a soft and flexible polymer network with a very high concentration of functional groups. This gives rise to unique surface properties that make polymer brushes interesting for several applications.[14] One is non-fouling, the repulsion of biomolecules from surfaces that prevent non-specific binding, as shown in Figure 2.1 A.[15, 16, 17, 18] Another is to selectively bind large quantities of proteins, Figure 2.1 B.[19, 20, 21, 10] A further possibility are brushes made of stimuli-responsive polymers that undergo reversible chemical change as a function of changes in their environment e.g. temperature,[22] light,[23] salt[24], and pH.[8] Such stimuli-responsiveness could enable the brush to reversibly switch between two modes: protein uptake, and protein repulsion.

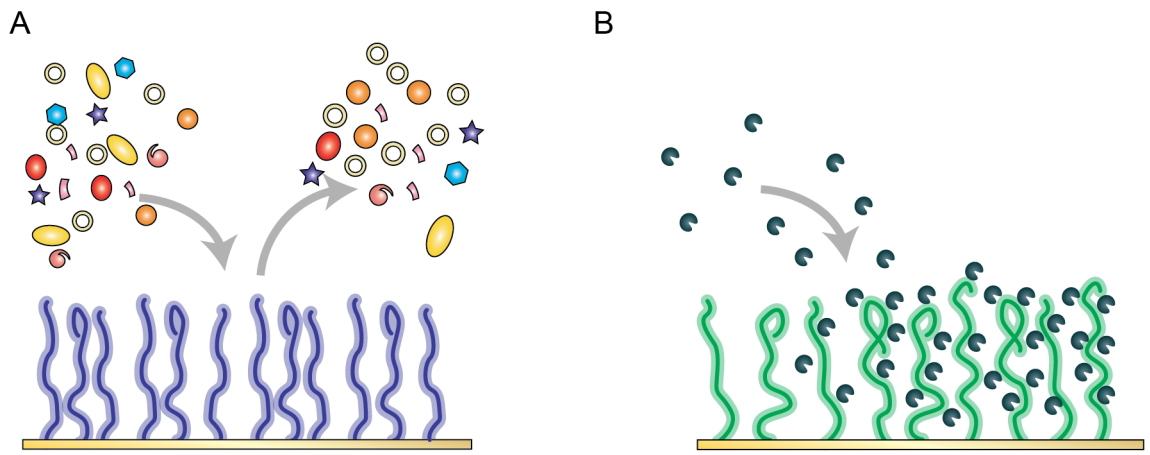

Figure 2.1: Two applications of polymer brushes: (A) preventing non-specific binding, (B) immobilization of protein.

pH-responsive polyelectrolyte brushes switch between a charged and neutral state, an attractive feature for biomolecular applications.[25] By tuning the pH and thereby the charge of the interface, the relative electrostatic interaction with proteins can be set, enabling control between attraction and repulsion. With sufficient control, applications in drug delivery, biosensors, and other biointerfaces are envisioned. Today, many synthetic techniques have been developed to prepare a variety of polyelectrolyte brushes, making applications in life science increasingly feasible.[26] However, lack in fundamental understanding of polyelectrolyte brushes, in particular of the interaction between polyelectrolyte brushes and biomolecules, prevent widespread use.[27]

In this thesis new methods are used to investigate how polyelectrolyte brushes behave as a function of the solution pH and salt concentration. First, we wish to determine brush heights in solution, as experienced by externally introduced macromolecules. Polyelectrolyte brush heights have traditionally been studied using techniques such as ellipsometry,[28, 29] AFM,[30, 31] SPR,[32] and QCM-D[33, 34]. These methods risk producing inaccurate brush height due to experimental limitations, or by employing models that require non-realistic assumptions. For instance, AFM typically only detects the brush after it has started to compress,[30, 22] while optical techniques often use models that assume a value for the refractive index despite strong hydration of the polymer layer. Measurement of the exclusion height, the distance from which macromolecules are expelled from the brush, is an interesting alternative.[35, 22] To this point, the exclusion height of polyelectrolyte brushes and how it changes with pH has not been investigated. In Chapter 5.1 I show how the exclusion heights of polyelectrolyte brushes can be determined using non-interacting probes.

While the salt concentration is known to affect the pK_a of polyelectrolytes in solution,[36] this effect has not been carefully studied in brushes.[37] Many polyelectrolyte brush studies fail to consider the potential effect of the salt concentration may have on the pK_a.[19, 38, 39, 40] Characterization of the pK_a of polyelectrolyte brushes, cationic and anionic, as a function of the salt concentration, showed striking differences in comparison with the solution pK_a, Chapter 5.2. This represent a second contribution to an improved understanding of polyelectrolyte brushes. In turn, knowledge of how the pK_a shifts, is crucial to correctly attribute by what intermolecular mechanism the polyelectrolyte brush

interacts with proteins.

Immobilization of proteins to polyelectrolyte brushes has been intensively studied, yet several fundamental questions remain insufficiently answered.[27] For instance, in numerous cases net-negative proteins immobilized to negatively charged brushes, a phenomenon called "immobilization on the wrong side of the pI".[41, 42, 43, 19, 39, 38, 44] Several plausible explanations have been proposed, including patches of opposite charge on proteins, since they have been shown to have a quantifiable free energy effect.[27] Furthermore, polyelectrolyte brushes are predicted to contain pH gradients, which if existent, could give rise to pH-displaced environments within the brush that trigger attractive protein-polymer interactions.[45, 46] In this work, accurate characterization of the brush pK_a enabled us to distinguish between non-electrostatic and electrostatic immobilization, which had not been considered. These results provide an alternative explanation to "immobilization on the wrong side of the pI". One of the most popular applications of protein immobilization is for use in biocatalysis. Enzyme immobilization to brushes is advantageous since the brush offers high loading capacity and constitutes a relatively soft and flexible support material.[47, 48, 42] The qualitative gain of placing enzymes in brushes has been shown.[49, 50, 20, 51, 42] However, the effect of placing enzymes inside polyelectrolyte brushes has not been systematically quantified and compared to alternative surfaces without brushes. In Chapter 5.3, I address this uncertainty by comparing the catalytic activity of glucose oxidase in polyelectrolyte brushes and on monolayers.

Protein immobilization techniques are often permanent and involve forming covalent bonds.[52, 53, 54] Even for non-covalent immobilization release of proteins may require extreme treatment of the surface with high pH,[39] use of surfactants,[55] or high salt concentration[19]. The cost of disrupting the relatively strong ionic or hydrophobic interactions between the brush and the protein risks degradation and denaturation. In many cases strong non-covalent bonding is desirable, as it minimizes leakage of enzymes in chemical process. For use in protein purification the opposite is desirable: a weak but sufficiently strong protein surface interaction that at any point can be conveniently broken by non-invasive means. In Chapter 5.4 I describe a new, generic method for binding large quantities of proteins to brushes, by an interaction which is still

sufficiently weak to fully release proteins by raising the solution pH above its pI.

Polyelectrolyte brushes compatible with electrochemistry constitute a thoroughly researched topic in materials science.[56, 57, 58, 59] Many electrochemical reactions produce or consume protons, which means that polyelectrolyte brushes can in principle be controlled electronically. This could be used to enable electronic control of protein uptake and release, as illustrated in Figure 2.2. However, the vision of polyelectrolyte brush electrodes that reversibly switches has not been realized. In part, this is due to the shortcomings of conventional methods of preparing brushes on electrode materials.[57] For instance, polymer brushes with thiol end-groups that are routinely used to functionalize metal surfaces are highly sensitive to electrochemical signals.[60] In Chapter 5.5 I describe the invention of a polyelectrolyte brush electrode for protein capture and release that utilizes electrochemical pH gradients and pH-responsive polymers anchored to the underlying electrode via electrochemically inert covalent bonds.

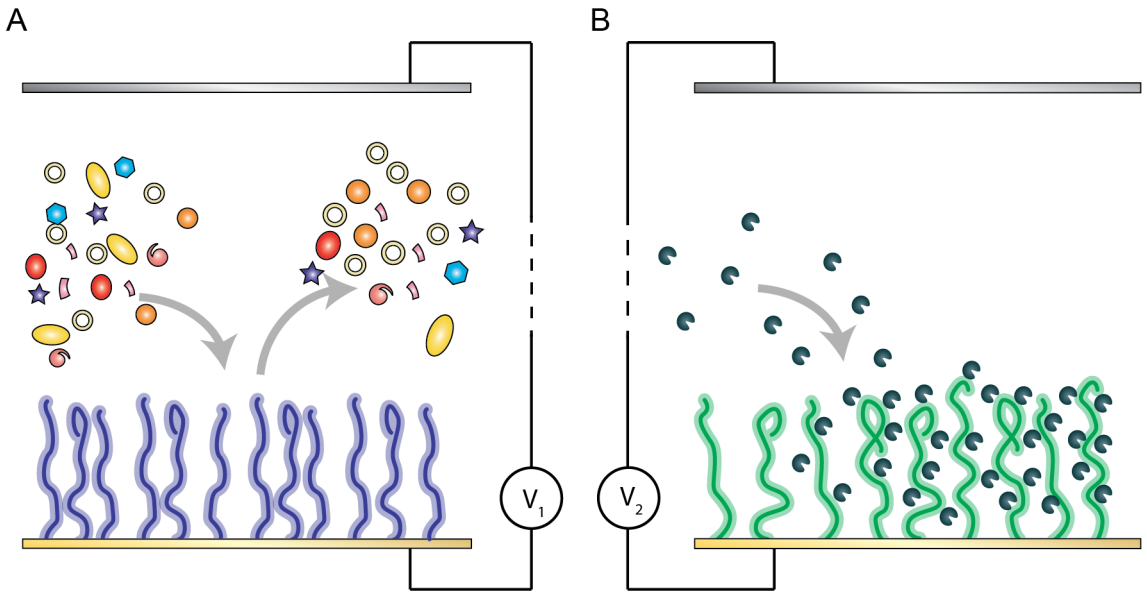

Figure 2.2: On-demand electrochemical switching between two modes of a stimuli-responsive polymer brush (A) protein repulsion and (B) protein immobilization.

Merging the two primary applications of polymer brushes, protein repulsion (Figure 2.2 A), and protein immobilization (Figure 2.2 B), into one electronically controlled solution creates opportunities for new applications. Some of these applications are discussed in the outlook section of this thesis. In addi-

tion to creating pH gradients in brushes by electrochemistry, I also discovered experimental evidence of spontaneous pH gradients in brushes. Although the results are preliminary, they corroborate the presence of so-called 'nanobuffering' in dense polyelectrolyte systems.[46, 45] Spontaneous pH gradients within brushes mean that charge re-normalization and distribution in polyelectrolyte systems is far from fully understood, and new theoretical explanations are required. Knowledge of how to experimentally produce nanobuffering and how to characterize it will create opportunities to utilize the effect in practical applications.

3

Theory

To place the content of this work into context a theory section is required that treats the following six main subjects: (1) Polymers, (2) Molecular interactions, (3) Enzymes, (4) Surface Plasmon Resonance (SPR), (5) Quartz Crystal Microbalance with Dissipation montoring (QCM-D), and (6) Electrochemistry. The theory behind polymers and polyelectrolyte brushes is presented as it is fundamental to understanding potential technological applications. Additionally, molecular interaction within the brush or with externally introduced molecules are discussed with emphasis on hydrogen bonding, electrostatic attraction and repulsion, and hydrophobic interactions. One particularly interesting application of polyelectrolyte brushes is using them as scaffolds for enzymes to perform biocatalysis. Enzyme catalysis theory is briefly described and methods for immobilizing them to brushes is covered. SPR and QCM-D are the central tools used for characterization of polyelectrolyte brushes, which requires a theoretical description of how these technologies work and operate that can be found in Section 3.4 and 3.5. In the last section, a brief theory section is given on electrochemistry with emphasis on electrochemical reactions that produce pH gradients.

3.1 Polymers

The following section begins by describing polymers and their basic properties in solution. Polymer brushes, polymer molecules bound to surfaces at a high density, are then considered. The theory behind polymer brushes composed of charged polymers, so-called polyelectrolyte brushes, is described in detail with special focus on properties that arise when the brush is charged compared to neutral. Finally, methods of preparation and the applications and potential ap-

plications of polymer brushes are considered.

3.1.1 Polymers

Polymers are macromolecules composed of many small repeating molecular units called monomers which are linked together by molecular bonds.[61] Polymers unlike small molecules vary in size and although the chemical identity of the monomers that make up the polymer matter, the size of the polymer the degree of polymerization, N, determines its molecular properties. Furthermore a collection of polymers (at least synthetic polymers) rarely all have the same length. The polydispersity, PDI, describes the variation in polymer lengths for a collection of polymers in a sample. In addition, the polymer hierarchical structure may vary from linear to highly branched. The conformational freedom of the monomers may be severely restricted giving it a stiff, rod-like structure, or the chain is highly flexible with a disordered highly entangled structure as a result. Finally, the length of the monomer, a, and another length scale called the Kuhn length which is an effective monomer length, b, are important parameters. Scaling laws are expressions which describe physical properties of polymers described by parameters related to their structure such as N, a, and b. Scaling laws reflect the fact that some physical properties may apply to a large class of polymers despite differences in specific composition may exist.

Consider a linear polymer coil in solution, the polymer spontaneously adopts a coil-like structure as shown in Figure 3.1.[62]

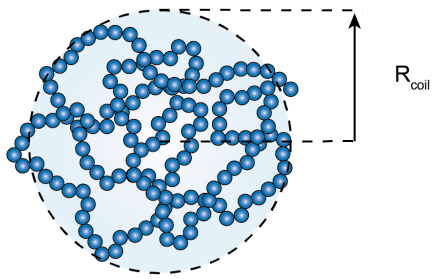

Figure 3.1: A polymer in solution that spontaneously adopts a spherical coil conformation with radius, R_{coil}.

The free energy of the coil in solution is a function of the coil radius, R, according to Equation 3.1, which contains three terms, (1) the excluded volume,

(2) configurational entropy of the polymer chain, and (3) the relative interaction between the solvent molecules and the polymer.[62] The excluded volume effect reflects the fact that each monomer occupies a volume which is inaccessible to other monomers. This gives rise to a repulsive contribution favoring a large radius of the coil in configurations with analogies to the result from the mathematical problem of random-walks. Excluded volume effects are balanced by the configurational entropy term which reflects the fact that for a highly stretched polymer chain there are fewer possible configurations to adopt. Similar to a spring, which contracts when it is stretched beyond its equilibrium, a polymer coil experiences a restoring force that is determined by loss of entropy. Finally, a term for describing the relative importance of interactions between the polymer and solvent reflects the fact that the coil size depends to a large extent on what solution it is in.

$$\mathrm{G_{free}(R)} = \underbrace{\frac{\mathrm{k_B T N^2 a^3}}{\mathrm{R^3}}}_{\text{excluded volume}} + \underbrace{\frac{\mathrm{3 k_B T R^2}}{\mathrm{2 N a^2}}}_{\text{configurational entropy}} - \underbrace{\frac{\mathrm{k_B T \chi N^2 a^3}}{\mathrm{R^3}}}_{\text{interaction}} + \text{constant} \tag{3.1}$$

In Equation 3.1, χ is the solvent-polymer interaction parameter and T is the temperature.[62] The free energy of the polymer coil in solution is minimized for a radius given by Equation 3.2.

$$\mathrm{R} = \left(1 - \chi\right)^{\frac{1}{5}} \mathrm{a N}^{\frac{3}{5}} \tag{3.2}$$

As Equation 3.2 shows, the value of χ plays an important role for the coil radius.[62]

1. For $\chi < 1$ interactions between the polymer and solvent are favourable, so-called good solvent behavior, the coil radius scales with respect to N as $R \propto \mathrm{N}^{3/5}$.
2. When $\chi = 1$ the contribution of excluded volume and polymer solvent interaction cancel out and the coil size scales $R \propto \mathrm{N}^{1/2}$.
3. Lastly, when $\chi > 1$ repulsion between the polymer coil and solvent induces polymer-polymer interactions and a compact globule is formed instead of a coil.

3.1.2 Polymer brushes

Polymer brushes are polymer chains grafted to a surface with a high surface density.[12, 63, 13] The crowded environment of chains close to the surface causes repulsion between the chains, forcing them to adopt a stretched out conformation away from the surface that would not be energetically favourable for an isolated polymer coil in solution. A very useful feature of polymer brushes is that they produce a high density of surface functional groups within a soft polymer network, while the strongly stretched chains effectively disguise the underlying surface. The former enables high capacity for binding of molecules to the surface. The latter prevents other molecules, in particular large ones, from entering the brush and reaching the underlying surface. If the polymer brush is highly flexible it acts as a kinetic entropic barrier, preventing sufficiently large proteins from entering the brush. However, the extent to which the polymer brush fulfills these two properties depends on the grafting density. For chains attached to a surface at a very low grafting density in the so-called "mushroom"-regime, the coils adopt a hemispherical structure despite being attached to the surface, Figure 3.2 B. Brushes in the mushroom regime poorly disguise the underlying surface from molecules in solution. If a critical density of surface anchored polymer coils is reached, a repulsion between polymer coils due to excluded volume effects will cause the polymer coils to stretch out with a length that exceeds the solvated polymer coil radius, $H_{brush} > R_{coil}$ as shown in Figure 3.2 C. Strongly stretched brushes effectively disguise the underlying surface which may be utilized for achieving non-fouling properties or ensure that molecules that bind to the surface primarily interact with the polymer brush and not the underlying support surface.

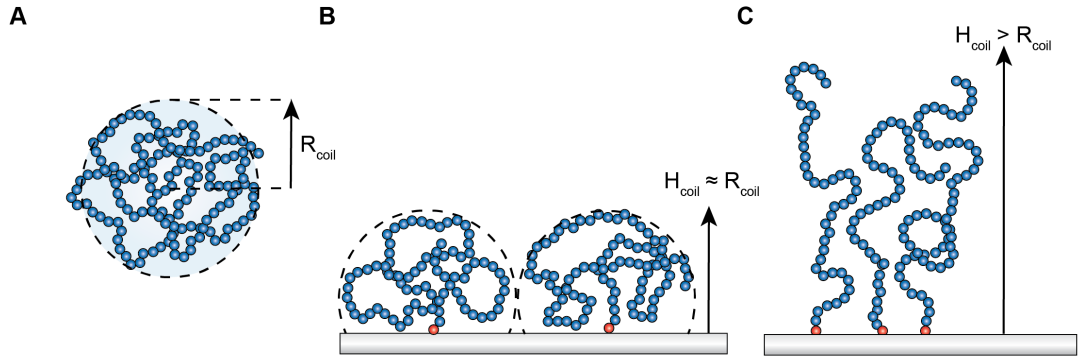

Figure 3.2: (A) A polymer coil in solution with a coil radius R_{coil}. (B) Polymer coil attached to a surface with low surface grafting density where the height of the polymer layer does not significantly differ from the radius of the free polymer coil in solution. (C) Polymer attached to a surface in brush conformation with a high density of surface grafting points.

Similar to a polymer coil in solution an expression for the free energy of a polymer coil as a function of brush height h, can be derived, Equation 3.3.[13]

$$G_{tot}(h) = \frac{3k_BTh^2}{2Na^2} + \frac{\sigma[1-\chi]k_BTN^2a^3}{h} + \text{constant} \tag{3.3}$$

Where σ is the grafting density of the brush, [number of chains $\times$ area^{-2}]. Similar to a polymer coil in solution the minimum in free energy of the brush gives an expression for the brush height Equation 3.4, if solvent interaction is neglected ($\chi = 0$).[13]

$$h = \left[\frac{\sigma}{3}\right]^{\frac{1}{3}} a^{\frac{5}{3}} N \tag{3.4}$$

Equation 3.4 shows that the polymer brush height scales with the grafting density by 1/3.[13] In contrast to the radius of a free polymer coil, the polymer brush height scales linearly with N.

It should be noted that the free energy expression for the brush is an idealized picture based on mean-field calculations.[64] Equation 3.3 and Equation 3.4 assume that throughout the brush the monomer density is constant up to a certain brush height value, after which there is a sharp cut-off, beyond which no monomers can be present. This implies that all the polymer coils are equally stretched with all ends located at the periphery of the brush. In reality this picture is false, the polymer coil configurations will vary to a great extent, and

terminal group of many coils will be buried within the brush because this corresponds to a lower free energy of the system. Consequently the density of monomers within the brush is not uniform but follows a parabolic relationship with respect to the distance from the surface, z, according to Equation 3.5.[64]

$$\Phi(z) \propto h^2 - z^2 \tag{3.5}$$

The parabolic density of polymer brushes has implications on the interfacial properties of the polymer brush.[64] There is a non-uniform solvent penetration within the brush and the degree of polymer-polymer interactions is larger deep within the brush compared to the exterior. Also the exterior of the brush, which has a low monomer fraction relative to the brush as a whole, is what particles and free macromolecules in solution first interact with when exposed to the polymer brush surface.

3.1.3 Polyelectrolytes

Polyelectrolytes are polymers that contain functional groups that are charged, or which become charged in certain environments.[63, 65, 66] Consider four examples of polyelectrolytes shown in Scheme 3.1. Polyelectrolytes may be composed of negatively charged, anionic monomers e.g. **1** (PSS), and **2** (PAA) or they may be positively charged, with cationic monomers e.g. **3** (PDAMAC) and **4** (PDEA) (see caption of Figure 3.1 for full polymer names).

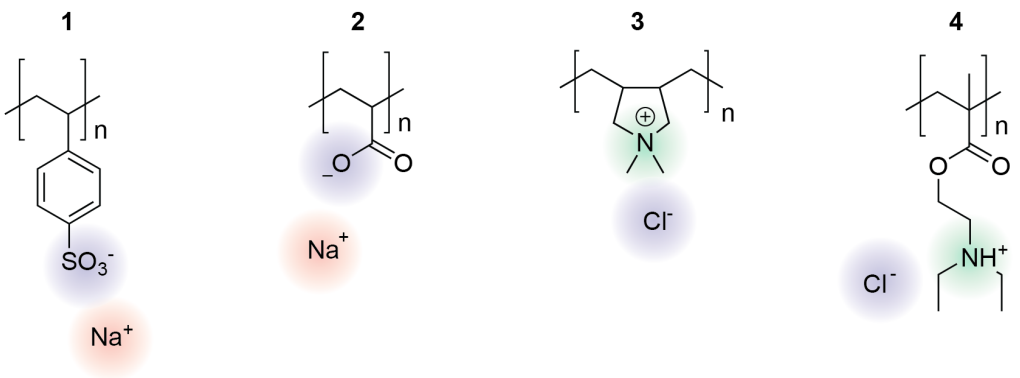

Scheme 3.1: Examples of polyelectrolytes, **1** sodium poly(styrene sulfonate) (PSS), **2** poly(acrylic acid) (PAA), **3** poly(diallyldimethylammonium chloride) (PDAMAC), and **4** poly(2-(diethylamino)-ethyl methacrylate) (PDEA).

Polyelectrolytes can be sorted into two classes: strong and weak. A strong polyelectrolyte contains functional groups that are strong acids or bases resulting in a permanently charged state of the polyelectrolyte in aqueous solution, PSS[67] and PDAMAC[68] are examples of strong polyelectrolytes. Weak polyelectrolytes can contrary to strong polyelectrolytes also exist in a neutral state, PAA[67] and PDEA[69] are weak polyelectrolytes which reversibly associate or dissociate protons, Scheme 3.2.[1]

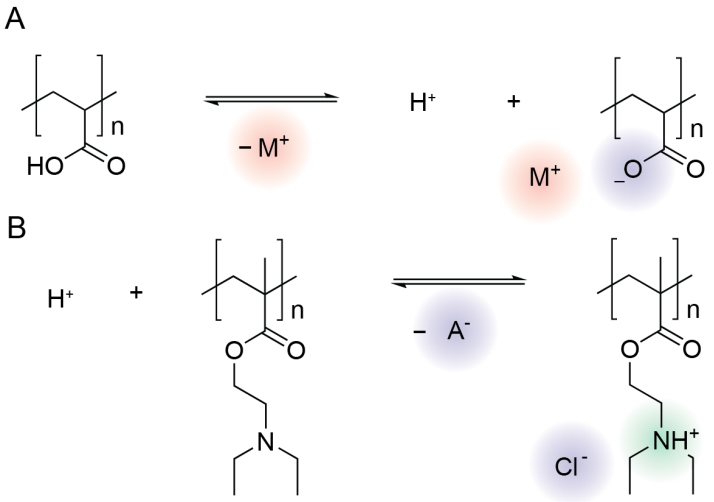

Scheme 3.2: (A) Dissociation reaction of protons from poly(acrylic acid) (B) Association reaction of PDEA

Formally, for weak acidic polyelectrolytes, the case of a basic polyelectrolyte is analogous, the proton association dissociation reaction is given by,

$$\mathrm{HA} \rightarrow \mathrm{H}^+ + \mathrm{A}^-. \tag{3.6}$$

We wish to relate the fraction of charged monomers, α to the pH of the solution. The fraction of charged monomers is given by,

$$\alpha = \frac{C_{\mathrm{A}^-}}{C_{\mathrm{A}^-} + C_{\mathrm{HA}}} \tag{3.7}$$

The dissociation constant, K_a, of monomers is given by

$$K_\mathrm{a} = \frac{[\mathrm{H}^+][\mathrm{A}^-]}{[\mathrm{HA}]}. \tag{3.8}$$

[1]Weak polyelectrolytes are mainly studied in this thesis, hence polyelectrolyte throughout this theses refer to weak polyelectrolytes unless stated otherwise.

where the $\mathrm{p}K_\mathrm{a} = -\log 10(K_\mathrm{a})$. Insertion of Equation 3.7 into Equation 3.8 and rearrangement results in the Henderson-Hasselbalch equation.

$$\mathrm{pH} = \mathrm{p}K_\mathrm{a} + \log 10\left[\frac{\alpha}{1-\alpha}\right] \tag{3.9}$$

This expression relates the dissociation of *a single* acid to the pH of the solution. However, a polyelectrolyte consist of many acid functional groups. For a charged polyelectrolyte the Henderson-Hasselbalch equation becomes inaccurate because of the proximity of charged functional groups along the polyelectrolyte chain.[36] Charge renormalization is when the ionization state of a functional group is altered by the surrounding molecular environment, in this case the electrostatic effects of surrounding monomers which influences the dissociation equilibrium.[70, 71] An alternative model for how the pH is related to the fraction of charges for polyelectrolytes is given by

$$\mathrm{pH} = \mathrm{p}K_0 + \log 10\left[\frac{\alpha}{1-\alpha}\right] + \mathrm{A}\alpha^{1/3}, \tag{3.10}$$

where $\mathrm{p}K_0$ is the $\mathrm{p}K_\mathrm{a}$ of a single acid and A is a constant where factors that influence the charge renormalization of the polyelectrolyte is included, such as the salt concentration, composition and polyelectrolyte concentration.[36]

In a polar solvent as water the dipole moment of the solvent molecule will result in polarization and orientation of water molecules in the vicinity of charges along the polyelectrolyte.[72] More importantly the charges species of the solvent, the counterions H^+ and OH^- and other ionic species e.g. Na^+ or Cl^-, will electrostatically interact with the polyelectrolyte. Counterions of opposite charge experience coloumbic attraction to the polyelectrolyte chain. This gives rise to a loosely associated cloud of counterions around the polyelectrolyte, called counterion screening. Counterion screening, or charge regulation as it is also called, gives rise to an effective charge of the polyelectrolyte in solution, which is often reduced in comparison to the true charge of the polyelectrolyte.[71, 72] This is highly relevant in the context of interactions with other charged molecules and interfaces in solution. For a polyelectrolyte in aqueous solutions with counterions present, the effective electrostatic interaction between two charges $z_1 e$ and $z_2 e$, is given by $z_1 z_2 v_\mathrm{DH}(r)$ where $v_\mathrm{DH}(r)$ is the Debye-Huckel potential,

$$v_{\mathrm{DH}}(r) = \frac{l_B}{r} e^{-r/\kappa^{-1}}, \tag{3.11}$$

where r is the distance between the two charges, $l_B = e^2/(4\pi\epsilon \mathrm{k_B} T)$ is the Bjerrum length.[72] The screening length, κ^{-1}, of a monovalent electrolyte species is determined by

$$\kappa^{-1} = \sqrt{\frac{\epsilon_0 \epsilon \mathrm{k_B} T}{\mathrm{N_A} c_s e^2}} \tag{3.12}$$

where e is the elementary charge, ϵ_0 is the vacuum permittivity, ϵ is the dielectric constant of the medium, and c_s is the salt concentration.[72] As Equation 3.12 shows, the screening of charges depends on the salt concentration. In biological fluids the salt concentration is high $c_s \approx 0.2$ M. The corresponding screening length in such a system is $\kappa^{-1} \approx 1$ nm, meaning that charges are effectively screened from objects beyond 1 nm of the polyelectrolyte molecule. The significant contributions of long-range coloumbic intramolecular repulsion and counterion attraction are difficult to include in theoretical models of polyelectrolytes. This is why simulations, models and predictions of the charged brush conformation and its scaling laws more complex to determine.[72, 62, 65, 66] Thus, the fundamental understanding of polyelectrolytes in brushes is lower compared to neutral brushes, as will be described in Section 3.1.4.

3.1.4 Polyelectrolyte brushes

Polymer brushes composed of polyelectrolytes display properties very different from neutral polymer brushes.[63, 72, 73, 74, 75] The presence of charges fundamentally changes the swelling properties of the brush. For a charged polymer the brush swelling and the height is no longer balanced by excluded volume and configurational entropy effects as is the case for a neutral brush. Instead the swelling behavior is primarily determined by electrostatic interactions and the osmotic pressure of the counterions. In an aqueous solution the charges along the polyelectrolytes in the brush are all accompanied by counterions. Within the brush charge neutrality must be preserved and it is established at the expense of the entropy loss of counterions that coordinate to functional groups within the brush. The free energy of the a polyelectrolyte brush is given by Equation 3.13, where in addition to the free energy of the polyelectrolyte $\mathrm{G_{pol}}$ terms for

the counterions G_{ion} and the interaction between counterions and the polyelectrolyte G_{int} are included.

$$G_{tot} = G_{pol} + G_{ion} + G_{int} \tag{3.13}$$

Weak polyelectrolyte brushes are classified into three regimes (1) the osmotic brush regime, (2) the salted brush regime, (3) and the neutral brush regime.[63, 74, 75, 76] The classification is based upon the salt concentration that the brush is exposed to. Figure 3.3 illustrates each polyelectrolyte brush regime for the case of a polyanionic brush where the counterions in solution are protons and dissolved monovalent metal ions. At low salt concentrations the charged functional groups are screened by protons in the water solution rather than by salt counterions, this is the osmotic brush regime. Due to osmotic pressure any salt counterions that may be present in the brush will diffuse out of the brush and into the bulk solution. However, to preserve charge neutrality protons replace the salt counterions in the brush. If the salt concentration increases protons are exchanged for salt ions. Eventually the salted brush regime is reached when there is a nearly equal concentration of salt ions within the brush and exterior of the brush. Upon even further increase of salt concentration the neutral brush regime is reached where the osmotic pressure of ions cause the brush to collapse. In the neutral brush regime charges are so efficiently screened that the electrostatic interactions between coils in the brush are low or even negligible.

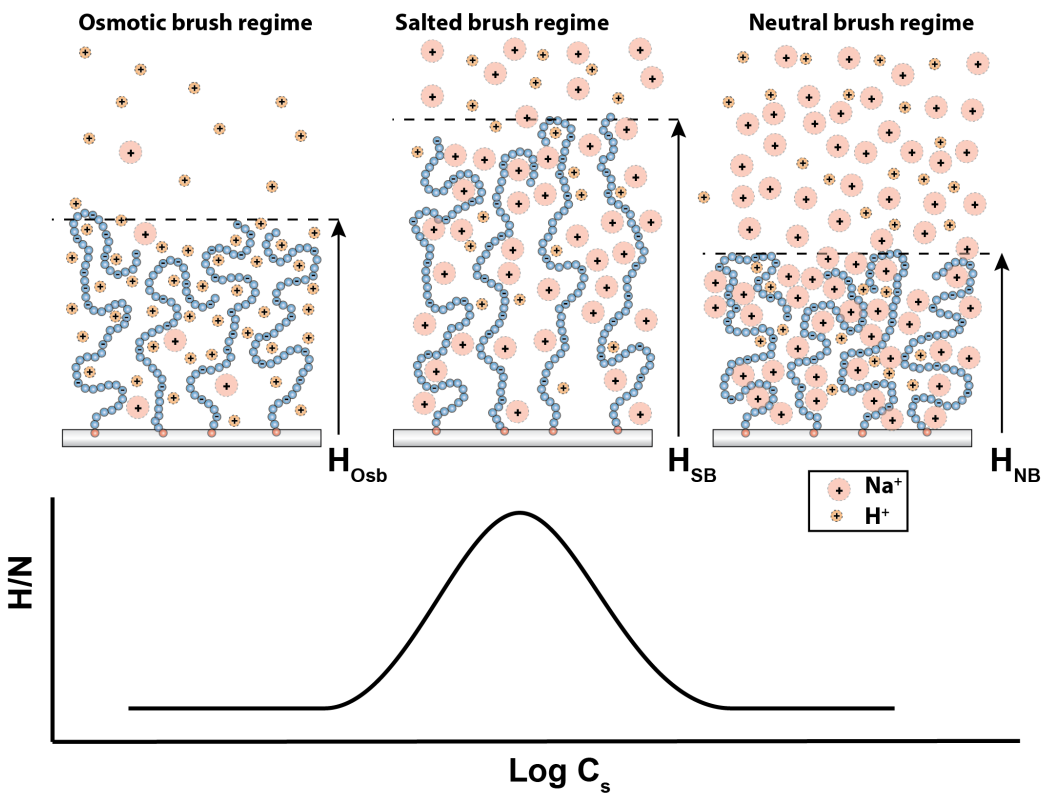

Figure 3.3: Three regimes of weak polyelectrolyte brushes, osmotic brush, salted brush and neutral brush. The brush height H/N is maximized at some salt concentration intermediate between the osmotic brush and neutral brush regime. The illustrations are an interpretation where protons (H^+) and sodium ions (Na^+) are present within and exterior of the brush at different salt concentrations (charge neutrality is preserved). The brush height as function of salt concentration is adapted with modification from the following references [76, 73]

At low salt concentration and in the osmotic brush regime the brush height is proportional to the square root of the fraction of charged monomers α, and linear with respect to degree of polymerization N according to Equation 3.14.[34, 63, 76]

$$H_{OsB} \propto N\alpha^{\frac{1}{2}} \tag{3.14}$$

Unlike neutral brushes (Equation 3.3) under osmotic brush conditions the height of polyelectrolyte brushes are under the osmotic brush regime independent of grafting density.[65] The situation changes as more salt is added to the

solution and the polyelectrolyte brush enters the salted brush regime. For the salted brush regime the brush height is given by

$$H_{SB} \propto N\sigma^{\frac{1}{3}} c_s^{\frac{1}{3}}. \tag{3.15}$$

As previously explained, in the salted brush regime the salt counterions begin to enter the brush and replace protons that previously screened charges.[74, 73] In the salted brush regime the height increases with increased salt concentration to the power of 1/3 up to the point where the concentration of ions within the brush is equal or near equal to the solution salt concentration. At some point a balance between electrostatic repulsion between the chains and liberation of protons as counterions leads to a brush height maximum. The maximum in height occurs because when the salt concentration of the bulk exceeds the local salt concentration the brush starts to shrink and collapse. The shrinkage is due to an osmotic pressure that builds up within the polyelectrolyte brush. The collapse of polyelectrolytes upon very high salt concentrations is observed in both weak and strong polyelectrolyte brushes.[63, 73] In the neutral brush regime the polyelectrolyte brush height scales according to

$$H \propto N\sigma^{\frac{1}{3}} c_s^{-\frac{1}{3}}. \tag{3.16}$$

The key point to observe is that there is a change in scaling with respect to salt concentration with increased salt concentration that leads to a maximum brush height for some salt concentration (Figure 3.3).[73, 74, 75] The salt concentration scales with brush height with the power of 1/3 (low salt concentration) to -1/3 (high salt concentration). The neutral brush or quasi-neutral regime reflects the increasing screening by counterions that conceal electrostatic interactions between the polyelectrolytes in the brush. Experimentally, the maximum in brush height as function of salt concentration has been observed for PAA, PDEA and PMAA brushes prepared by grafting-from polymerization techniques.[34, 73, 76, 30, 77]

Discrepancies between theoretical and experimental results are common in polyelectrolyte brush literature.[63] Partly this is due to the fact that scaling laws of polyelectrolyte brushes are not developed theoretically or validated experimentally to the same extent as neutral brushes. Primarily the difficulty is

due to the difficulty in modelling polyelectrolytes themselves. Theoretical approaches to understanding polyelectrolyte brushes rely on several simplifying assumptions. Although theoretical models of polyelectrolytes require simplification, discrepancies between experiments and theory are also linked to experimental difficulties in preparation of polyelectrolyte brushes and mixed results between preparation methods. Achieving a sufficiently dense and strongly stretched polyelectrolyte brush with sufficient knowledge of the polymer properties is challenging, a topic discussed in the next section.

3.1.5 Protonation behavior of polyelectrolyte brushes

It is well known that the pK_a of weak polyelectrolytes shifts as a function of the salt concentration through charge regulation (Equation 3.9).[36] In a highly concentrated PAA solution, the pK_a of PAA shifted by approximately 0.3 units between 10 and 100 mM total salt concentration.[78] Such a shift should in principle also occur for polyelectrolyte brushes. In fact, polyelectrolyte brushes might display even larger shifts in the pK_a as function of salt concentration due to the proximity of polyelectrolyte chains within the brush that produce a very high density of acidic/basic functional groups, difficult to achieve in bulk polymer systems. For instance, the pK_a of PMAA brushes was observed to change when the grafting density was varied[79], which indicates the role of the concentration of functional groups. The swelling and collapse of polyelectrolyte brushes as a function of the total salt concentration and of different salt chemistry e.g. valencies and ion types has been tested extensively but only for a few fixed values of pH.[30, 29, 40] However, pH switching measured for many pH values especially surrounding the pK_a has rarely been reported. In a few published experiments where multiple pH are measured, the number of data points are too few to accurately judge if the pK_a is shifted as function of salt concentration or not.[80] Furthermore, the range of concentrations tested is limited to 10 mM to 100 mM. A very recent study (performed simultaneously and independently of this thesis) studied the pK_a of PAA as a function of the salt concentration.[34] Indeed, the results showed shifting pK_a as function of the salt concentration. However, it is still not fully understood if this is a general feature of all pH-responsive polyelectrolytes, and what the effect of changing the salt concentration over a large

concentration and pH window is.

The possible existence of a pK_a shift of polyelectrolyte brushes as a function of salt concentration has large implications in correctly attributing the mechanisms behind its interactions with other molecules. In multiple studies of polyelectrolyte brushes the salt concentration is kept low since it extends the Debye length and enhances electrostatic effects such as attraction and repulsion by other charged macromolecules.[40, 43, 19, 39] These studies neglect to take into account that at low salt concentration the pK_a might be different compared to pK_a measured at regular ionic strength (e.g. physiological salt concentration).

3.1.6 Locally displaced pH within polyelectrolyte brushes

Nanobuffering is the displacement of the pH from the bulk solution established by a confined molecular environment that displays an increased (or depleted) proton concentration (H^+).[46] Polyelectrolyte brushes are predicted to display a lateral pH gradient.[76] Simulations show that the salt concentration and polymer surface coverage both affect the local pH within the brush and that the pH within the brush can differ by at least two units compared to the solution pH.[76, 81]

To date most experimental evidence of nanobuffering are indirect observations of the phenomenon.[82] Charge regulation has been suggested to be evidence of nanobuffering.[78] As discussed it is reasonable to expect that charge regulation occurs in polyelectrolyte brushes since it is displayed even for polyelectrolytes in solution. This may be manifested in shifts in pK_a as function of salt concentration,[34, 78] or by the existence of lateral gradients in the dissociation state of polyelectrolyte brushes,[76, 81, 34, 83] or both. This is unsurprising since polymer brushes have a non-uniform lateral density distribution,[13] which can be expected to favour dissociation at the fringe of the polyelectrolyte brush solution interface, compared to deep within the polyelectrolyte brush.[83] However, an altered dissociation state does not necessarily a displaced local pH. A functional group which is normally charged, can be protonated in some other molecular environment (all other things being equal: pH and salt concentration etc.) without necessitating a shift in the pH of the surrounding solution. Biocatalysis and other biological interactions with polyelec-

trolytes is another, arguably indirect, method of detecting nanobuffering of polyelectrolytes.[82, 45] For instance, conjugation of PMAA to Cytochrome C (Cyt-C) resulted in increased catalytic activity at high pH of the Cyt C-PMAA conjugate compared to the native enzyme activity.[82] The retention of catalytical properties even at high magnitudes of pH was attributed to a locally decreased pH microenvironment within the Cyt-C-PMAA conjugate. However, boosted enzyme activity can occur due to other effects than nanobuffering, increased turnover of the enzyme can also be explained by altered enzyme structure induced by the bioconjugation.

Direct measurement of the local pH can be measured by microscopy using pH reporting fluoresent molecules. This was done in layer-by-layer (LbL)[2] assemblies of strong polyelectrolytes (poly(allylamine chloride) (PAH) and PSS).[84] This approach is appealing since it directly senses the pH within the confined polyelectrolyte environment. Evidence of pH-gradients within the polyelectrolyte layers were found, providing perhaps the strongest experimental evidence of nanobuffering. However, this system is very different compared to pH-responsive polyelectrolyte brushes. First, the system consists of a highly compact thin layer of strong anionic and cationic polyelectrolytes that collapses to the surface by electrostatic attractions. Contrary to weak polyelectrolytes the system is permanently charged which means that this system cannot regulate proton concentrations by protonation to the same extent, which is a very relevant process with respect to the free proton concentration. Consequently there are a number of factors that prevent the direct translation of nanobuffering in films of strong polyelectrolytes to weak polyelectrolyte brushes.

Experimentalists address nanobuffering by trying to detect it,[82] and theoreticians perform molecular simulations to track the protons distribution by ambitious computations.[76, 81] However, the existence of nanobuffering can be addressed by a different method. One can try to answer why nanobuffering should exist in the first place? Charge renormalization is often used to explain nanobuffering, since counterions are needed to screen charges in dense polyelectrolyte systems, this should result in a sequestering of protons (proton "sponge") to screen charges within a heavily charged anionic brushes for instance.[46]

[2]Contrary to polymer brushes which are end-tethered polymers to surfaces layer-by-layer surfaces are stacked layers of oppositely charged polyelectrolytes onto a charged substrate

While counterion screening is to be expected, it does not answer why other more abundant counterions are not sufficient to achieve screening. The theory of nanobuffering requires some explanation to why specifically protons are favoured ahead of other cations such as sodium (Na^+). At very low total salt concentration it is understandable that protons participate in screening since there is a lack of counterions that can perform screening. Consequently this means that if nanobuffering should exists then low salt concentration is plausible. But this contradicts some examples where nanobuffering is claimed to happen at physiological salt concentration, in solutions where $[Na^+] = 10^{-3}$ and $[H^+] = 10^{-7}$.[82, 45, 46] Consequently more research is needed, which provide methods for direct detection of nanobuffering, and which provides an explanation to why protons are favoured as cations in highly concentrated polymer systems ahead of other cations.

3.1.7 Preparation of polymer brushes

Polyelectrolyte brushes can be prepared either by grafting-to or grafting-from method, as shown in Figure 3.4 A and B, respectively.[63] The grafting-to approach relies on attaching already synthesized polymers to a bare surface, while grafting-from is a bottom-up method where the brush is grown from the surface directly using surface-initiated polymerization. Grafting-to often leads to relatively low grafting density within or close to the "mushroom"-regime. This is due to the kinetic barrier of attachment that arises on a partly covered surface which is due to an increased steric hinderance experienced by polymer coils which are not yet attached but are in the vicinity of the surface. The method of attachment sometimes relies on forming chemical bonds with the functional groups along the polymer chain, causing a multiple point attachment of the polymer to the substrate surface. Multiple anchor points affect the conformational freedom of the polymer chain and the effective polydispersity of the polymer brush produced. To circumvent this problem end-functionalized polymers are preferable. Temporary shrinking of coil size by using high salt concentration can substantially increase the grafting density and give rise to strongly stretched polymer brushes.[17] However, achieving high grafting density by grafting-to is challenging. An advantage of grafting-to is control of the polymer properties by

characterization of the free polymer.

Another method for preparing polymer brushes is to synthesise them directly on the surface by a polymerization reaction shown in Figure 3.4 B, known as grafting-from or surface initiated polymerization. High grafting density is possible to achieve since a monolayer of initiators can be present during polymerization.[85, 26] In addition the number of initiator molecules can be set to control the grafting density. The disadvantage with grafting-from is the low control and knowledge about the final polymer properties such as grafting density, PDI, and molecular weight. There is no way to guarantee that all the initiator molecules initiate polymerization which means the grafting density of the polymer brush will not necessarily match the surface density of surface initiator.

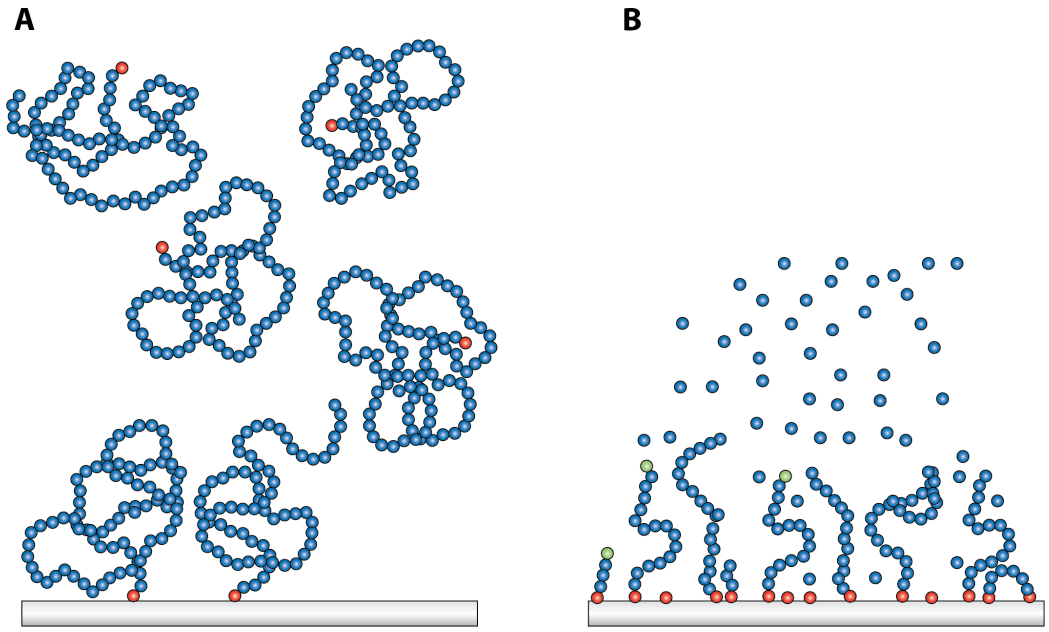

Figure 3.4: Illustration of two strategies for preparation of polymer brushes in (A) by grafting-to (of end-functionalized polymers) where the surface binding group is shown in red and by (B) grafting-from, through activated radicals on growing brushes, shown in green.

In this thesis polymer brushes were prepared by grafting-from using a controlled radical polymerization reaction called Atom Transfer Radical Polymerization (ATRP), Figure 3.3. ATRP was reported in 1995 followed by surface initiated ATRP in 1997.[85, 26, 86] It has become a popular polymerization technique for preparation of polymer brushes due to its relative robustness and versatility. It is

compatible with a wide range of solvents, different catalyst/ligand combinations can be used to tune the reaction rate for a specific need, and works for a large variety of different acrylate and methacrylate monomers. ATRP proceeds through transfer of a halogen between a transition metal catalyst ligand complex (e.g. Br-Cu(I)/L) and a polymer chain end-capped with an alkyl-halide (P_n-Br), the alkyl radical propagate at a rate of k_p, and are reversibly formed where the equilibrium is heavily shifted to the dormant reduced state state by K_{ATRP}, enabling synthesis of polymers with low PDI (Figure 3.3).

In ATRP a large concentration of copper is required to sustain the reaction, although the copper can be washed away the risk of copper contamination during subsequent use of the brush limits the scope for applications in biological and semiconductor applications.[86] A further complication of ATRP is the oxygen sensitivity of the Cu(I) species. Unless a very rigorous oxygen-free environment can be established, side-reactions quickly terminate the polymerization reaction. To circumvent these issues a less oxygen sensitive method which also requires a lower concentration of copper was developed. In Activator Regeneration Electron Transfer (ARGET) ATRP a reducing agent e.g. ascorbic acid is used, which produce Cu(I) species (Figure 3.3). Instead of having Cu(I) species present in the reaction vessel at the start, ARGET ATRP initially only contains Cu(II) and the polymerization reaction starts when the reduction agent is added to the polymerization solution which reduce Cu(II) complexes into Cu(I). The copper concentration can be significantly reduced with this method because if there is an excess of reduction agent present it not not only reduces Cu(II) into Cu(I) to start the reaction, but it also removes oxygen and radical inhibitors. Contrary to copper, relatively high concentration of reduction agents (ascorbic acid, sugars, and tin(II) 2-ethylhexanoate) can be tolerated for applications.

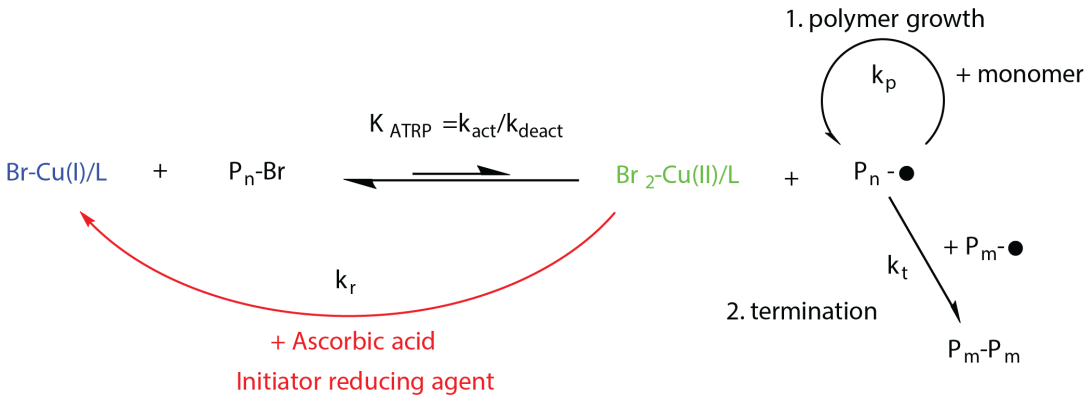

Scheme 3.3: Reaction scheme that shows one example of ARGET ATRP using ascorbic acid reduction agent and bromine halogen. The equilibrum constant for the catalyst and polymer radical activation reaction is given by K_{ATRP}, the rate of polymerization reaction is k_p, the rate of the termination reaction is k_t, and the rate of initiation by reduction is k_r.

Although, grafting-from by controlled radical polymerization is a robust and versatile method its main disadvantage is precise knowledge of the polymer molecular weight and the grafting-density of the brush. Therefore large efforts have been dedicated to characterize polymers grown by surface-initiated polymerization.[87, 88] The grafting density (σ) is calculated by

$$\sigma = \frac{\rho h \mathrm{N_A}}{\mathrm{M_n}}, \tag{3.17}$$

where ($\mathrm{M_n}$) is the number average molecular weight, h is the brush height and $\mathrm{N_A}$ is the Avogadro's number. A common approach to calculate the grafting density without direct knowledge the molecular weight is to perform a solution polymerization in parallel, under equal conditions.[19, 29, 34, 30] This method is controversial: On the one hand some experiments support that solution phase polymerization can be compared to surface-initiated polymerization.[26, 89] On the other hand there are also several reported cases of when solution polymerization fails to predict grafted-from polymer properties.[87, 88, 90] Despite conflicting experimental evidence, polymer properties based on solution polymerization is frequently used to calculate grafting density of brushes.[19, 26, 29, 30, 34] At best, there is experimental verification that supports the validity in that particular case. At worst, it is assumed to be valid in general that polymerization from surfaces and in solution proceed at equal rates. One should be es-

pecially cautious in making this assumption when the grafting density of surface initiators is high.[88] Results from experiments and simulations of surface initiated polymerization with a high density of surface initiators show mass-transfer limitations of reactants that slow down the reaction rate, and that the proximity of actively growing chain ends leads to increased rate of chain termination. Resulting in significant discrepancy between surface-initiated and bulk-initiated polymer molecular weight and PDI.

Ultimately, the lack of non-invasive characterization methods currently, means destructive analysis is still required where the brush is de-grafted and the free polymers are characterized by standard polymer characterization methods like size exclusion chromatography (SEC) or matrix assisted laser desorption/ionization (MALDI). This is the only reliable method for determining the true number average molecular weight that allows determination of the grafting density with certainty.[26, 87, 88] This can be accomplished by initiator groups that are anchored to the surface with photo-cleavable bonds.[26] Another option are functional groups that cleave in acidic conditions or by exposure to some reactant that specifically cleaves the initiators off of the surface. It is crucial however that only the bond that anchors the polymer to the surface breaks and that further degradation of the polymers does not occur in the process. An appealing non-destructive method for determining grafting density would be assays that detect the end-groups of the polymer chains.[87] Obviously this requires a highly controlled polymerization reaction such that every end group of the polymer was terminated when the reaction stopped, making them available for subsequent detection. A very small fraction of chains need to be prematurely terminated by two chains growing together, since these would go undetected in the assay. Some promising results on this area has been produced, but it has not become a standard practice.

3.2 Molecular interactions

Electrostatic repulsion between polyelectrolytes and attraction of counter-ions are significant contributors to the free energy of the polyelectrolyte brush system. If external molecules are introduced, such as proteins or polymers, the molecular interactions between the proteins and the brush polymers occur *in addition* to

the above mentioned interactions. This adds complexity to an already complex system. To provide a theoretical general description of molecular interactions is obviously a very ambitious task. I chose to focus on molecular interactions that may occur between proteins and pH-responsive polyelectrolytes.

3.2.1 Electrostatic repulsion and attraction

The majority of amino acids with charged side groups (95%) are located on the protein surface.[91] Contrary to the polyelectrolyte brushes we consider in this thesis (which are exclusively either cationic or anionic), proteins are polyampholytes with both positive and negative charged functional groups.[3] Similar to the pK_a of polyelectrolytes, proteins have isoelectric point pI describing the net charge as a function of pH. It is instructive to sum up the charged natural amino acids, shown in Scheme 3.4.

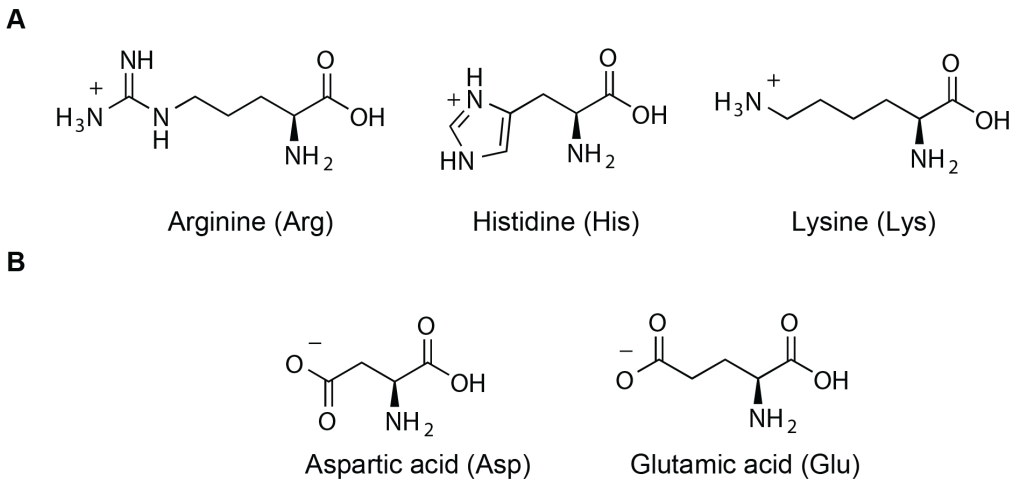

Scheme 3.4: Charged amino acids with (A) cationic and (B) anionic side groups at pH 7.4.[92]

The net charge of a protein can be obtained by a summation of the charged functional groups of the protein.[70, 71, 72] However, this is a highly simplified picture. Similar to synthetic polyelectrolytes, proteins in solution display an effective charge due to charge renormalization and charge regulation. The surface of a protein consists of a compact environment with a high density of differ-

[3]It is possible to synthesize a large range of polyampholyte and so called zwitterionic polyelectrolyte brushes, but these were not studied in this theses.

ent charged and polar functional groups which will affect the effective charge. Charge regulation will also occur as a function of the buffer chemical composition and in particular the salt concentration which will screen charges. The net effective charge of the brush and of the protein depends on the pH of the solution. This sets a window, the relative overlap between the pK_a and the pI, for when net electrostatic attraction between the protein and polyelectrolyte brush occurs.

Figure 3.5 A, demonstrates an example where avidin (pI $\approx$ 10.5) at neutral pH displays electrostatic attraction to PAA (pK_a = 4.5), the relatively high pI exceeds the pK_a of the brush. Conversely, in Figure 3.5 B, a cationic brush such as PDEA can electrostatically attract a protein with relatively low pI e.g. glucose oxidase around neutral pH. In both cases, if the pH is increased or decreased, the net charge of the protein and the brush become equal, with electrostatic repulsion as a result. If the brushes are neutral, electrostatic interactions are suppressed, giving rise to other non-electrostatic molecular interactions.

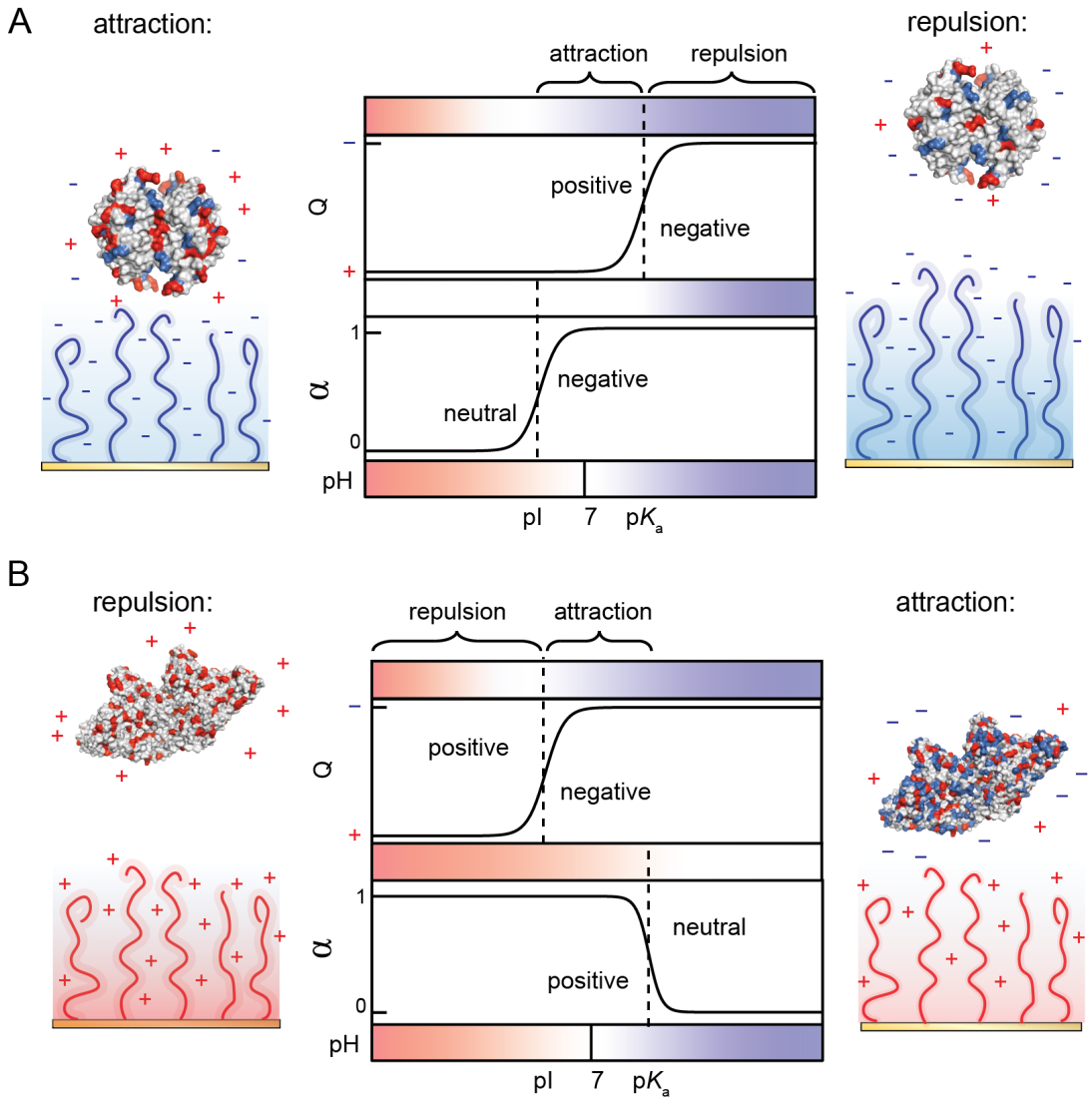

Figure 3.5: Examples of electrostatic interactions between proteins (Q: net charge) to polyelectrolyte brushes (α: degree of charging) as function of pH. In (A) between avidin and PAA and in (B) between BSA and PDEA. The conditions for attraction and repulsion are determined by the pI and pK_a of the protein and brush respectively.

When protein binds to the brush by electrostatic immobilization, the protein replaces the counterions associated with the charged functional groups of the brush, liberating the counterions from being confined to the brush.[27] Conversely, the counterions associated with the charged functional groups on the protein surface must also release from the protein when electrostatic immobilization occurs. Even if net electrostatic attraction exists it is not obvious that

electrostatic immobilization will lower the free energy of the system. The free energy and in particular the entropic penalty of counter-ions to coordinate with the protein and the brush, play an important role in promoting or preventing the formation of electrostatic immobilization.

The simplified picture shown in Figure 3.5 works as a rule of thumb in many cases.[19, 42] However, proteins are diverse and complex polyelectrolytes which means the net charge of proteins cannot be drawn as a simple single sigmoidal function. There are several reports of examples where proteins immobilize to brushes even when the brush and protein are reported to have same sign of charge.[27, 44] In addition, many protein surfaces contain binding pockets and surface domains with a local concentration of a certain ionic species, which create a "patch" of a charge opposite of the net charge of the protein. This patchiness of charges of the protein means that the net charge might not decide if electrostatic immobilization occurs or not. Hence, protein which contains a patch with a permanent charge that is opposite of the net charge may still bind strongly to the brush regardless of net repulsion. The reason for apparent electrostatic attraction on the wrong side of the pI is a topic which we will return to in Chapter 5.2.

3.2.2 Hydrogen bonds

Protonated polyacids (PAA and PMAA) engage in hydrogen bonding with other polymers and molecules that contain functional groups with complementary hydrogen bond donors and acceptors.[93] Hydrophobic interactions is the driving force for self-assembly of the proteins, which includes the forming of hydrogen bonds between amino acids to form the secondary and tertiary structure of proteins.[91] The amino acids shown in Scheme 3.5 all contain side groups with hydrophilic polar functional groups that form hydrogen bonds. These amino acids are predominantly displayed towards the hydrophilic exterior surface of the protein.

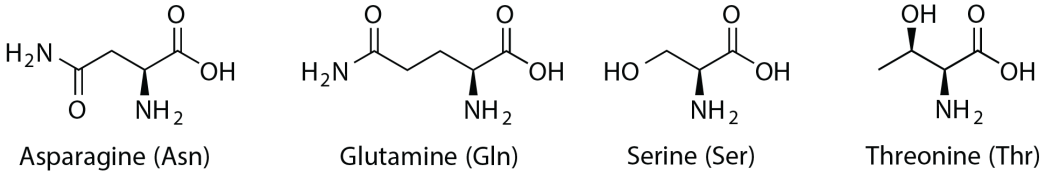

Scheme 3.5: Amino acids with polar uncharged side groups

The polar amino acids displayed on the surface of proteins enable hydrogen bonds with other polar molecules. In addition to neutral polar amino acids, charged amino acids (in Scheme 3.4) are also capable of forming hydrogen bonds with molecules in solution. Consequently, if a protein is exposed to a hydrogen-bonding polymer e.g. a neutral PMAA or PAA brush, a range of hydrogen bonds can form between the polyelectrolyte and the exterior surface of the protein (Scheme 3.6).

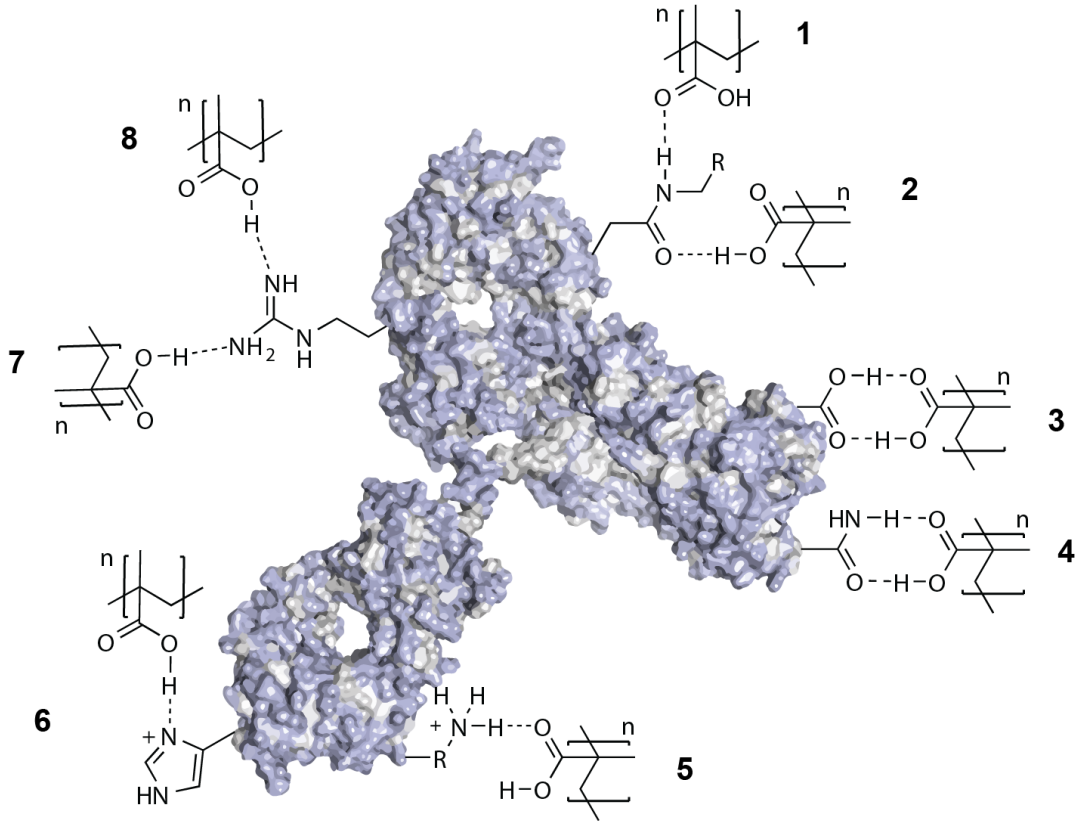

Scheme 3.6: Examples of some of the many hydrogen-bonds that may form between neutral poly(methacrylic acid) brush and the exterior functional groups of a protein: (1-2) peptide bond, (3) aspartic and glutamic acid, (4) asparagine and glutamine, (5) lysine, (6) histidine, (7-8) arginine.

In survey of the literature the impression is, that the only means for binding protein to polyelectrolyte brushes is by electrostatic attraction.[19, 41, 42, 94] However, Figure 3.6 shows multiple ways in which proteins can immobilize to polyelectrolyte brushes by hydrogen bonds. Charged brushes could in principle also immobilize proteins by hydrogen bonding, since hydrogen bonds can form between ionic functional groups.[95] Consequently, there are is good reason to suspect that non-electrostatic interactions by hydrogen bonds between the protein surface and polyelectrolyte brushes could play a role in protein immobilization.

3.2.3 Hydrophobic interactions

To this point we have discussed water soluble proteins that interact with hydrophilic, charged or polar materials. However, if proteins interact with a hydrophobic material this may trigger unfolding of the protein that exposes its hydrophobic interior. Amino acids with non-polar, uncharged, and therefore hydrophobic side groups (Scheme 3.7) are buried into the core of the protein. A water soluble fully functional protein generally relies on retaining its self-assembled structure to perform its biological function within an extracellular or cellular environment. But, if a protein unfolds the hydrophobic interior is exposed, not only will this cause the protein to loose its function, the unfolded protein will rapidly interact with other hydrophobic molecules in solution and phase separate, resulting in aggregation.

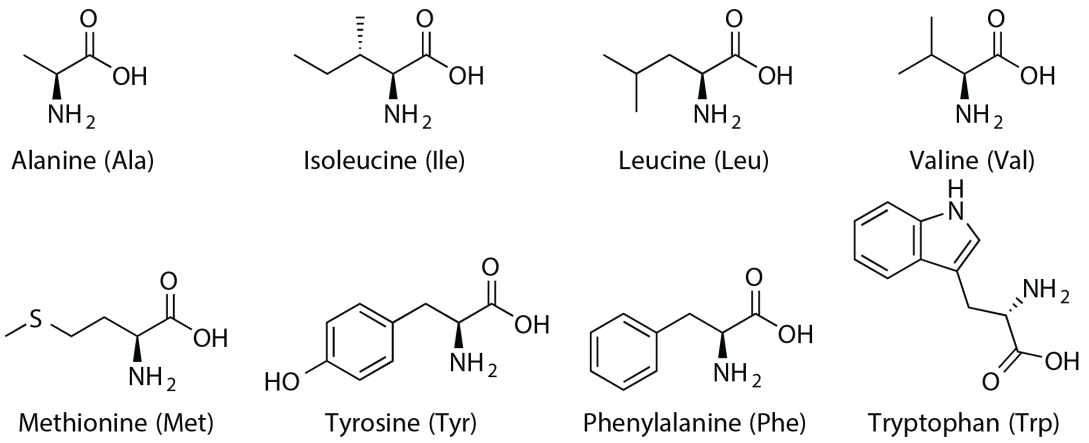

Scheme 3.7: Amino acids with hydrophobic side groups

A charged polyelectrolyte is highly hydrophilic and thus unlikely to undergo attractive interactions with an unfolded hydrophobic surface of a protein. However, a neutral, collapsed polyelectrolyte will have hydrophobic properties and readily bind unfolded and denatured protein. Charged amino acids are expected to interact primarily with the charged functional groups of the polyelectrolyte. But if the polyelectrolyte in question contains aromatic groups, alkane side groups, a hydrophobic polymer backbone or hydrophobic ligands, they may engage in hydrophobic interactions in addition to electrostatic interactions.

3.2.4 The combined picture

The exterior of a protein is composed predominantly of amino acids with hydrophilic, charged and polar functional groups.[91] Binding to the surface of proteins is a useful strategy to prevent protein unfolding, denaturation and aggregation.[42, 48, 96] One of the main motivations for using polyelectrolyte brushes for protein immobilization is the electrostatic attraction between the protein surface and the polyelectrolytes. However, polar side groups of the protein surface can also form hydrogen bonds with the polyelectrolyte brushes, in fact surface exposed amino acids with hydrogen bonding side groups outnumbers those with charged side groups (Figure 3.6). The relative occurrence of electrostatic and non-electrostatic interactions depend on many parameters, salt, pH and temperature. But it is important to highlight that both both electrostatic and non-electrostatic interactions may have a significant contribution for protein immobilization to polyelectrolyte brushes.

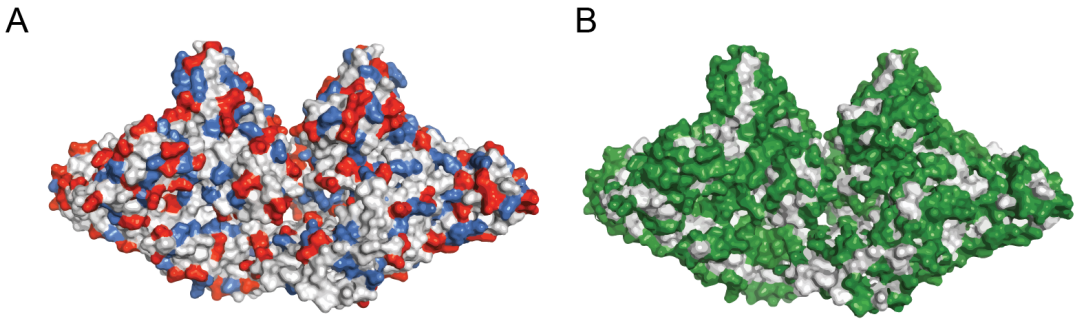

Figure 3.6: BSA side groups of amino acids with (A) charged side groups (cationic in blue: Arg, Lys, His and anionic in red: Glu, Asp) and (B) side groups that hydrogen bond (shown in green: Tyr, Trp, Lys, Ser, Thr, Glu, Asp, Arg, Asn, His, Gln), charged side groups constitute a sub-set of polar side groups

The molecular interactions discussed here are only a few of many possible. The surface of proteins rarely only consists of the surface exposed peptides.[97] Proteins in particular those expressed by eukaryotic organisms, undergo glycosylation, a post-translational modification of proteins where carbohydrates, glycans, are attached to the surface of proteins. Consequently, the first interaction between a polyelectrolyte brush and a protein may be between a glycan and the brush and not with sidfe groups of surface exposed amino acids. How-

ever, glycans are generally equipped with both hydrogen-bonding and charged functional groups meaning this does not fundamentally alter the mechanism by which polyelectrolyte brushes and proteins interact.

In summary, polyelectrolytes and proteins interact by electrostatic and hydrophobic interactions and through hydrogen bonds. The pH of the solution determines if electrostatic interactions are attractive or repulsive and depend on the pI and pK_a of the protein and polyelectrolyte brush in question. Non-electrostatic interactions like hydrogen bonds occurs between the hydrophilic surface of the protein and the polyelectrolyte. In fact, the very high density of hydrogen-bond donors and acceptors on the surface of proteins make this a highly probable form of protein polyelectrolyte interaction. Hydrophobic interactions may take place between neutral polyelectrolytes, with hydrophobic ligands will may result in immobilization by protein unfolding. This however, is detrimental to the preservation of protein structure and thereby function. Polyelectrolytes which contain a high number of polar functional groups and are charged like PAA and PMAA have the capability of interacting with the surface of proteins to a high extent making them suitable as scaffolds for proteins while preserving their structure.

3.3 Enzymes

The enzyme theory section is divided into three parts. In the first part a motivation for working with enzymes in synthetic environments is given. Secondly, different techniques for enzyme immobilization are described. The main model enzyme used, Glucose Oxidase (GOX), is described. Finally since the catalytic kinetics of GOX was studied in brushes, a brief description of basic enzyme kinetics is given.

3.3.1 Biocatalysis

Enzymes are proteins that functions as catalysts, they accelerate the reaction rate of chemical reactions without undergoing permanent change.[98] Enzymes catalyze the majority of chemical reactions that extract energy and materials from the environment to sustain life, making enzymes not only essential for life

but also the most powerful and complex catalysts known. Knowledge of how enzymes and biological reaction pathways function could potentially serve our societal need of improved access to energy and chemicals. For instance, use of enzymes in a cell-free environment offers a supplement to, or replacement for; (1) inorganic non-biological catalysts used to make complex chemicals by bottom-up synthesis,[99] and (2) top-down biosynthesis of biomolecules.[100]

Enzymes have a long tradition of industrial use, primarily for food and in house-hold consumer products.[101] For instance in the removal of lactose from dairy or gluten from beer, to remove fat and dirt from laundry, and to convert starch into glucose. In these applications, the cost of producing enzymes is very low and can be made in large quantities.[102] Most of these applications of enzymes require only the decomposition of some component. However, the efficiency does not have to be very high in terms of turnover rate per enzyme. Some applications of enzymes are more demanding like in the production of pharmaceuticals, an extremely regulated process with high demands in terms of performance, contamination and patient safety.[103] Their use in pharmaceuticals production is motivated by the enantioselectivity of enzymes which results in enantiopure products, which acoids racemate mixtures. Furthermore enzymes often have regiospecificity, meaning selectivity towards specific subsets of functional groups, which also translates into considerable savings. Consequently, enzymes are today used in several late stage transformations of pharmaceutical compounds.[99]

Recent developments in enzyme engineering techniques have further contributed to generate enzymes with new catalytic abilities at a very rapid rate.[104] This is important, since biocatalysis offers to reduce the environmental impact of chemical manufacture through the use of relatively low temperatures, ambient pressure, aqueous synthesis, replacement of metal catalysts, and high selectivity.[103, 99] However, in most cases biocatalytic synthesis steps are still introduced in isolated cases where costs of traditional methods are exceptionally high.[99] To unlock the potential of bottom-up synthesis enzymes need to constitute the platform of synthesis rather than act as a supplement to the current chemical processes.

Biosynthesis is a top-down approach of producing complex compounds where a living organism e.g. bakers yeast or *E. coli* produce a high value product. It

is widely used for large-scale production of valuable substances that are too difficult or expensive to produce synthetically (e.g. small but complex molecules with therapeutic activity,[100] and therapeutic antibodies[105]). The synthesis pathway to create these target molecules require a host of complex enzymatic transformations which are interconnected with and compete with other reaction pathways of the host organism. Cell cultures, microorganisms or animal models are therefore genetically engineered to produce a the desired compound and to increase the yield.[100] The yield can in this way reach impressive quantities considering that the microorganisms must stay viable and healthy simultaneously as producing high turnovers of the molecule in question.[106] However, the subsequent purification of the molecule of interest after harvest from the host organism molecules and cellular debris requires substantial effort and downstream purification resources that significantly contributing to the cost of compounds produced by biosynthesis.

The inherent limitation of sustaining the livelihood of microorganisms throughout the production cycle and the cost of downstream purification has inspired alternative approaches. A cell-free approach use enzymes extracted from the host organism placed within synthetic materials to produce desired chemicals. Outside the cellular environment enzymes in synthetic materials could operate in conditions with much larger chemical variation than within the cell, potentially increasing the output of product. Two strategies may be used (1) The first strategy for expressing cell-free protein expression, lysate the cells containing enzymes, along with all the other native molecules, the desired recombinant DNA sequence is introduced to the mixture and the protein of interest is expressed.[107] This crude strategy is not very different from conventional biosynthesis, but it simplifies the introduction of foreign DNA but also require purification of the molecule of interest from the native microorganism molecules. (2) The second strategy employs a purification of the lysate to avoid side-reactions and to facilitate the downstream purification of products.[108] The PURE system by New England Biolabs, is an example of this approach.

The production cost of purified enzymes limits the potential use of biocatalysis.[99] However, the potential gain of using enzymes is still very large and the reason why is quite simple. Currently, only a very small proportion of enzymes are used in industrial processes. A few more can be commercially obtained in

small quantities albeit at a high cost. But the vast majority of enzymes have not yet been produced, purified and characterized, meaning there is an enormous amount of different enzymes that have existed since life itself begun, and that exists today expressed by organisms in nature. In extension, we have the tools and methods at our disposal to evolve new and improved versions of interesting enzymes by a directed approach that allows us to tailor the properties of interesting enzymes once found. [104]

3.3.2 Enzyme Immobilization

As with inorganic heterogeneous catalysis, a requirement for practical applications is immobilization of the catalyst to an insoluble support that enables easy reuse and continuous collection of products.[103] In biocatalysis this is an extraordinary challenge since enzymes often loose their activity upon immobilization to surfaces of synthetic materials, characterized by being hard, and hydrophobic, contrary to their native cellular environment which is free suspension a soft gel-like liquid. Thus, interactions with synthetic materials often lead to loss of the enzyme structure and denaturation. Consequently, large efforts have been spent on techniques for achieving free suspension of enzymes by gentle interactions, that prevent degradation of the enzyme yet, able to store a large amount per surface area and volume.[109, 110]

Methods for enzyme immobilization onto synthetic materials ideally combine high enzyme loading (enzymes per area) and high specific activity (turnover per molecule). The material in question should make the enzymes accessible for reactants and allow for efficient evacuation of products, transported by convective and diffusive mass transfer. To optimize loading porous materials are popular, since high internal area and maximized porous volume offer increased possibility of immobilization. Examples of porous materials used for enzyme immobilization are mesoporous inorganic materials e.g. silica,[111, 112], and cross-linked gels or foams which entrap enzymes within polymeric materials.[103, 113] For all synthetic materials, the interaction between it and the enzyme needs to be considered. Enzymes are amphiphilic, which means that they are composed of both hydrophilic and hydrophobic domains.[114] Spontaneous enzyme-surface interaction may consist of predominantly hydrophobic interactions or polar at-

traction, or a combination of the two. Both hydrophobic and hydrophilic materials have been shown to reduce activity of enzymes upon immobilization. In the case of hydrophobic support materials, loss of activity is often due to an unfolding of the enzyme structure that exposes hydrophobic domains. The unfolding of the enzyme interior on the surface acts to spread the enzyme across the surface. This may act to produce an even more hydrophobic surface that may affect new enzymes immobilizing to the surface subsequently. Hydrophilic interactions with the surface may also lead to loss of enzyme activity through competitive hydrogen bonding with the hydrophilic surface, hydrophilic amino acid groups, and water. Regardless of immobilization strategy, loss of structure generally leads to lower activity but exceptions exist.[115, 116]

A general problem with high immobilization to porous or polymeric materials is achieving sufficient fluid exchange through the material. If the fluid exchange is low, efficient mass-transport that exchange products with new reactants will become a problem.

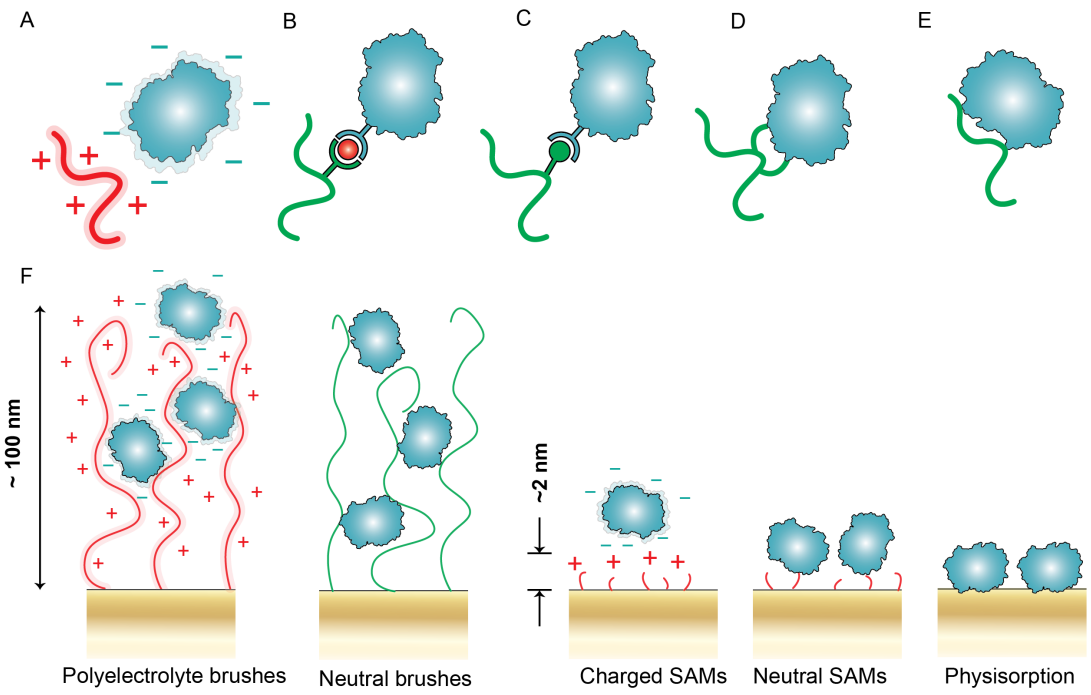

Figure 3.7: Enzyme immobilization strategies by polymer brushes: (A) electrostatic attraction, (B) ion chelation (C) affinity interaction, (D) covalent attachment, (E) hydrophobic interactions. (F) Options for enzyme surface immobilization: polyelectrolyte and polymer brushes, charged and neutral SAMs, and physisorbed enzymes on surfaces.

In this thesis enzyme immobilization was performed on polyelectrolyte brushes and SAMs by electrostatic immobilization and covalent attachment (Figure 3.7). The choice of immobilization method depends on the desired outcome and which specific enzyme that is considered.[109] Electrostatic attraction is a common and simple to use strategy for enzyme immobilization because neither the polyelectrolyte brush or the enzyme requires pre-treatment.[19, 42] However, a match between the polyelectrolyte pK_a and the pI of the enzyme is required, furthermore loss of electrostatic attraction due to changes in salt concentration or pH risks release of immobilized enzymes.[19] Affinity interactions can immobilize enzymes like metal ion chelation (e.g. histidine, Nickel, and nitriloacetic acid),[20, 51] or by various biological affinity tags (e.g. streptavidin-biotin),[54, 117, 118]. Binding by affinity requires additional steps for functionalization of polymers with the affinity tag, but with the added gain of immobilization by highly specific protein-enzyme interactions. Introduction of His-tags for metal ion affinity capture is highly effective and can store large quantities of enzymes. However, this method requires recombinant expression to add polyhistidine tag to the N-terminus or C-terminus of the enzyme, which in many cases is located close to the active site.[119, 120] Indeed, it is widely acknowledged that polyhistidine tags alter enzyme activity. When enzymes were immobilized by this method to polymer brushes a large decrease in activity per enzyme was observed.[20, 51] This highlights that it is not sufficient to immobilize enzymes to brushes to retain activity, the protein-polymer interaction used must also be sufficiently non-invasive for activity retention. Furthermore, ion-chelation requires metal ions (e.g Ni^{2+}) that may be harmful to living organisms. The binding strength of affinity tags are similar to electrostatic interactions highly dependent on pH, making release due to pH change induced by for instance biocatalytic reactions a potential problem.[53]

Covalent enzyme immobilization relies on activating the enzyme surface groups, or the polymer functional groups to form intramolecular covalent links fixating the enzyme to the brush e.g. epoxy formation,[121] glutaraldehyde,[122] and EDC/NHS[54, 123]. A primary advantage is the permanent multipoint attachment, which minimizes the risk of leaching in relation to non-covalent approaches. A disadvantage, is the lack of specificity to where on the enzyme the polymer reacts, which risks interfering with the catalytic properties of the

enzyme. The state-of-the-art in enzyme immobilization are scaffolds made of DNA origami in combination with tags that bind specific enzymes to specific sites of the DNA nanostructure.[117] A disadvantage with such structures, and flat surfaces in general is the limitation of binding only a single layer of protein. Furthermore, the proximity of the underlying surface significantly distorts the enzyme and is generally found to be detrimental to the catalytic activity, especially when physisorbed to surfaces.[124, 125]

For polymer brushes larger quantities of enzymes can be bound as Figure 3.7 suggests.[19, 20, 51] However, if retention of enzymatic activity is the end-goal, accurate quantification of enzymes within brushes is crucial to obtain the turnover rate per enzyme. This is especially important for three-dimensional materials such as polyelectrolyte brushes that are not limited exclusively by the area of the surface but which can bind enzymes in multilayers.

As a final remark it should be noted that the need of immobilization for preserving enzyme activity varies extremely from case to case.[109] Some enzymes increase their activity upon immobilization by unfolding and distortion. Enzymes may also gain higher stability, and tolerance to solvents, pH, and temperature compared to the native enzyme in solution.

3.3.3 Glucose Oxidase

Glucose oxidase (GOX) is a globular enzyme from *Aspergillus Niger* that consists of two subunits (80 kDa) of equal size. It catalyzes the reaction between D-glucose and oxygen forming hydrogen peroxide and D-glucono-lactone, (Scheme 3.8).[126]

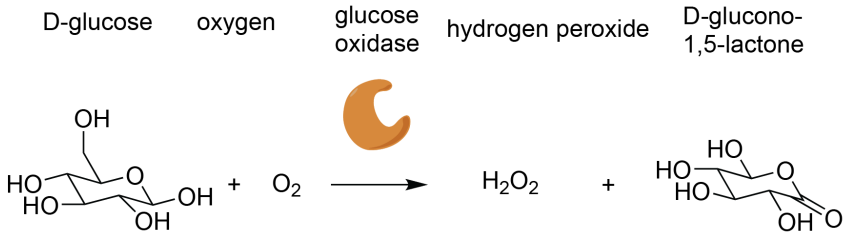

Scheme 3.8: Glucose oxidase catalyses the reaction of D-glucose and oxygen to produce hydrogen peroxide and D-glucono-lactone.

Glucose oxidase is inhibited by elevated concentrations of hydrogen peroxide, and D-glucono-lactone.[127] D-gluconolactone degrades relatively rapidly into gluconic acid which lowers the pH. With hydrogen peroxide significant inhibition of activity occurs already around concentrations of 10-50 mM. Hydrogen peroxide does not affect the two non-covalently bound cofactors flavin adenine dinucletotides but instead it causes amino acid degradation, methionine and possibly tryptophan.[128]

Glucose oxidase is a thoroughly studied and characterized enzyme.[127] A list of useful GOX properties within the context of this thesis is given in Table 3.1. Its biological function is to act as an antibacterial and anti-fungal agent since it consumes oxygen and produces hydrogen peroxide. This property has been utilized in the food industry where it is used for food preservation.[127] The most frequent and useful application of GOX is in making glucose sensors.[127, 129] Since it is a redox enzyme both electrochemical sensors and colorimetric assays have been developed for the detection of hydrogen peroxide and GOX activity.[130]

Table 3.1: Properties of GOX, a GOX has a broad activity range between 4−7,[129], b The density of proteins varies as a function of the molecular weight,[131], c under the following conditions: T = 0 °C in 0.13 M PBS, pH 5.6, 0.01 M D-glucose, ambient oxygen concentration, and for an enzyme concentration of 11.7 μM.

Property	
Molecular weight, [g/mol]	160 kDa
Isoelectric point, pI	4.2[129]
Optimal pH	5.5^a
Density, [g/cm^3]	1.35^b
Bulk activity, [s^{-1}]	17^c

3.3.4 Enzyme kinetics

Characterization of individual enzymes and their reaction kinetics helps to understand how living systems function, and why they malfunction.[98] Enzymes are also a source of inspiration for how to improve synthetic catalysts, and methods for evaluation of enzyme kinetics can be combined with genetic engineering to systematically develop enzymes with desired properties.[104] A famous model of enzyme kinetics is the Michaelis-Menten model given by the following scheme

$$\mathrm{E} + \mathrm{S} \underset{k_r}{\overset{k_f}{\rightleftharpoons}} \mathrm{ES} \xrightarrow{k_{cat}} \mathrm{E} + \mathrm{P}$$

where the enzyme, E and the substrate, S reversibly react, with a forward rate, k_f and reverse rate, k_r, to form an Enzyme-substrate complex ES.[98] The dissociation of the enzyme-substrate complex, ES is assumed to be irreversible and proceeds at a rate of k_{cat}. The reverse reaction, where E and P recombine to EP, and in turn ES, is assumed to occur so rarely, that we can ignore it. According to the law of mass action the reaction rate is proportional to the concentration of the related species, $r_f = k_f[E][S]$, $r_r = k_r[ES]$, $r_{cat} = k_{cat}[ES]$, giving us:

$$\begin{aligned}\frac{d[S]}{dt} &= -k_f[E][S] + k_r[ES] \\ \frac{d[E]}{dt} &= -k_f[E][S] + k_r[ES] + k_{\text{cat}}[ES] \\ \frac{d[P]}{dt} &= k_{\text{cat}}[ES]\end{aligned} \tag{3.18}$$

Michaelis and Menten assumed that the first reaction of the model is sufficiently rapid to be in instantaneous equilibrium with the complex meaning that

$$k_f[E][S] = k_r[ES]. \tag{3.19}$$

The total enzyme concentration is conserved since it is a catalyst, meaning that $[E]_0 = [E] + [ES]$, where $[E]_0$ is the total concentration. By insertion of enzyme conservation into Equation 3.19 and simplification it is possible to show that the reaction rate v, the rate of formation of product P, can be expressed in terms of the concentration of product S according to

$$v = \frac{\delta[P]}{\delta t} = \frac{V_{\text{max}}[S]}{[S] + K_M}. \tag{3.20}$$

Where $V_{\text{max}} = k_{\text{cat}}[E]_0$ is the maximum reaction rate and K_M is the Michaelis-Menten constant, which in the original model becomes the dissociation constant of the enzyme complex, $K_M = k_f/k_r$. An alternative assumption was proposed by Briggs and Haldane.[98] The quasi-steady-state approximation assumes that the enzyme-substrate complex concentration does not change over the timescale that product is formed giving

$$k_f[E][S] = k_r[ES] + k_{cat}[ES]. \tag{3.21}$$

The Michaelis-Menten constant is then given by

$$K_M = \frac{k_r + k_{cat}}{k_f}. \tag{3.22}$$

The Michaelis-Menten equilibrium model, is based on the assumption that equilibrium is much faster than the formation rate of the product

$$\frac{k_{cat}}{k_r} << 1. \tag{3.23}$$

While the Briggs-Haldane assumption of quasi-steady state relies on that the enzyme concentration needs to be much lower than the sum of the substrate concentration and the K_M

$$\frac{[E]_0}{[S]_0 + K_M} << 1. \tag{3.24}$$

As stated above, both models assumes the law of mass action is valid. This relies on free diffusion of reactants to the enzymes which in biochemistry is not always the case, especially within cellular environments which are often extremely crowded molecular environment, where enzymes and substrates are compartmentalized into organelles and phase separated domains, and where the cytoplasm as a whole is more reminiscent of a gel than a liquid.[132] Thus the assumption of free diffusion of reactants may be violated in several cases. In fact, the situation might be similar for enzymes immobilised into polyelectrolyte brushes. This also constitutes an environment that is highly crowded, where the assumption that reactants can freely diffuse might be inaccurate.

3.4 Surface Plasmon Resonance

A surface plasmon resonance (SPR) is produced by irradiation of light on a thin metal film, resulting in an oscillation of electrons that propagates across the metal film.[133] The conditions for producing an SPR changes due to very small changes in the refractive index near the surface of the metal film. This is useful for the detection of molecular binding events where bound matter to the surfaces produce a refractive index change.[134] Today SPR has become a standard surface sensing technique with commercial devices that has a sensitivity of 0.01 ng/cm^2. In this thesis SPR was used to characterize polyelectrolyte brushes and their ability to immobilize proteins and other macromolecules.

3.4.1 Conditions for Surface Plasmon Resonance

A surface plasmon, also called surface plasmon polariton (SPP), is produced when free electrons, mobile charges, of a metal oscillate collectively upon irradiation of light as shown in Figure 3.8.[133] The charge oscillation propagates along and is confined to the metal-dielectric interface. Associated with the

charge oscillation is an evanescent electromagnetic field which extends perpendicularly from the interface into both materials and decays exponentially with increased distance from the interface.

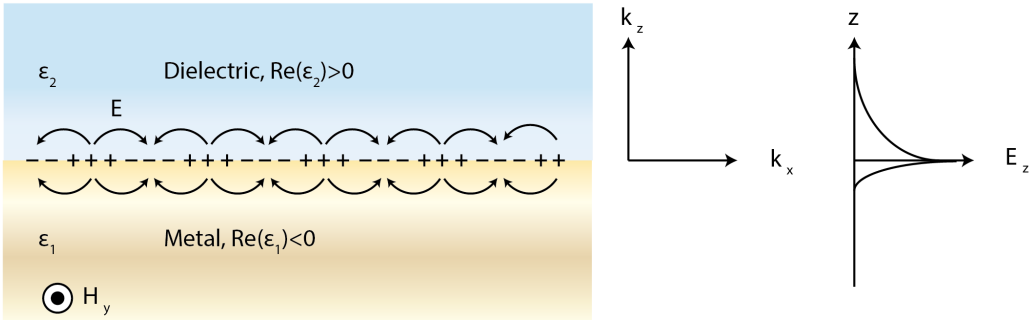

Figure 3.8: The collective oscillation of charges at the interface of a dielectric and metal is illustrated. The evanescent electromagnetic field decays exponentially as a function of lateral distance from the interface (z-direction).

A single interface between a metal and a dielectric is the most simple system capable of sustaining a SPP, illustrated in Figure 3.8.[133, 135] The dielectric function of the metal is described by the dielectric function, $\epsilon_1(\omega) = \epsilon_1^{'}(\omega) + i\epsilon_1^{''}(\omega)$ where a metal has a negative real part, $\mathrm{Re}(\epsilon_1) < 0$, and where the dielectric material has a positive dielectric constant $\epsilon_2 > 0$. If Maxwell's Equation is applied to such a system the following expressions are obtained when applying appropriate boundary conditions:

$$\frac{\mathrm{k}_{z,1}}{\epsilon_1} = -\frac{\mathrm{k}_{z,2}}{\epsilon_2}, \tag{3.25}$$

$$\epsilon_i\left(\frac{\omega}{c}^2\right) = \mathrm{k}_x^2 - \mathrm{k}_{z,i}^2. \tag{3.26}$$

Equation 3.25 and 3.26 combined gives the dispersion relation that describes how frequency of oscillation ω relates to momentum k_x for SPPs, Equation 3.27.[133]

$$\mathrm{k}_x = \frac{\omega}{c}\sqrt{\frac{\epsilon_1\epsilon_2}{\epsilon_1 + \epsilon_2}} \tag{3.27}$$

For a metal film in vacuum the dispersion relation between incident light $\sqrt{\epsilon_2}\omega/c$ and the SPP never intersect.[133] There is a mismatch in momentum and energy of light and plasmon resonance prohibiting excitation of SPPs in air

or vacuum. To excite SPPs we require some other additional means of providing momentum such that the resonance conditions are met. It turns out that using a different dielectric, a dielectric material with higher dielectric constant (refractive index since $\epsilon_2 = n_2^2$) causes an intersection between light and plasmon dispersion relations.

3.4.2 Prism coupling and evanescent field

The conditions for SPP excitation are not fulfilled directly by light irradiation on a metal surface.[133] However, the mismatch in energy and momentum between incoming light and the SPP dispersion relation may be overcome by using a dielectric material with higher dielectric constant. Prism coupling, also called Attenuated Total Reflection (ATR) coupling shown in Figure 3.9 makes use of this. If light is irradiated at an angle, θ_0 through a prism of for instance silica and is reflected at the metal/prism interface then the projection on the metal surface is given by Equation 3.28.

$$\mathrm{k}_x = \mathrm{k}\sqrt{\epsilon_0}\sin(\theta_0) \tag{3.28}$$

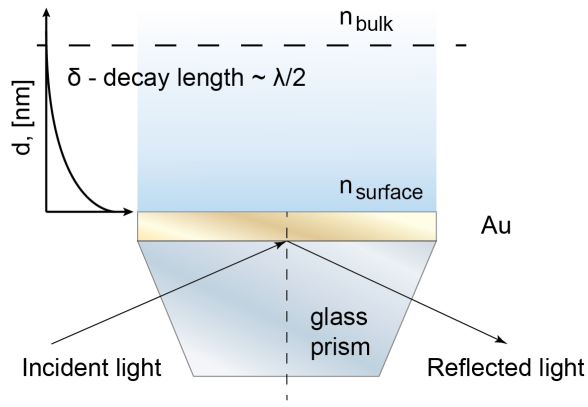

Figure 3.9: Configuration of SPR where a high refractive index prism is used to compensate for the mismatch between photon and plasmon resonance dispersion relations.

One method of ATR coupling is the Kretschmann configuration where a thin metal film is deposited on a glass prism.[133] The Kretschmann SPR design

is a common experimental set-up, used in this thesis. An alternative to ATR techniques is grating-coupling where a periodic roughness on the metal surface leads to excitation of SPPs.

The lateral distance to which refractive index changes are detected, is confined within an electromagnetic field produced by the SPR. The field extension only stretches a few hundred nanometers perpendicularly away from the metal film making SPR a highly surface sensitive refractometric detection technique (Figure 3.9). But the restriction of the volume caused by the evanescent field is there regardless of if there is a gold film that produces plasmon resonances or not. It is there because light is incident at an angle exceeding the total internal reflection (TIR). The exponential decay of the evanescent field is not only useful for SPR but also for microscopy where the aim is to study a very small volume. Microscopy performed under TIR restricts the sample volume to include only a small number of molecules, present near the surface. This microscopy technique is known as Total Internal Reflection Fluorescence (TIRF) microscopy, only fluorophores within the evanescent field are excited enabling characterization of only fluorescent molecules within the evanescent field at a given point in time.

3.4.3 The SPR spectra

A method to detect the SPR is to scan the surface through many angles while simultaneously recording the reflectivity (Figure 3.10).[133, 136] At some angle of incidence (θ_{SPR} in Equation 3.28), beyond TIR, the SPR is excited. The surface plasmon resonance is identified as a sharp minimum in reflectivity as a function of the incident angle of light. If a change in the refractive index of the sample occurs this changes the coupling conditions between the incident light and the SPR, i.e. it changes at what conditions SPR excitation is observed. However, the SPR angle alone cannot distinguish between surface-specific refractive index changes and bulk liquid refractive index changes. To make this distinction the bulk refractive index needs to be measured.

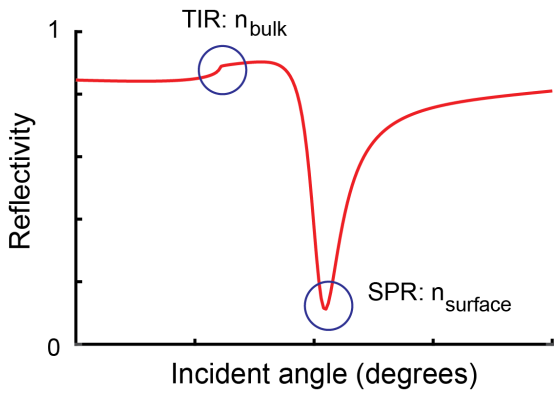

Figure 3.10: SPR spectra where reflectivity is shown as a function of incident angle of light. In the spectra the angle of total internal reflection (TIR), which provides knowledge of the bulk liquid refractive index n_{bulk} and the angle of surface plasmon resonance (SPR) which detects the local refractometric index, $n_{surface}$ in the nanoscale vicinity of the metal surface are highlighted.

In addition to the surface plasmon resonance angle the TIR angle is also obtained when measuring SPR in angular scan mode identified by a sharp increase of reflectivity as a function of increasing incident angle (Figure 3.10). The conditions for TIR is in general given by Snell's law,[136] which states that when light with incident angle, θ_i, reaches a planar interface of two materials with refractive index n_1 and n_2, it may be transmitted with an angle, θ_r according to

$$n_1 \sin\theta_i = n_2 \sin\theta_r. \tag{3.29}$$

However, if light passes through material 1, with a higher refractive index compared to the material opposite of the interface such that $n_1 > n_2$, it will at some critical angle of incidence, θ_c , reach TIR according to

$$\theta_c = \arcsin\left(\frac{n_2}{n_1}\right). \tag{3.30}$$

When the value of the refractive index is known for the material in which light is internally reflected, n_1, this allows for the determination of the unknown bulk refractive index of the unknown medium, n_2. As Figure 3.10 shows, when angular scans technique is used within a range that covers both the TIR and the SPR, we can distinguish between surface refractive index changes and solution refractive index changes.

3.4.4 Fresnel models of the SPR spectra

Fresnel models simulate the SPR spectra (Figure 3.10) where the thickness and refractive index of the molecular layer are two parameters incorporated into the Fresnel coefficient matrix.[136] When light travels through a planar interfaces of materials with different refractive indexes such as in a Kretschmann SPR sensor configuration, light may either be reflected, transmitted or both. Fresnel coefficients determine the relative proportion of the light that is reflected or transmitted (Equation 3.31 and 3.32). The coefficients assume a value in between 0 and 1 which depends on how light is polarized in relation to the interface. Since SPPs are excited by p-polarized light we only need to consider coefficients for p-polarized light.

$$\mathrm{F}_{rp} = \frac{\mathrm{n}_1 \cos\theta_t - \mathrm{n}_2 \cos\theta_i}{\mathrm{n}_1 \cos\theta_t + \mathrm{n}_2 \cos\theta_i} \tag{3.31}$$

$$\mathrm{F}_{tp} = \frac{\mathrm{n}_1 \cos\theta_i}{\mathrm{n}_1 \cos\theta_t - \mathrm{n}_2 \cos\theta_i} \tag{3.32}$$

Figure 3.11 illustrates a single layer in which light is reflected and transmitted through. For the topic of this discussion we are interested in cases where the distance d is small in comparison with the beam width and the light coherence length.[136] Such circumstances introduce coherence effects where the effective Fresnel coefficients are given by Equation 3.33 and 3.34.

$$\mathrm{F}_r = \frac{\mathrm{F}_{r,12} + \mathrm{F}_{r,23} e^{i2\mathrm{k}_0 \mathrm{d} \mathrm{n}_2 \cos\theta_2}}{1 + \mathrm{F}_{r,12}\mathrm{F}_{r,23} e^{i2\mathrm{k}_0 \mathrm{d} \mathrm{n}_2 \cos\theta_2}} \tag{3.33}$$

$$\mathrm{F}_t = \frac{\mathrm{F}_{t,12} + \mathrm{F}_{t,23} e^{i2\mathrm{k}_0 \mathrm{d} \mathrm{n}_2 \cos\theta_2}}{1 + \mathrm{F}_{t,12}\mathrm{F}_{t,23} e^{i2\mathrm{k}_0 \mathrm{d} \mathrm{n}_2 \cos\theta_2}} \tag{3.34}$$

For the calculation of Fresnel coefficients we utilize Snell's law, Equation 3.29.[136] Also, in addition to the relative intensities of reflected and transmitted light we may obtain the new angles of refraction in each new material through Equation 3.35.

$$\theta_{j+1} = \mathrm{Re}\Big(\arcsin\Big(\frac{\mathrm{n}_j}{\mathrm{n}_{j+1}} \sin\theta_j\Big)\Big) - i\Big|\mathrm{Im}\Big(\arcsin\Big(\frac{\mathrm{n}_j}{\mathrm{n}_{j+1}} \sin\theta_j\Big)\Big)\Big| \tag{3.35}$$

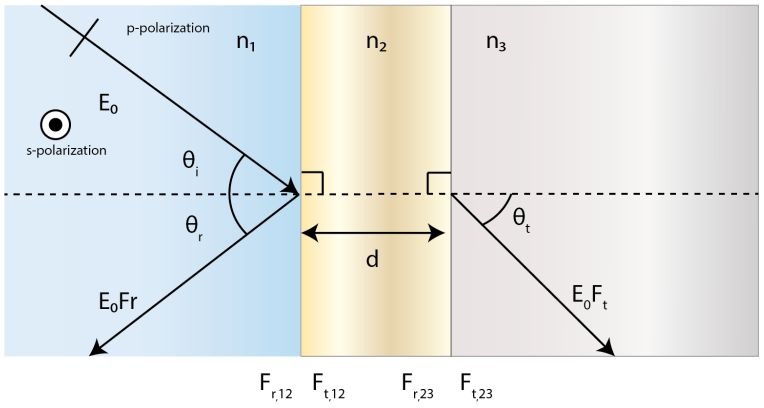

Figure 3.11: Reflection and transmission of incident p-polarized light for wavelengths larger than the distance d of material 2.

Equations 3.33 and 3.34 describe the case shown in Figure 3.11 where a single layer is considered, a system with three materials and two interfaces.[136] However, the SPR sensor is composed of more than one layer. To model the SPR spectra shown in Figure 3.10 requires a method to calculate angle of refraction and relative intensities of light in many layers in a systematic way. The matrix transfer method, Equation 3.36 is useful for calculating reflection and transmission of light travelling in an arbitrary number of layers and is given by Equation 3.36.

$$\Phi = \Pi_{j=2}^{m-1}\left(\frac{1}{\mathrm{F}_{t,[m-1]m}}\begin{bmatrix} 1 & \mathrm{F}_{r,[j-1]j} \\ \mathrm{F}_{r,[j-1]j} & 1 \end{bmatrix} \times \begin{bmatrix} e^{-i\mathrm{k}_0\mathrm{d}_j\cos\theta_j} & 1 \\ 1 & e^{i\mathrm{k}_0\mathrm{d}_j\cos\theta_j} \end{bmatrix} \times \frac{1}{\mathrm{F}_{t,[m-1]m}}\begin{bmatrix} 1 & \mathrm{F}_{r,[m-1]m} \\ \mathrm{F}_{r,[m-1]m} & 1 \end{bmatrix}\right) \tag{3.36}$$

The output of calculating Equation 3.36 becomes Fresnel coefficients produced for a set of refractive indexes and thicknesses of the layers included in the model.[136] A representative example of a commercial SPR sensor which consists of a glass substrate, a chromium adhesive layer, the sensor gold surface, which is coated with a SAM that anchors a polymer brush in air (Figure 3.12). By inserting the thickness of each layer and the corresponding refractive index, the reflectivity Fresnel coefficients are calculated as a function of the incident angle using Equation 3.36.

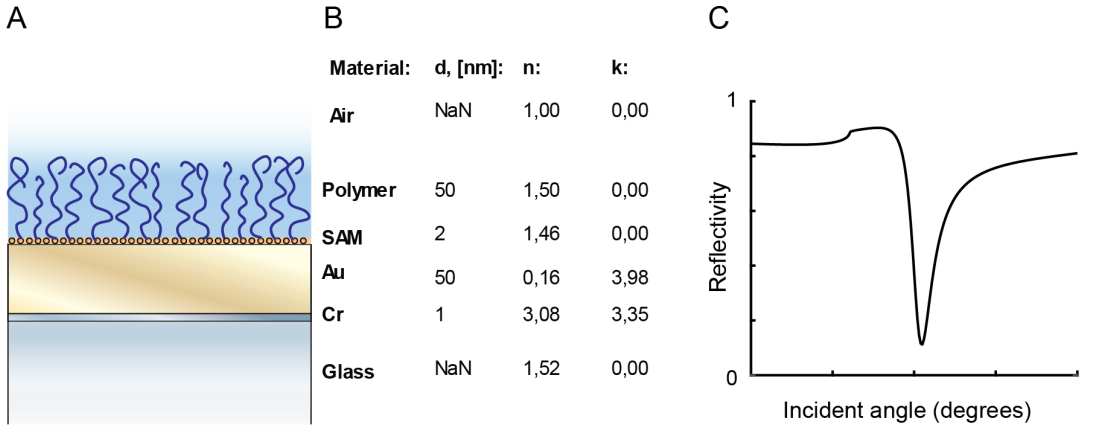

Figure 3.12: Model of commercial SPR sensor coated with a polymer brush where, (A) shows a schematic of each of the different layers, (B) shows an example model with thicknesses and refractive index of each layer, (C) shows the output result from calculation of the reflectivity as a function of incident angle.

Fitting of the Fresnel SPR model to experimental values can be used to determine the refractive index or thickness of a specific layer. However, if several parameters are unknown a well-defined solution cannot be obtained.[35] In this case the experiment needs to be re-designed such that a unique solution can be obtained.

3.4.5 Non-interacting Probe Method

SPR is a powerful technique for analyzing molecular coverage when information about the size of the molecular layer or the refractive index properties are well known.[134, 137] However, SPR measurement when the refractive index and thickness of the molecular layers are unknown become problematic.[35] Polymer brushes which contain high volume fractions of solvent e.g. PNIPAAM, PEG or polyelectrolyte brushes are primary examples: the effective refractive index of the layer and the thickness of the molecular layer are convoluted. The non-interacting probe method enables simultaneous determination of refractive index and height of molecular layers without the need to make assumptions of either parameter to estimate the other.[22, 35]

Any method that utilize the non-interacting probe method relies on finding a macromolecule, or nanoscale object, that: (i) Does not bind to the brush.

(ii) Is sufficiently large to be kinetically hindered from entering the brush, thus completely expelled from the brush. (iii) Sufficiently aqueous soluble. (iv) Furthermore it must have a sufficiently high refractive index increment as function of concentration that it permits its detection in the bulk. The lack of binding to the sensor surface, is manifested through a proportional shift between the SPR and TIR angle, Figure 3.13 A. This is further verified by a linear slope when the SPR signal is plotted against the TIR signal with minimal hysteresis as a result, Figure 3.13 B.

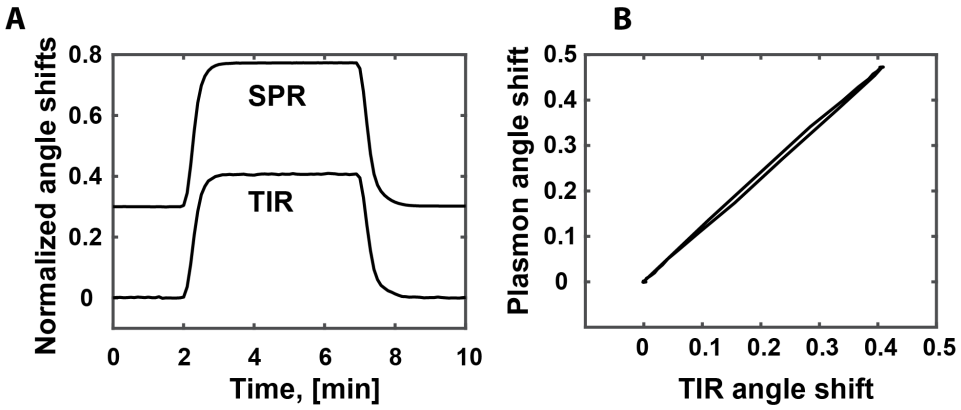

Figure 3.13: Non-interacting probe injections in an SPR experiment where (A) shows SPR and TIR angle shifts shown as function of time when injecting a higher refractive index liquid and (B) shows normalized SPR signal plotted as a function of TIR angle signal.

The presence of a non-interacting probe shifts the SPR spectra proportionally due to bulk liquid refractive index and the surface refractive index changes (Figure 3.14 A). In these two spectra the polymer brush is unchanged, only the bulk solution refractive index is different due to the absence or presence of the non-interacting probe. This can be exploited to generate a set of Fresnel models with different refractive index and brush height values (n_i,h_i). These pair values, produce a unique solution upon comparing the spectra with and without the probe. The unique value for the refractive index and brush height can be graphically represented, shown in Figure 3.14 B.

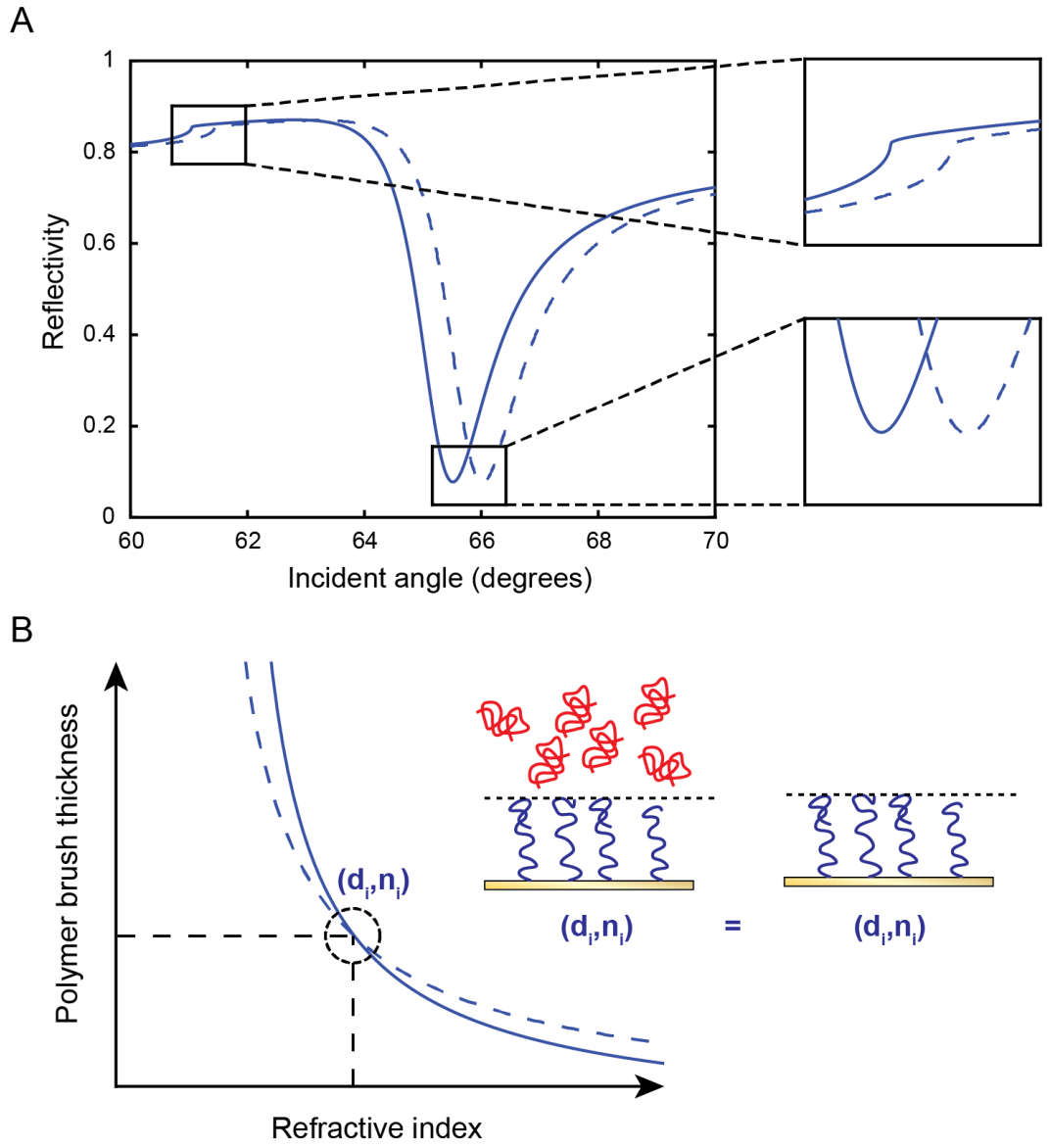

Figure 3.14: Brush height determination by non-interacting probes where (A) shows solution induced refractive index change of the SPR spectra (both the TIR angle and the SPR angle shift proportionally), (B) shows the unique intersection that determines the polymer brush height and refractive index.

In this thesis we require the brush heights of polyelectrolytes. Ideally, these requirements hold at both high and low pH, such that the brush thickness in both the neutral and charged state can be determined using a single non-interacting probe, as shown in Figure 3.15.

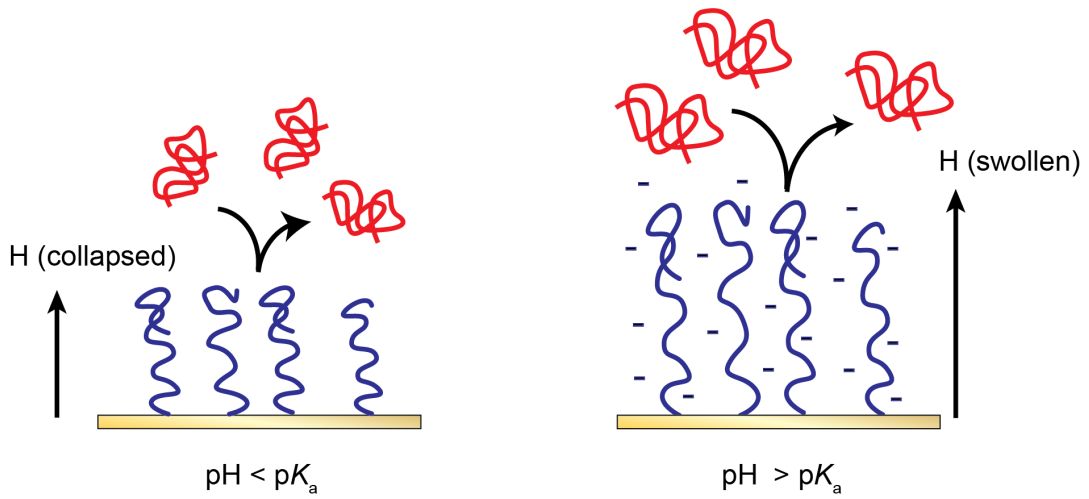

Figure 3.15: Requirement for a non-interacting probe exemplified for polyacidic polyelectrolyte brush, the probe should resist binding to the polyelectrolyte brush in both neutral and charged state.

3.4.6 Alternative methods

Several approaches using refractometric techniques have been used to determine brush heights, many of which estimate the wet brush thickness with SPR or ellipsometry by making certain parameter assumptions related to the refractive index of the polymer brush layer.[29, 31, 32, 34, 73, 138] With such methods there is a risk that the brush height is incorrectly defined due to invalid choice of refractive index. Even if the refractive index is included in the fitting procedure, the problem of not finding a unique solution for both the hydrated brush refractive index *and* height remains. Two alternative methods (other than the non-interacting probe method that employs Fresnel calculations studied in this thesis) have been developed to determine the hydrated polymer brush: the non-interactive probe technique without Fresnel calculations, and the $\delta n/\delta c$ method.

The non-interacting probe method without Fresnel models introduces a model surface where the brush is replaced by a well-defined molecular layer, e.g. a SAM of OEG thiols, where the refractive index and height is known.[35] The reference surface is used to determine two parameters, the sensitivity (S [angular degree shift per unit of refractive index]), and the decay length of the evanescent field, (δ [nm^{-1}]), and uses these to estimate the brush height and refractive index. The SPR response is given by,

$$\mathrm{R} = \mathrm{S}(\mathrm{n}_b - \mathrm{n}_0) \times (1 - \exp(-2\mathrm{d}/\delta)), \tag{3.37}$$

where n_b and n_0 are the refractive index of the brush and the bulk liquid respectively, d is the brush thickness and delta is the decay length of the evanescent field. By re-arrangement of Equation 3.37 the brush thickness of interest, d_2 in Equation 3.38 is determined by the quotient of the SPR response between the reference surface and the unknown surface of interest.[139, 35]

$$\mathrm{d}_2 = \frac{\delta}{2} \log\left(\frac{\mathrm{R}_1}{\mathrm{R}_2}\right) + \mathrm{d}_1 \tag{3.38}$$

A limitation of Equation 3.38 is it assumes that the modelled film has a uniform refractive index only slightly exceeds the bulk solution (1.33-1.4).[35] First, brushes do not have a uniform refractive index. Secondly, even within this refractive index range an error of 15% in absolute error can be expected. Equation 3.38 can provide wet brush heights to a reasonable degree in highly hydrated polymer layers like PEG brushes which contains 90% water.[35, 140] However, for layers with higher refractive index of stimuli-responsive polymer brushes such as those considered in this thesis it becomes invalid.[22] Thus, non-interacting probe method with Fresnel models, which determines the brush height and the refractive index without requiring S and δ is more suitable for non-interacting particle measurements over a broader range of refractive indexes.

The other alternative method investigated uses the refractive index increment as function of polymer concentration ($\delta n/\delta c$).[19, 141] The mass surface coverage of the dry polymer brush (Γ), the brush (n_b) and bulk (n_0) refractive index to calculate the brush thickness, d_b according to

$$\mathrm{d_b} = \frac{\frac{\delta n}{\delta c} \times \Gamma}{n_\mathrm{b} - n_0}. \tag{3.39}$$

The refractive index as function of concentration is either obtained from literature or easily determined using a refractometer or by an angular scan SPR system that can measure TIR. Similar to the non-interacting probe method without Fresnel model, use of Equation 3.39 inaccurately assumes that the polymer brushes constitute a homogeneous polymer layer with uniform density with respect to lateral distance to the surface.

3.5 Quartz Crystal Microbalance

Quartz Crystal Microbalance with Dissipation monitoring (QCM-D) is a technology that can measure processes that occur on surfaces with very high sensitivity.[142] Unlike SPR, QCM-D is not an optical sensing method but a weighing device that operates by a mechanism called piezoelectricity. Piezoelectricity is the transduction between a mechanical perturbation that produces an electrical field. Or conversely, when an electrical field is applied across a material it induces a movement of the material. Crystals cut along the crystallographic axes of the quartz start to oscillate at a resonance frequency when an alternating current (AC) electrical field is applied across the crystal. Specifically, the oscillation starts when the applied voltage frequency strikes the resonance frequency of the crystal. The Sauerbrey relationship relates the absorbed mass on the sensor surface, Δm, is then linearly related to the shift in the resonance frequency,

$$\Delta m = -(\mathrm{C_{QCM}}/\mathrm{n})\Delta f. \tag{3.40}$$

where $\mathrm{C_{QCM}}$ = 17.7 $\mathrm{ng\ cm^2\ Hz^{-1}}$ at f = 5 MHz), is called the mass sensitivity constant and n denotes the overtone number of the resonance oscillation. The use of the Saurebrey relationship relies on the deposited mass to be rigid in its conformation on the surface, say for instance an inorganic oxide.[142] The relationship also holds for stiff molecular layers bound to the surface e.g. self-assembled monolayers of alkane thiols. But when the deposited material is flexible, such as a polymer brush, the oscillation of the crystal will not induce a simultaneous response in the polymer film. Since the soft polymer film is viscoelastic it deforms under shear stress, and dissipates energy as the surface oscillates. Under such circumstances the linear relationship between frequency and mass changes are not applicable. In addition hydrophilic polymer materials in water will hydrate and trap water within its structure thus coupling water to the surface and if charged in addition to this coordinate counter-ions (and with these more water) into the polymer film. Thus the sensed mass of the crystal surface includes not only the "dry" polymer weight but all the mass associated with the viscoelastic polymer film. Since in this thesis hydrophilic polymer brushes are mainly considered the Saurebrey relation cannot be used. But the viscoelas-

tic properties of the polymer film can still be measured. The dampening effect due to dissipation losses of the viscoelastic film, e.g. the polymer brush, that occur due to its flexible and hydrophilic properties is described as

$$D = \frac{1}{Q} = \frac{\mathrm{E_{dissipated}}}{\mathrm{E_{stored}}}. \tag{3.41}$$

Where D, dissipation is the quotient between dissipated and stored energy. QCM-D is a further development of the QCM technique that rapidly and simultaneously measure, both f and D. Experimentally f and D are determined by fitting a numerical function to the exponentially dampened sinusoidal oscillation that is recorded when the resonance of the quartz crystal is disconnected, where D is defined as

$$D = \frac{1}{\pi f \tau}. \tag{3.42}$$

With QCM-D measurement data of f and D together with a theoretical representation, properties of the viscoelastic film such as layer height, density, or water content can be modelled.[142] The theoretical representation is often a Voigt model for which, the parameters included are, the film and bulk solvent viscocity, density, and in addition to the thickness and elastic modulus of the film. In this thesis quantitative analysis of the QCM-D data was not performed, the Voigt model will not be described in detail, but it is important to point out that such a characterization is possible. Another important remark is that QCM-D measurements alone can rarely provide the necessary data to accurately model the polymer film, complementary techniques, such as SPR, ellipsometry, AFM are important, and experimental material values for density and dynamic viscocity are required for the model to produce reliable results. An approximation often made in the viscoelastic model is that the film layer has uniform density, similar to the decay length model of SPR. This does not reflect the real parabolic density profile of polymer brushes and it is a shortcoming of the model.

Although quantitative analysis from QCM-D experiments were not made, qualitative interpretations were extensively used to study biomolecular interactions with polymer brushes and polymer brushes transitions in response to external stimuli. Throughout this thesis QCM-D is used to monitor protein immobilization and stimuli-response switching of brushes in real-time.

3.6 Electrochemistry

Electrochemistry describes the relationship between chemical and electrical change.[143] The field of electrochemistry is large as it encompass many technologies, from digital displays to batteries and fuel cells, and it is central to the description of many natural phenomena such as corrosion and how signals are transmitted through the neural system. In general, the study of electrochemical processes involves transport of charged species across an interface of chemical phases. Most often, the two chemical phases are a solid electrode and a liquid electrolyte. The electrode conducts current in the form of electrons (and holes), while in the electrolyte charges are transported by ions, charged atoms and molecules. The charge transfer between the electrode and electrolyte is either spontaneous, galvanic, or electrolytic (driven by supply of external electrical energy). Here we consider the latter case, electrochemical reactions that result from applying a variable or constant potential.

3.6.1 Electrochemical cells

To facilitate the study of electrochemical processes one usually divides an electrochemical system into electrochemical cells.[143] Even though there are generally two or three electrodes immersed into the electrolyte it is simpler to focus on one electrochemical process at the time. The working electrode is the electrode on which the electrochemical process of interest occurs, and the secondary electrode is called the counter electrode. A schematic representation of a three electrode set-up is illustrated in Figure 3.16. Three-electrode set-ups are used to introduce a reference electrode, to be able to accurately, consistently, and repeatably set a specific voltage between the working and counter electrode. As Figure 3.16 shows the working electrode is coupled with the reference electrode of a known potential. Appropriate choice of the reference electrode material and programming of the potentiostat ensures that only a minor proportion of the current is passed, enough to allow the voltage to be controlled accurately. A common choice of reference electrode are silver/silver chloride (Ag|AgCl) electrodes. These electrodes are suitable as reference electrodes as they are simple to maintain, easy to make by home fabrication, and commercially abundant.

The counter electrode is ideally a material with inert properties and with a large surface area in relationship to the working electrode.

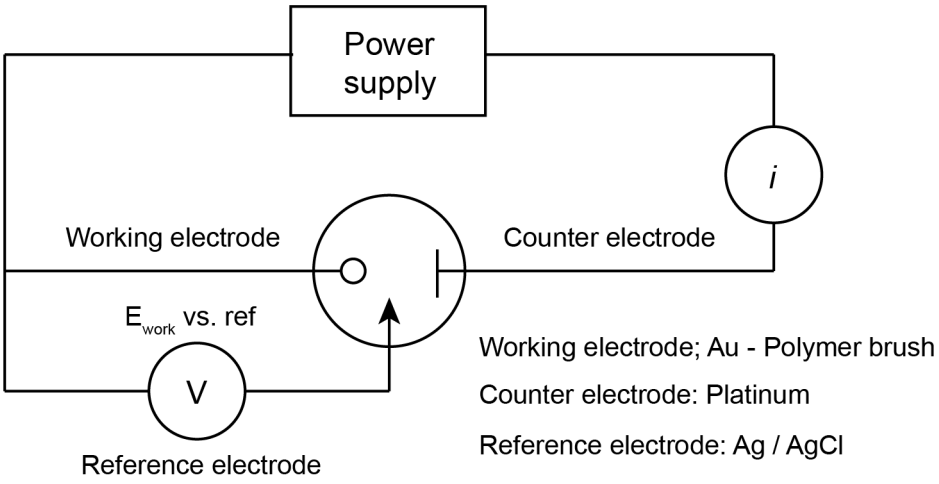

Figure 3.16: Schematic of a three-electrode set-up.

3.6.2 Oxidation reactions that produce protons

This thesis investigates methods for changing the pH locally on surfaces. One convenient method for accomplishing this is to utilize conductive surfaces that can act as electrodes. There are many electrochemical reactions that produce or consume protons. Electrochemical signals can be used to drive these electrochemical reactions resulting in a temporary pH gradient at the vicinity of the electrode surface throughout the duration of the electrochemical potential.

When a negative potential is applied to an aqueous acidic solution oxygen is reduced producing water or hydrogen peroxide according to:[59]

$$\mathrm{O_2 + 4H^+ + 4e^-} \longrightarrow \mathrm{H_2O}$$

$$\mathrm{O_2 + 2H^+ + 2e^-} \longrightarrow \mathrm{H_2O_2}.$$

Water forms already when a potential of -0.5 V vs. (Ag|AgCl), is applied, and for even larger negative potentials, -1.0 V both water and hydrogen peroxide are formed. In general, water contains dissolved oxygen (0.3 mM at ambient conditions), which makes these reactions a useful tool for electrochemical increase of the pH. The reactions have been performed on carbon, indium tin oxide and other conductive materials, which makes them a convenient electro-

chemical reaction for producing locally increased pH on a variety of different electrodes.[144, 145, 146, 59] Use of the same reactions, but driving them in the reverse direction, to locally decrease the pH at the electrode surface is much more challenging. Electrochemical water splitting typically requires noble metals such as platinum and palladium as catalysts.[147]

To achieve local reduction in pH by an electrochemical process, an additional molecule, a reduction agent that in the process of donating an electron also sheds a proton, is required.[146] But, even then conventional molecules might be unsuitable. Methanol oxidizes to produce hydroxonium ions, but this reaction is kinetically hindered and proceeds too slowly in ambient conditions without a catalyst. The ideal molecule readily donates protons and is non-toxic for optimal utility in applications.

In living systems there are many small molecule reduction agents. An obvious example is NADH which is a reduction agent in cellular metabolism. A possible limitation of NADH is that electron transfer within the cell occurs as a co-factor in enzymatic reactions. However, there are even simpler reduction agents such as ascorbic acid and signalling substances such as dopamine that readily participate in electrochemical reactions. Scheme 3.9 shows a selection of biologically occurring molecules which all produce protons upon oxidation. Some of these molecules spontaneously oxidize even without electrochemistry in aqueous solutions. Most, are known to, at relatively low concentrations 1 mM, oxidize at the electrode interface upon application of a relatively small positive potential (+0.2 to +0.5 V).[146, 148]

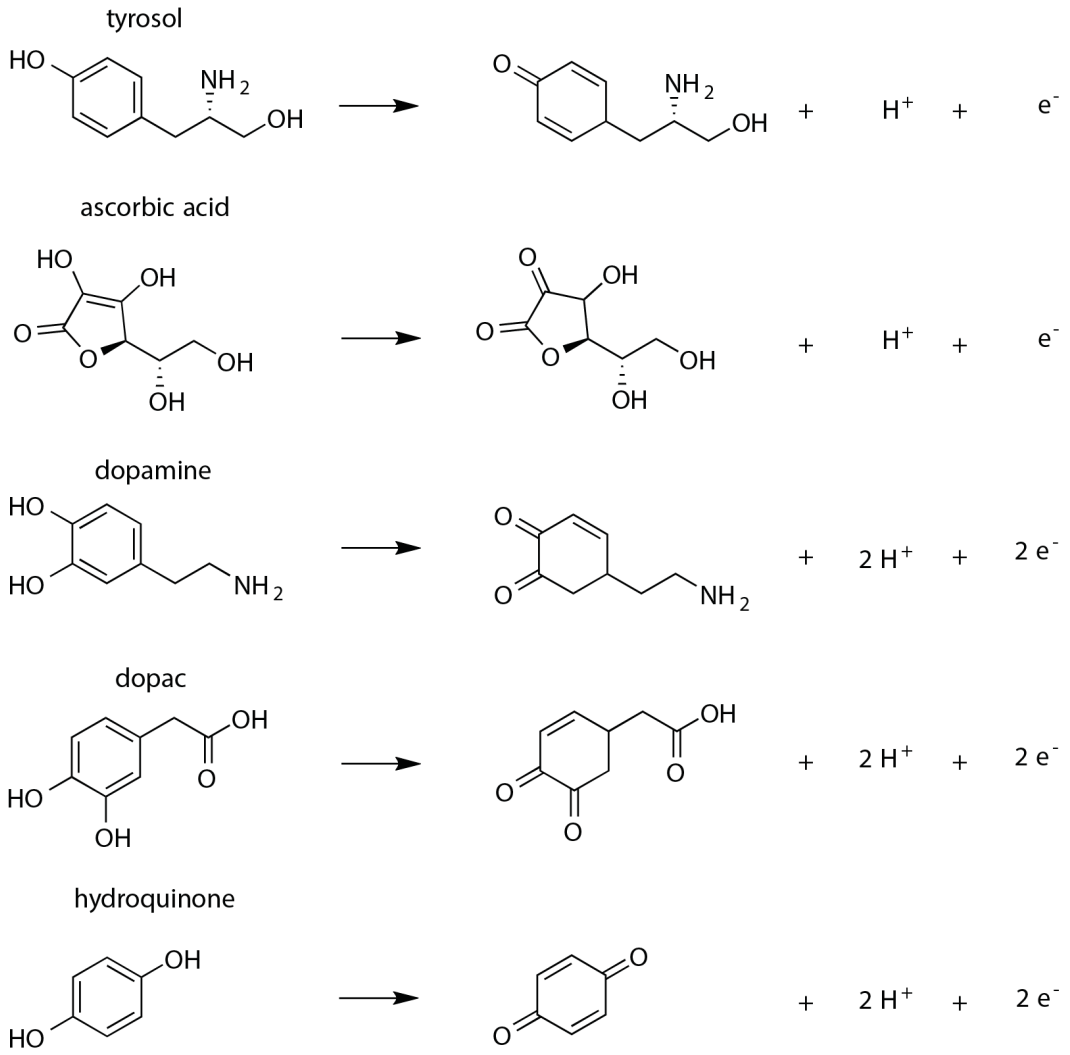

Scheme 3.9: Selection of biologically occurring molecular reduction agents which produce protons upon oxidizing.

Scheme 3.9 shows how oxidation results in loss of proton(s) in addition to electrons, when hydroxyl bond breaks, resulting in formation of a carbonyl bond and by electron pair rearrangement within the aromatic benzene ring. Some of the molecules, dopamine, dopac, and hydroquinone contain more than one hydroxyl group. This enables multiple oxidations per molecule and release of multiple protons making these molecules potent for pH reduction.

In summary, the most straightforward practical method for producing a proton gradient by electrochemistry is to reduce oxygen to produce water or hydrogen peroxide by applying a negative potential resulting in a basic pH gradient. But there are also several molecular candidates for producing an acidic proton

gradient at the electrode surface. Many of which exists in living biological systems.

4

Experimental

Here a summary of the experimental techniques and methods, used in the appended papers is given. The aim is to share key experimental knowledge required to produce the results. It will not repeat experimental information, for specific protocols, quantities or instrument setting used the reader is referred to the appended papers. Instead I will describe recipes and techniques in general, and motivate choices and strategies taken relative to other options.

4.1 Surface chemistry

Three different methods for chemical surface functionalization were considered: (1) self-assembly of thiols, (2) silanization, and (3) diazonium salt deposition. For all methods it is possible to deposit thin, well-defined layers. However, each method has some distinct advantages depending on what interface is synthesised and the intended application. The Schemes shown in this section emphasize the chemically modified surface, eventual side-products are omitted for clarity.

4.1.1 Thiol self assembly

Alkane thiols are amphiphilic molecules that spontaneously bind to metal surfaces to form a self-assembled monolayers (SAM) on the surface.[149] The thiol head group binds forming a metal-thiol bond that anchors the alkanethiol to the surface. As increasing number of thiols bind to the surface the thiols begin to stack by self-assembly into a two-dimensional layer on the surface. The other end of the alkane chain, opposite of the thiol, can be synthesized to contain a large variety of different chemical groups. The relative ease of preparation of self-assembled alkane thiols layers combined with many different areas of ap-

plication has made them a popular strategy for surface functionalization. For instance in this thesis I used commercially available alkane thiols that contain a tertiary bromine end group for use as initiator for ATRP, see Scheme 4.1.[26, 63]

The standard choice of substrate is gold, it is historically the most studied SAM substrate and there are several reasons for why.[149] Gold is practical because it is relatively inert in ambient conditions, it does not form oxides below its melting point and does not react with oxygen at ambient temperatures. Thus SAMs on gold are conveniently prepared without the need of inert atmosphere or under vacuum conditions compared to other substrate materials. Although metal oxides also forms SAMs the reaction mechanism is more complex at the expense of the SAM quality. Another advantage with gold substrates is the high affinity of thiols for gold and that SAMs formed on gold are known to be relatively stable over time. Compared to other metals and oxides such as silver where the SAM has been observed to rapidly degrade by oxidation when stored in air.[149] Therefore, although SAMs can technically be prepared on other materials than gold, in this thesis I chose to prepare alkanethiol SAMs on gold.

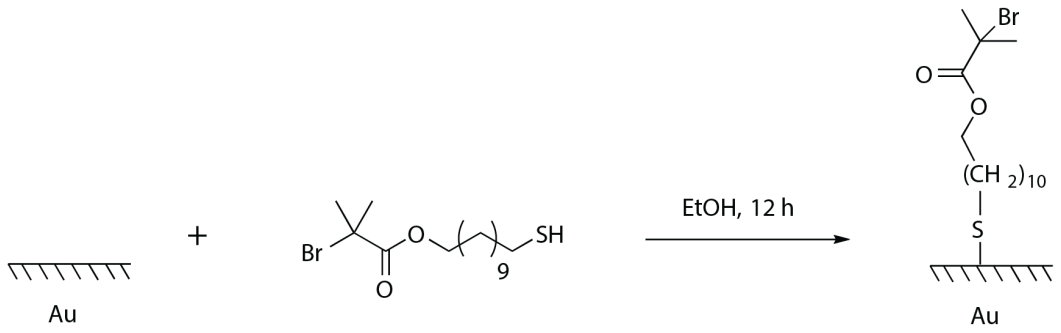

Scheme 4.1: Thiol bond formation to a gold surface in ethanol.

A common method of forming SAMs is shown in Scheme 4.1.[149] It requires a clean gold surface, which can be obtained by a chemical wash protocol (e.g. pirahna wash) or plasma cleaning (e.g. oxygen plasma) of the surface. Immediately after cleaning and rinsing in water and ethanol the surface is exposed to approximately 1 mM of alkane thiol dissolved in ethanol. The self-assembly process proceeds on a timescale of hours. After 12 hours the surface is rinsed in ethanol and ready for use or for a subsequent functionalization step.

Alkane thiol SAMs desorb from gold upon application of electrochemical po-

tentials.[150, 60, 149] In aqueous solution the electrochemical stability window of SAMs on gold was found to be between −0.8 V and +0.4 V. [60]. In addition, when the pH is lower the reductive potential required to break the thiolate (Au-S) bond becomes considerably higher in value, by up to −0.5 V, which narrows the stability window considerably.[151] A thiol anchored polyelectrolyte brush are unsuitable for electrochemical applications, like those we explore in Chapter 5.5, because it is highly likely to de-graft even within small potential windows.[57] The electrochemical instability at low pH is unsuitable since the purpose with working with weak polyelectrolyte brushes is to be able to change the pH. Although electrochemical desorption of thiol SAMs are considered to be a disadvantage in this context, several clever methods for electrochemical release of molecules and even entire cells have been devised that utilize electrochemical thiol desorption.[152, 153]. Table 4.1 summarize some of the advantages and disadvantages of thiol self-assembly.

Advantages	**Disadvantages**
Simple protocol	Electrochemically unstable
Robust	Works best on gold
Stable in air	
Self-assembly favors monolayer	

Table 4.1: Summary of advantages and disadvantages of thiol surface chemistry

4.1.2 Silanization

Silanization is the reaction between a silica substrate surface with an organosilane, an organic molecule containing a silane functional group e.g. 3-aminopropyl triethoxysilane (APTES).[154, 155] As shown in Scheme 4.2, the silica substrate reacts with the APTES silane forming siloxane bonds O−Si−O. Silanization is generally agreed to occur by two steps.[156, 154] In the first step the etoxy group of the silane undergoes hydrolysis with surface bound water or with trace amounts of moisture in the gas phase, or from water in the solvent. In the second step the siloxane bond binds covalently to surface exposed hydroxyl groups on the silica surface. Silanization is more difficult to control than preparing an alkane thiol SAM because silanization is not a self-assembly process.[154, 157]

It is not self-limiting and does not necessarily become an ordered two dimensional layer. Many protocols for silanization of alcoxysilanes have been developed to address the challenge of forming well-defined molecular layers of silanes.[158, 159, 154, 160, 157, 156]

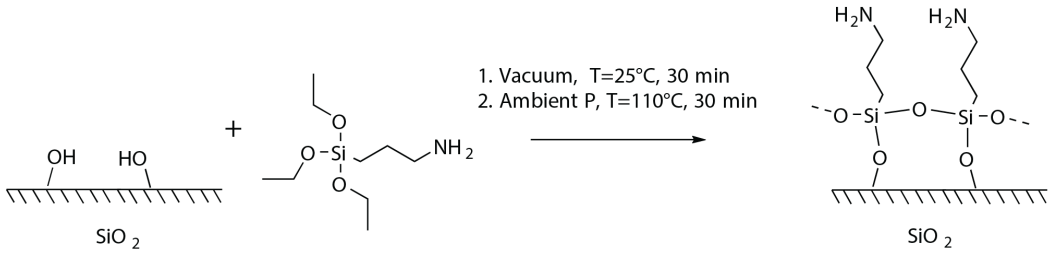

Scheme 4.2: Silane vapor deposition performed in two steps, first a hydroxylactivated silica surface was exposed to a vapor of APTES in vacuum, followed by annealing of loosely bound APTES on the surface.

Multiple different versions of silanes have been tested and there are examples where engineering of the silane functional groups can benefit the quality of the silanization. Apart from altering the silane functional group, the functional group at the opposite end of the organosilane is known to affect silanization. For instance, the amine functional group of APTES has been suggested to bind to the silica surface and to promote the formation of disordered multilayers of silane molecules on the surface.[157] However, the presence of water is probably the most challenging aspect of silanization since it is necessary to initiate the silane layer reaction, but in too large quantities it causes uncontrolled polymerization producing a rough surface with multilayers of silane molecules. This is critical for silanization in solution since even trace amounts of water in the solution can trigger uncontrolled polymerization of APTES already in solution.[156] Therefore, protocols for solution phase deposition involve careful removal of water and drying of the solvent. Silanization can also be performed under vaccuum.[159] This allows for a more controlled deposition with minimal siloxane polymerization since it is easier to remove humidity in a vaccuum chamber. There is no established consensus on which is the best method for silanization for or achieving a uniform and close to monolayer of APTES.[160, 158] Vacuum deposition is generally found to be the preferred method if monolayer deposition is the intended outcome of the chemical modification. However, recently good

alternatives to APTES that have been developed which produce monolayers even by solution phase deposition.[161]

Briefly the protocol for making APTES films used in this thesis was as follows. Cleaning pre-treatment of the surface is essential to remove carbon impurities on the surface and to produce reactive hydroxyl groups on the surface which can bind to the siloxane groups of the silane.[158] Piranha wash is highly effective in producing hydroxyl groups on silica. If the sample in question was too sensitive for piranha wash oxygen plasma cleaning was used.[161] Oxygen plasma in vacuum breaks carbon bonds and evacuates volatile compounds loosely bound to the surface and generates sufficient hydroxyl bonds on the surface. In a vacuum chamber that contains the activated glass or silica samples a droplet of APTES liquid is placed. The chamber is sealed and a vacuum of around 2 mBar is sufficient to produce a vapor of APTES. Once this vacuum has been reached the chamber is sealed for 30 min. At this point a loosely bound silane layer is produced, by annealing the surface at 110 °C etoxy groups hydrolyze which forms siloxane bonds between APTES molecules creating a more robust silane layer. The silanization protocol described here is specifically developed for APTES. The suitability of using this protocol also for other silanes depends on which specific silane is considered. Some silanes do not have three etoxygroups for instance, then it does not make sense to anneal the surface after vapor deposition because it will not have the intended effect. Similarily some silane compounds are difficult to evaporate which makes vacuum deposition unsuitable.

Aminosilanes deposited on silicon dioxide have been shown to be susceptible to degradation in aqueous solution on a timescale of hours.[160] Therefore long term stability of polyelectrolyte brushes on glass anchored with APTES is low. In addition to degradation during storage the siloxane bond stability may be too weak anchor for hydrophilic polymer brushes. In fact, the swelling of siloxane anchored brushes has been found to induce de-grafting of the polymer brush.[162, 163] A summary of the advantages and disadvantages of APTES silanization in vacuum is presented in 4.2 below.

Advantages	Disadvantages
Specific for glass, silica	Requires vacuum
Solvent free	Sensitive to water
	Low stability
	Optimiziation to prevent multilayers

Table 4.2: Summary of advantages and disadvantages of silane surface chemistry

4.1.3 Diazonium salt

Diazonium salt was the third option used for surface functionalization, which reacts with carbon, silicon, polymer and metal surfaces to form an aromatic organic layer that is covalently bonded to the substrate.[164] A third option for surface functionalization was required in order to use the underlying gold surface as an electrode and to use electrochemistry to modulate the brushes. Thiols, as discussed earlier are unsuitable due to electrochemical instability. Silanes, which deposits on silicon dioxide is not conductive. Silanes can deposit on conductive substrates but these electrode materials are generally not as inert, or convenient, to work with as gold. Diazonium salts are electrochemically[164, 165, 166] or chemically[167, 168, 169] reduced on gold to form a covalent (Au−C) gold-carbon bond with nitrogen gas as a side product. This bond is electrochemically inert once formed.[164] Scheme 4.3 shows chemical deposition of diazonium salts on gold with ascorbic acid as the reduction agent.[167]

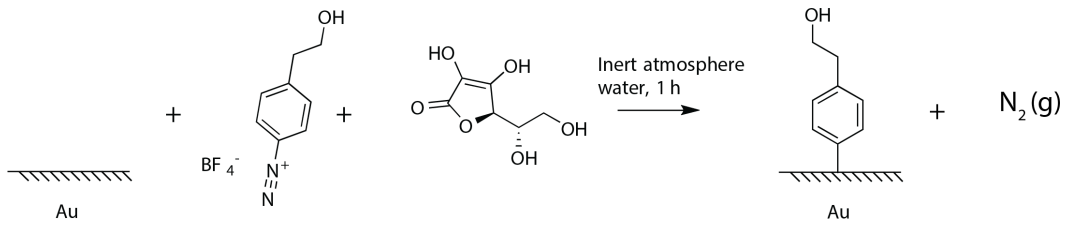

Scheme 4.3: Aryl monolayer prepared on gold by exposure of the gold surface to an aqueous solution of diazonium salt and ascorbic acid.

As a coupling agent the diazonium salt is powerful as it can interface molecules

with almost any conductive electrode and material.[164] The covalent carbon anchor bond to the substrate is stronger and more stable than the siloxane bond and the thiol-gold bond. The disadvantage with diazonium salts is the risk of producing too many aromatic organic layers on the electrode. Like with silanization diazonium salt deposition easily proceeds to form multiple and rough layers up to micrometer thick unless the deposition process is controlled. In particular electrochemical deposition risks producing thick layers and tuning of the electrochemical reduction process is difficult.[165] Consequently, new methods for aryl functionalization of surfaces have been investigated. By generation of electrochemical pH gradients aryltriazene was converted to diazonium salts at the immediate vicinity of the electrode surface, which resulted in drastically improved control of film thickness by electrochemical deposition.[170] Another strategy for avoiding the risk of forming thick layers is to chemically deposit the diazonium salt like shown in Scheme 4.3. In this thesis chemical deposition was chosen as it was found to reproduce molecular thin aryl layers on the electrode, which made electrode surface accessible for use in electrochemical reactions after synthesis. The advantages and disadvantages of chemically depositing diazonium salts are summarized in Table 4.3

Advantages	**Disadvantages**
Electrochemically stable	Oxygen sensitive
Works on many materials	Requires synthesis
Works in water	

Table 4.3: Summary of advantages and disadvantages of diazonium surface chemistry

4.1.4 Converting monolayers to ARTP initiators

The goal of the chemical surface functionalization was to produce a molecular layer of tertiary bromine which can act as ATRP initiators. A post-functionalization was performed where a tertiary bromine was introduced according to Scheme 4.4. ATRP initiator groups are formed on the surface by the addition of isobutyryl and triethylamine in dichloromethane (DCM). Within 10 minutes sufficiently many bromine groups were converted to produce a polymer brush by subse-

quent surface initiated polymerization.

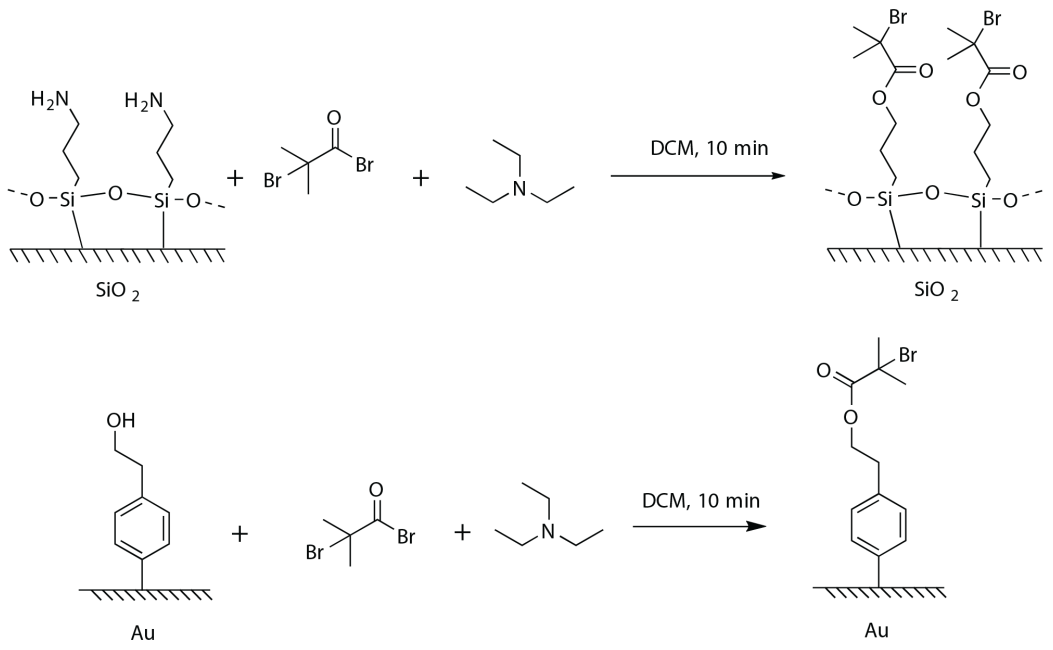

Scheme 4.4: Conversion of silane and diazonium surfaces into ATRP initiators.

4.2 Synthesis of polyelectrolyte brushes

ARGET ATRP (described in Chapter 3.1.7) was used to synthesize three different types of polyelectrolyte brushes, PAA, PMAA, and PDEA. Shown in Scheme 4.5 are the protocols for preparation of PAA using two different reaction protocols (**I** and **II**), and the protocol used to synthesize for PDEA brushes (**III**). The synthesis protocol of PMAA was analogous to that of PAA apart from that the monomer was *tert*-butyl methacrylate (later converted to methacrylic acid by post-modification).

Synthesis of acidic polymer brushes like PMAA and PAA using ATRP is challenging since acidic monomers inactivate the catalyst.[85] Two common approaches to produce acidic polymer brushes is either to polymerize the deprotonated (meth)acrylate under basic conditions or to synthesize a non acidic brush for post-modification conversion later.[26] The disadvantage of the former method is the use of aqeuous polymerization medium, which is difficult to control, while the latter method require a post-modification step. In this thesis I primarily chose to polymerize *tert*-butyl (meth)acrylate for subsequent conver-

sion into poly(meth)acrylic acid.

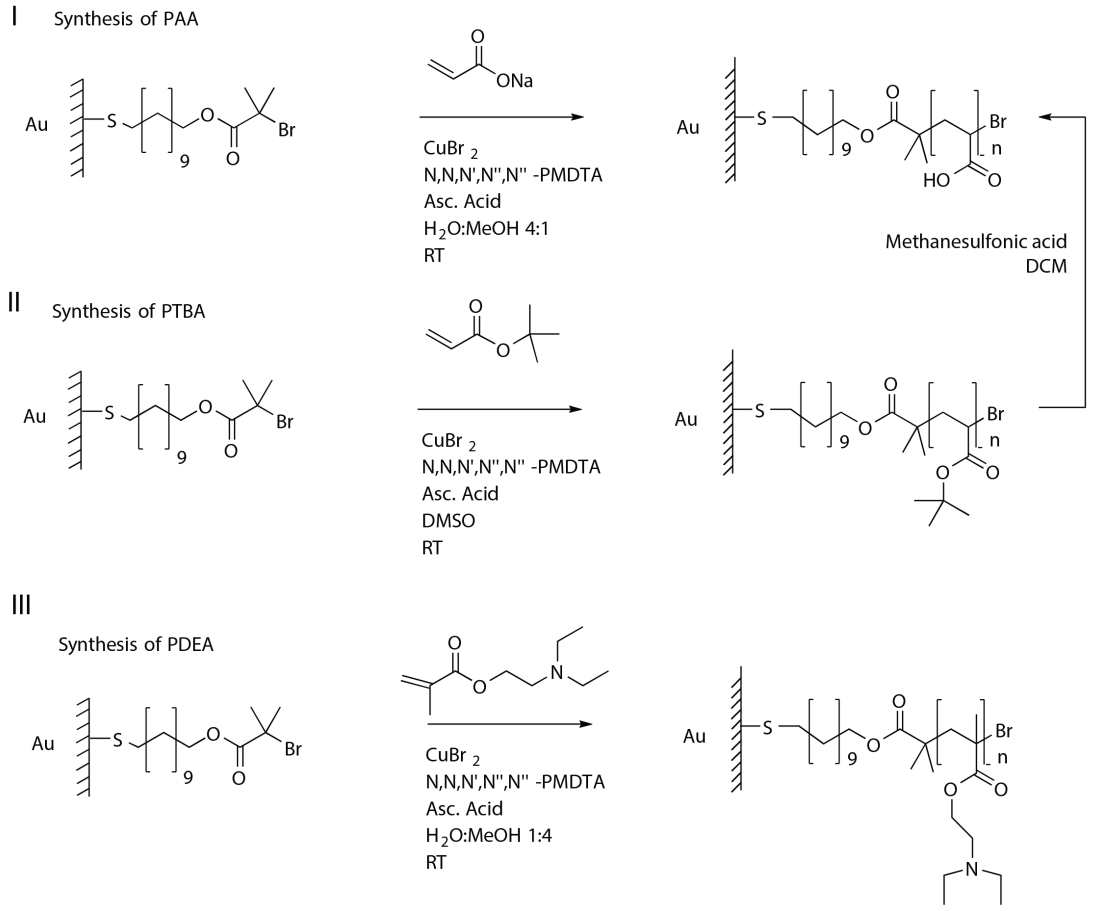

Scheme 4.5: Polymerization reaction schemes for **I**, PAA polyacrylic acid, **II**II, PTBA, poly(tert-butyl acrylate) including conversion scheme to PAA, and III, poly(2-(Diethylamino)ethyl methacrylate)

4.3 Protein conjugation

Bioconjugation reactions were utilized to produce covalent bonds between proteins and three different synthetic molecule targets: polyacidic brushes, PEG, and fluorophores. Covalent immobilization of enzymes to PAA required pretreatment of PAA with EDC and sulfo-NHS (Figure 4.1) that targets the carboxylic acid group and amines on the surface of proteins.[54] First EDC reacts with PAA (Step I), this intermediate is unstable and undergoes rapid hydrolysis, but it enables a subsequent reaction (Step II), with the sulfo-NHS ester, which has higher stability.[171] Mainly the EDC intermediate, but also the sulfo-NHS

ester are susceptible to hydrolysis, a side reaction where the carboxylic acid is restored.

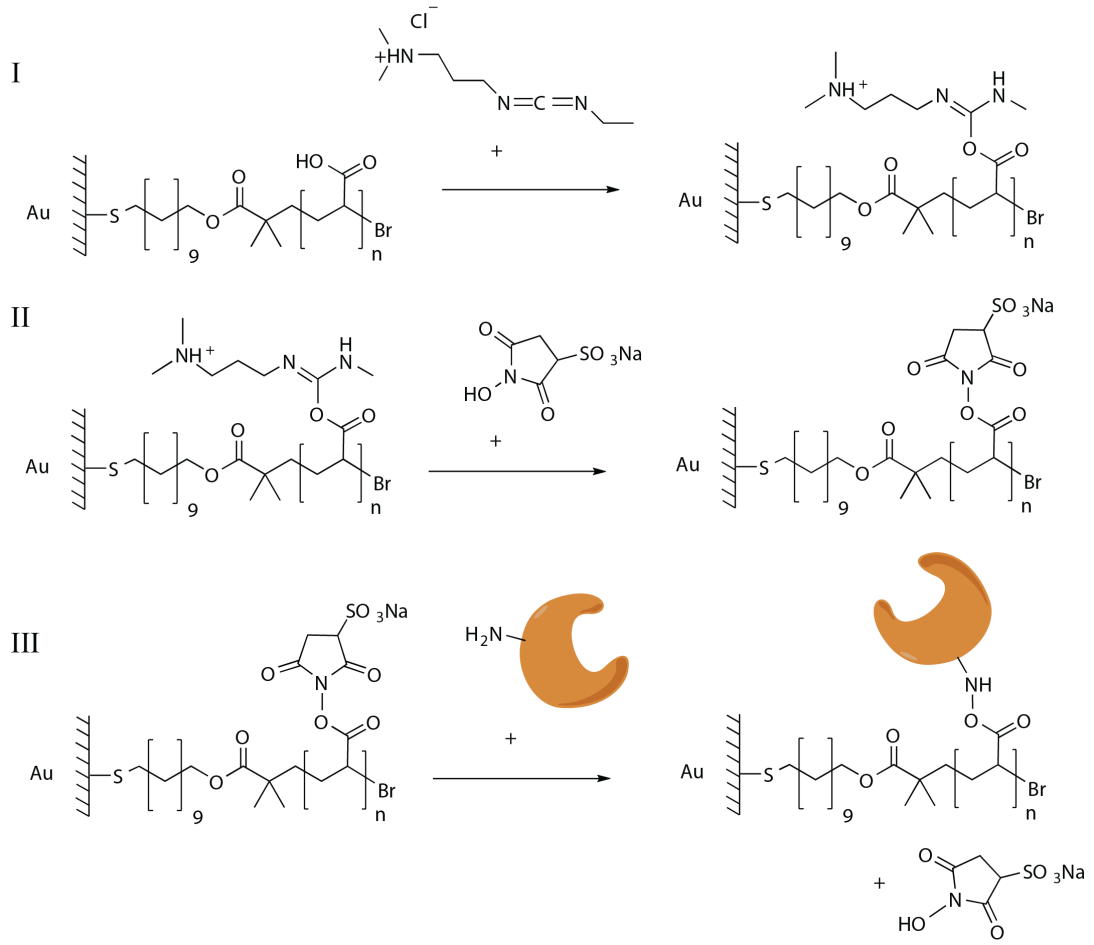

Figure 4.1: Conversion of the carboxylic acid groups of PAA brushes into sulfo-NHS carboxylate groups by (I) reaction with NHS followed by (II) replacement of EDC by sulfo-NHS and (III) binding of primary amine on a protein

The protocol used for EDC/NHS conjugation was to first expose the PAA brushes to a mixture of EDC (40 mM) and NHS (20 mM) in MES buffer for 45 minutes, following this the surfaces were rinsed removing excess EDC and NHS, then exposed to the protein sample resulting in a reaction between the sulfo-NHS carboxylates with primary amines on the protein surface.[54] Proteins which did not react with the surface were removed simply by rinsing surfaces. Finally ethanolamine (0.1 M) was used to quench eventual sulfo-NHS groups which did not react with a protein. The different conjugation reactions between the synthetic target molecule R^1 with a biological molecule R^2 are summarized

in Figure 4.2. PEG-succinidimyl valerate (PEG-SVA) was used to attach PEG to the surface of proteins.[171] Since the NHS group was already attached to the PEG polymer the conjugation reaction was carried out simply by mixing these in sodium carbonate solution for one hour. Separation between unreacted PEG, protein and PEGylated protein was performed by SEC. Fluorophores with NHS or TFP esters were similarly conjugated to proteins.[171] Like with PEGylation, the reaction is spontaneous and subsequent separation can be accomplished by size exclusion filters.

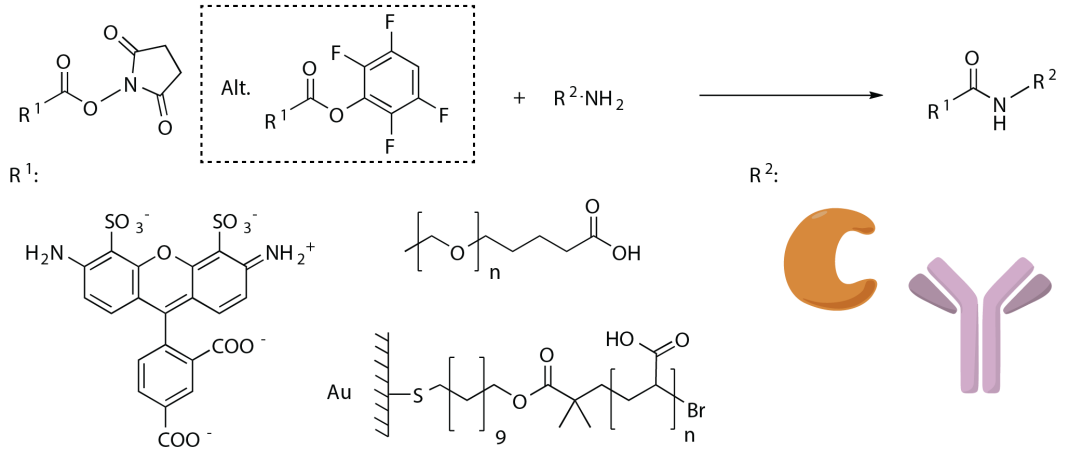

Figure 4.2: Conjugation reactions between some synthetic molecule that is NHS functionalized e.g. fluorophores, PEG, and polymer brushes, with a biomolecule e.g. enzyme and antibody.

4.4 Enzyme activity

With immobilized enzymes it is central to understand if the enzyme activity is in any way altered by the immobilization treatment. Here I describe strategies for enzyme activity measurements and the assays that were used.

Figure 4.3 shows how the activity of immobilized enzymes were measured. A droplet containing the reactants was confined within a poly(dimethylsiloxane) (PDMS) well with a bottom area of 49 mm^2 placed on top of the functionalized surface, or for the case of bulk enzyme on a glass surface. The total reactant droplet volume was 200 μL. The activity measurements were initiated by placing the reactant droplet onto the functionalized surface. From the reaction medium samples of 10 μL were collected at the time points 0, 1, 2, 3, 4, 5, 10 and 15

min into the experiment and mixed with 790 μL of assay liquid. A standard curve with concentrations of H_2O_2 within the concentration range was made to quantify the produced quantity of H_2O_2 during the activity measurements. Absorption spectra for different dilution of the GOX stock solution (2.0 g/L) were measured at 280 nm.

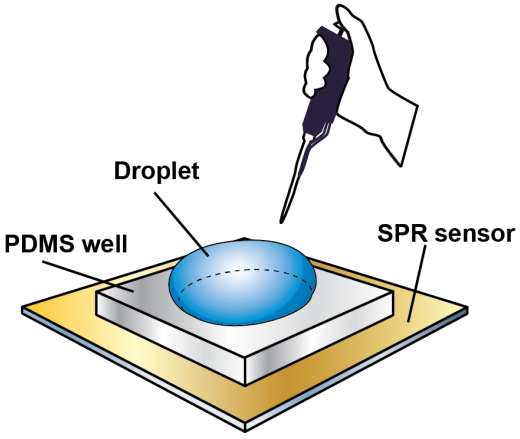

Figure 4.3: Activity measurement method of immobilized enzymes. The activity is measured directly on surface by sampling from a droplet that is fixed to the surface by a PDMS mask.

GOX is widely used as a biosensor and as a model enzyme for research.[129] Several protocols for determining its activity have been developed. To measure enzyme activity liquid exposed to the enzyme is either sampled or measured directly. Direct measurement of the activity is convenient since it enables rapid measurements. But direct measurement of enzyme activity might be impractical when measuring on immobilized enzymes. The surface to volume ratio of the system might introduce inaccuracies tied to insufficient mixing and produce local concentration surface gradients. The immobilized enzyme activity on surfaces has been measured by electrochemical measurements.[172, 173] Since our substrate was a conductive material, technically we could have done the same. However, for enzymes immobilized to brushes, the enzymes are not in close contact with the electrode. We cannot guarantee that the electrochemical method senses activity of enzymes situated wihtout direct contact with the electrode surface. Although electrochemical measurement would work to measure enzyme activity on SAMs, conductive polymer films, and bare inorganic surfaces,

it is unsuitable for brushes.[172, 173] Furthermore, we want to compare the activity of immobilized enzymes with the native enzyme activity in solution. But the electrochemical methods does not measure the native bulk enzyme activity in solution. Consequently we used colorimetric assays for the detection of the GOX reaction product hydrogen peroxide.

The first assay used measured activity by the oxidation of iron xylenol orange complexes in the presence of hydrogen peroxide (Scheme 4.6).[174] The recipe for the assay solution was 25 mM H_2SO_4, 100 μM xylenol orange, 250 μM ammonium iron(II) sulfate hexahydrate, similar to a previously developed protocol for detection of H_2O_2.[174, 130] The reactant solution was composed of 0.1 - 0.001 M glucose in PBS at pH 6.0 and dissolved oxygen present at ambient conditions. By visible light spectroscopy the change in oxidation state of iron xylenol complexes was monitored at 480 nm and 560 nm as a function of time.

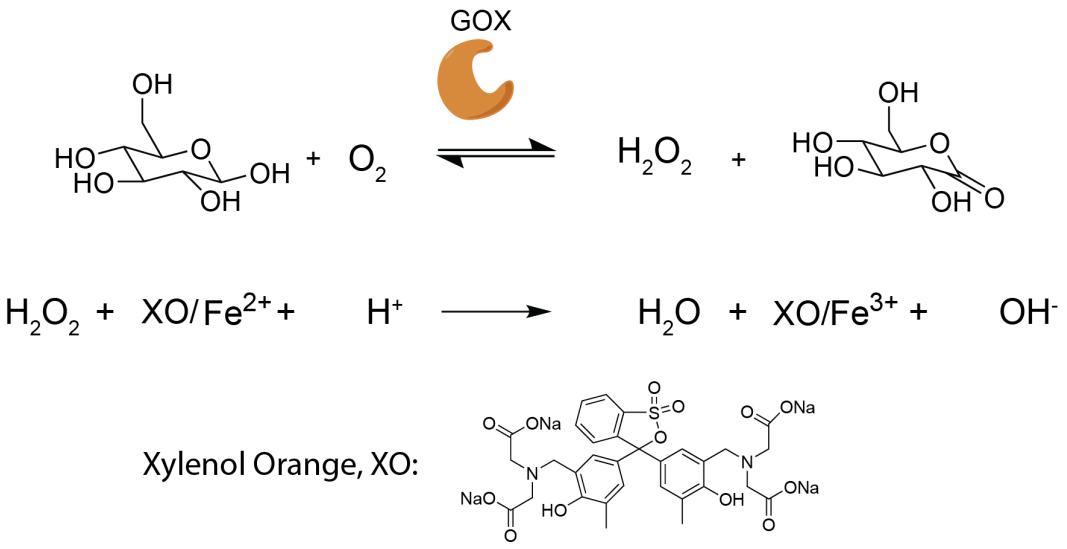

Scheme 4.6: Assay reaction where the oxidation of Iron-Xylenol Orange complex is used for the detection of glucose and oxygen consumption into hydrogen peroxide and gluconolactone.

The second assay used was a coupled enzyme reaction between glucose oxidase and horse radish peroxidase. Similar to the first protocol, this protocol also detects hydrogen peroxide produced according to Scheme 4.6. The composition of the assay was 2 mM ABTS, a variable amount of glucose between 1 and 100 mM, 20 nM HRP and 2 nM GOX. The concentration of HRP was kept ten

times higher than that of GOX to ensure that this enzymatic reaction was not the bottleneck of the kinetics. Oxidation of ABTS was detected at 420 nm by spectroscopy. The second assay was used to compare the enzyme activity in solution before and after immobilization meaning the enzyme activity was measured by standard methods through a cuvette.

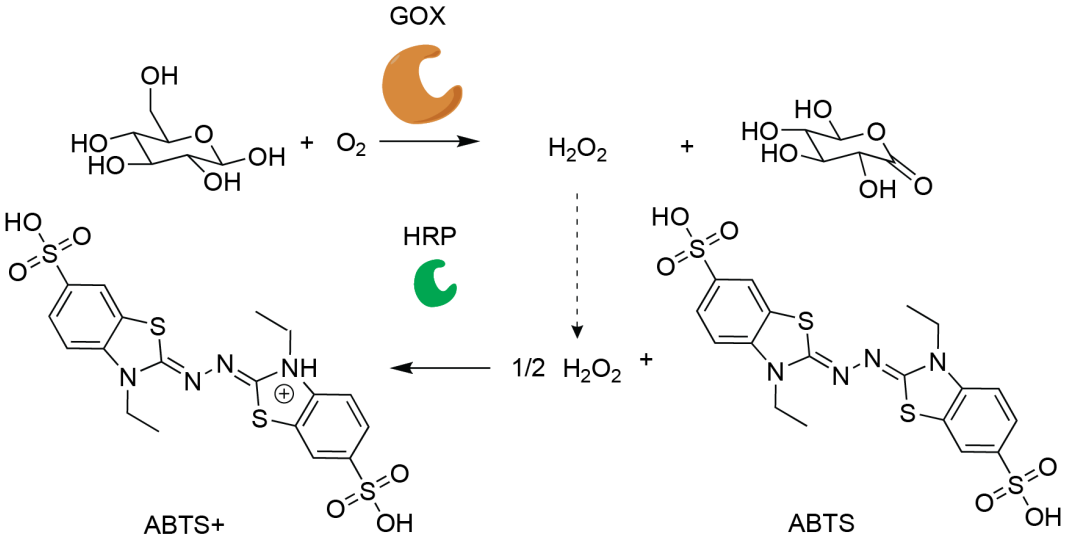

Scheme 4.7: ABTS assay where oxidation of ABTS by HRP detects the presence of hydrogen peroxide produced by catalytic conversion of glucose and oxygen by GOX.

The activity of a collection of enzymes was studied within a polyelectrolyte brush (Scheme 4.8). Detection of the chain reaction requires at least analytical verification that the last step of the chain reaction occurs. As assay for detecting chain reactions of enzymes was done by adding Galactosidase (GAL) to reaction between GOX and HRP from Scheme 4.7 where lactose constitute the first reactant. Oxidation of ABTS was then used to verify and quantify the final cascade reaction output. Other assays for cascade reactions can include multiple colorimetric or fluorescent substrates, that change their emissive properties upon participating in the chain reaction, that allows not only detection of the final product, but also the activity of the individual enzymes in the chain reaction.[175]

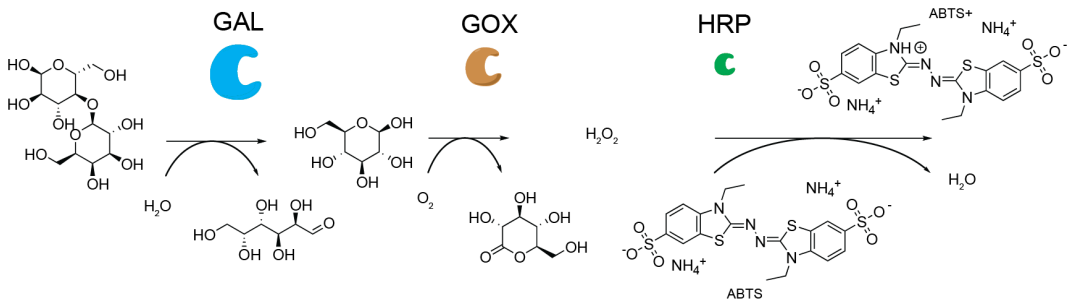

Scheme 4.8: An enzyme cascade reaction between GAL, GOX and HRP where lactose is the first reactant of the cascade reaction and the final product is oxidized ABTS detected by visible light spectroscopy.

4.5 Electrochemical methods

Two electrochemical cells were considered, ex-situ and in-situ cells (Figure 4.4). The ex-situ cell consisted of immersing the working electrode and reference electrode within a counter electrode mesh, while the in-situ cell was a QCM-D flow cell designed for in-situ electrochemical measurements (QEM 401, by Q-Sense). An in-situ cell has the obvious advantage of real-time information of surface changes when electrochemical signals are applied, while an ex-situ cell is simple to use and set-up.

With both the in-situ and ex-situ cell designs the quality of the electrochemical measurements might be hampered by sub optimal electrode configuration. For the ex-situ electrode the large surface area of the counter-electrode relative to the working electrode is beneficial since it allows for improved current collection.[143, 176] However the distance between the electrodes is large, and non-uniform which means that the current density will vary across the surface of the working electrode. The placement of the reference electrode can be made in close proximity to the working electrode which is beneficial to reduce uncompensated resistance. In contrast the in-situ electrode separates the counter and working electrode by a small and uniform distance. However, this is at the expense of the sub-optimal location of the reference electrode, behind the counter electrode.

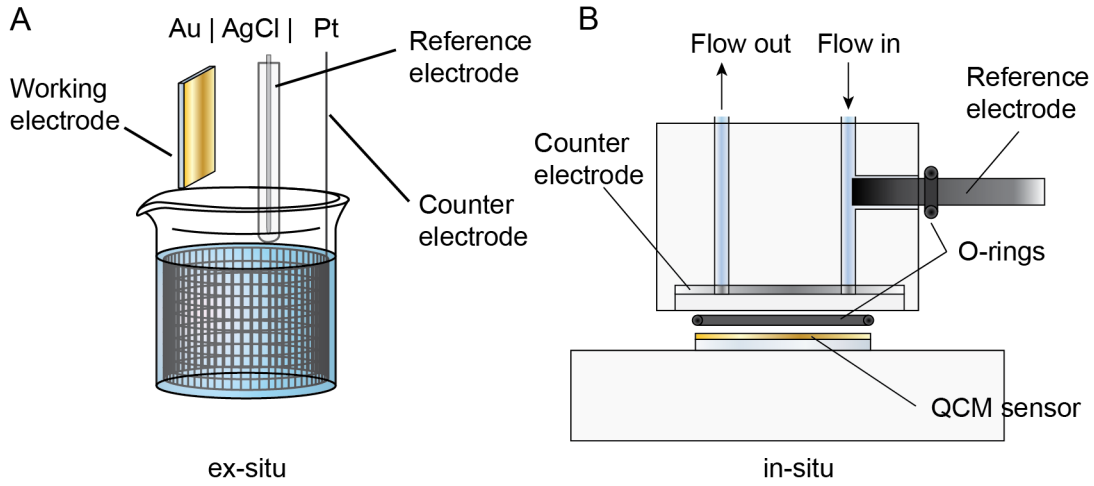

Figure 4.4: (A) Ex-situ and (B) in-situ electrochemical cells used in this thesis.

The working electrode functionalized with polyelectrolyte brushes was unless stated otherwise made of gold. The electrolyte was phosphate buffered saline it was filtered serum (with a 22 μm sized hydrophilic filter) used to model how the electrode would perform in a biological setting. For local electrochemical acidification of the electrode a reduction agent, e.g. hydroquinone, was added at a millimolar concentration.

4.6 Spectroscopy

Different methods of spectroscopy were used in this thesis to obtain information about the polyelectrolyte brushes and about proteins that bound to them. Here a brief summary of the working principles of each spectroscopy method is given.

4.6.1 Infrared reflective absorption spectroscopy

IR spectroscopy excites vibrational modes of bonds in molecules, revealing chemical information of the analyzed sample. By Fourier transform of the IR signal a spectrum is produced where bands of different bonds can be identified and analyzed. Some functional groups produce exceptionally strong IR bands that are easy to detect and where the frequency of the vibration is unique in comparison with other IR excitable covalent bonds. The carbonyl functional group is a good example of an easily detectable functional group. The monomer chemical

structure of PAA, PMAA and PDEA all contain carbonyl groups and are therefore easy to detect and characterize using IR. The carbonyl group of PAA and PMAA is particularly interesting to study because the frequency of the carbonyl band vibration shifts strongly depending on if the carboxylic acid is protonated or deprotonated.[177] Thus the IR spectra of PAA and PMAA can detect if the carboxylic acids within the brush are predominantly charged or neutral.

A problem with performing infra-red spectroscopy on polyelectrolyte brushes is the very small amount of sample per surface area. If the IR beam is directed perpendicularly towards the surface very little IR light would be absorbed preventing the detection of the polyelectrolyte brush. However, by sending the IR beam with grazing incidence towards the sample, reflection as well as transmission of light light occurs at the air polymer interface. Since the underlying gold film is reflective, a proportion of the transmitted light will internally reflect within the polymer brush film extending the light path that travels through the polymer film. The effect becomes larger IR absorption from the brush, and an amplified signal as a result. The technique is called Infrared reflective absorption spectroscopy (IR-RAS) and it is useful for studying monolayers of molecules on metal surfaces(Figure 4.5),[178, 179] and it has also been frequently utilized to study also polymers on metal surfaces.[177, 30, 31, 180]

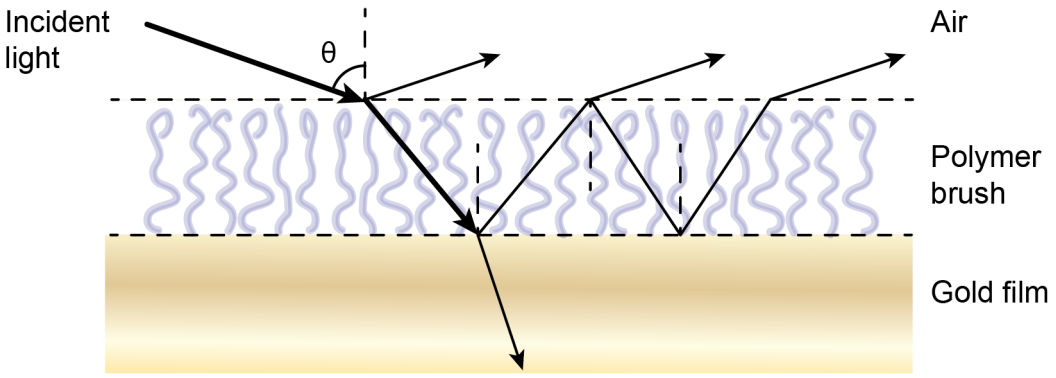

Figure 4.5: Principle of Reflective Absorption Spectroscopy showing light irradiation with grazing incidence towards a molecule layer on a reflective surface e.g. gold producing partial absorption and reflection through the polymer film.

IR-RAS was used by us to determine the degree of charging of the polyelectrolyte brushes[177, 30, 31, 181] and it was one of the techniques we used to

verify and characterize protein binding to brushes[42, 182]. Figure 4.6 shows an example of how the IR-RAS spectra in the carbonyl band region of PMAA varies as a function of pH, at pH 3, pH 8, and pH 10. At low pH a peak at 1730 cm^{-1} dominates the spectrum, while at high pH this peak is absent and replaced by a peak positioned at 1650 cm^{-1}. At an intermediate pH both peaks are visible.

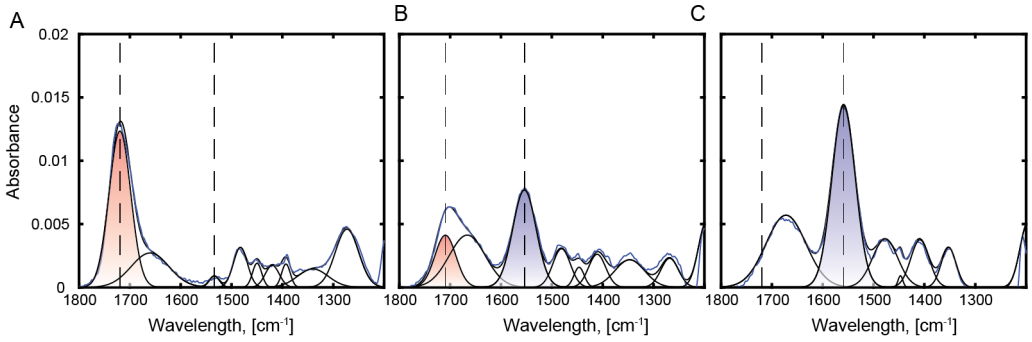

Figure 4.6: IR-RAS spectra of PMAA at (A) pH 3, (B) pH 8 and (C) pH 10.

The spectra was modelled by a sum of Gauss functions, each representing a band of the measured spectrum.[177]

$$f(w) = \sum_{n=1}^{m} g_n(w, a(i)), \text{where,} \quad g(w,a) = a(1)exp\left[\frac{-(w-a(2))^2}{2*a(3)^2}\right] \tag{4.1}$$

Minimization of the model with respect to the experimental data was performed after which integration of the peak areas was made. The relative dissociation of the carboxylic acids α, was calculated according to

$$\alpha = \frac{\text{A(COO-)}}{\text{A(COO-)} + \text{A(COOH)} \times \epsilon} \tag{4.2}$$

Where $\epsilon = 1.8$ reflects the ratio between the extinction coefficients of the charged and neutral carboxylic acid.[177] The degree of charging was obtained by normalization of α, between completely neutral polyacidic brush, at very low pH, and completely charged polyacidic brush, at very high pH according to,

$$\alpha_N(\text{pH}) = \frac{\alpha(\text{pH}) - \alpha(\text{pH}=2)}{\alpha(\text{pH}=12) - \alpha(\text{pH}=2)}. \tag{4.3}$$

Titration of PAA and PMAA brushes at for each unit of pH between 2 and 11 was performed, producing a vector $\alpha_N(\text{pH})$. The α_N obtained by IR-RAS were

used to validate the corresponding α_N that was obtained by SPR and QCM-D titrations.

4.6.2 Circular dichroism spectroscopy

Circular dichroism (CD) is a spectroscopy technique for determining the secondary and tertiary protein structure of proteins.[183, 184] CD is the detection of unequal absorption of left-handed and right-handed polarized light. Proteins are optically active molecules which means that when circularly polarized light passes through protein there is an unequal absorption of right and left-handed circularly polarized light (Figure 4.7). A CD instrument detects the difference in absorption of right and left polarized light or it calculates the degree of ellipticity of the detected light beam.

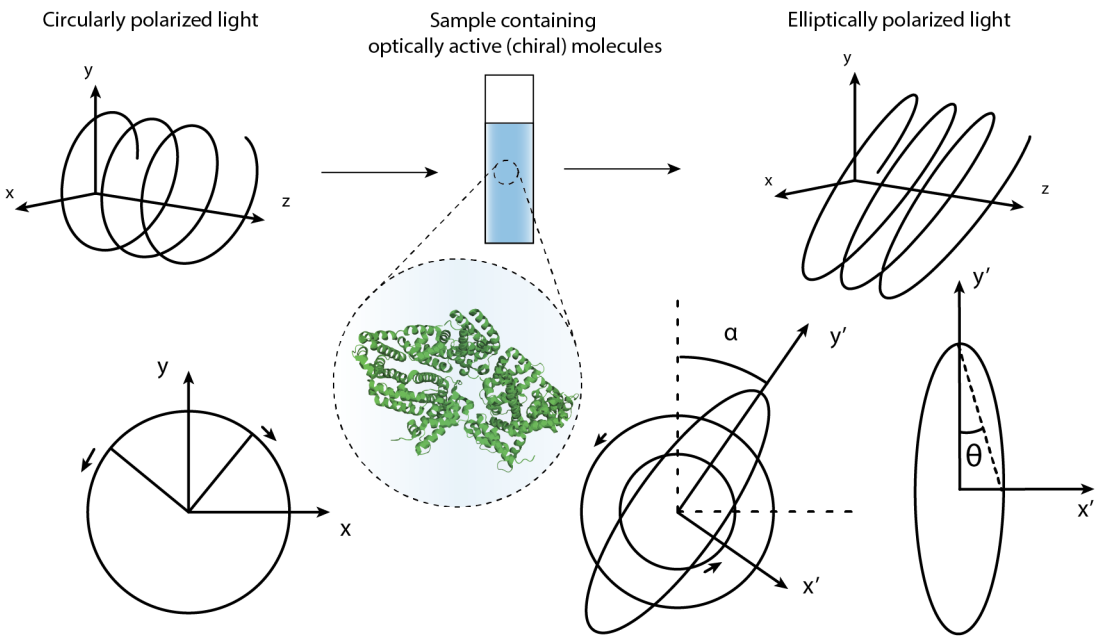

Figure 4.7: Principle of Circular dichroism spectroscopy.

The peptide bonds absorb light in the UV region (240 - 180 nm), here the CD spectrum detects the presence of secondary structure in the protein, α helix and β sheet structures.[183] At higher wavelengths (320 - 260 nm) of the CD spectrum information of the tertiary structure may be obtained as it reflects the structures around aromatic amino acid groups. BSA displays a characteristic CD spectra where the peak located around 190 nm, represent the relative presence

of α helix structure, and in the wavelength region between 210 and 230 nm two peaks reflect the β-sheet structures (Figure 4.8).

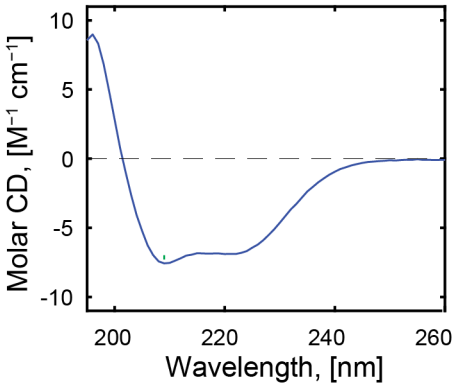

Figure 4.8: CD spectrum of BSA.

Circular dichroism has been used to measure the protein structure while immobilized on surfaces and protein structure after immobilization.[96, 115] In this thesis CD was used as a test of structure before and after, to determine the retention or possible loss of the native protein structure after immobilization to polyelectrolyte brushes. CD has previously been used to show that proteins which immobilize to polyelectrolyte brushes by electrostatic interactions retain their structure while inside the polyelectrolyte brush.[96] We used it to show that immobilization of proteins to pH-responsive polyelectrolyte brushes in the neutral state equally well preserves the protein structure.

4.6.3 Fluorescence spectroscopy

Fluorescence spectroscopy with pH sensitive fluorophores was used to detect the pH within polyelectrolyte brushes. To restrict the fluorophore excitation to occur only within the polyelectrolyte brush, a TIRF optics (see Chapter 3.4.2) set-up was used. The eventual discrepancy between the solution and brush pH would provide evidence supporting the existence of a pH gradient within polyelectrolyte brushes, see illustration in Figure 4.9.

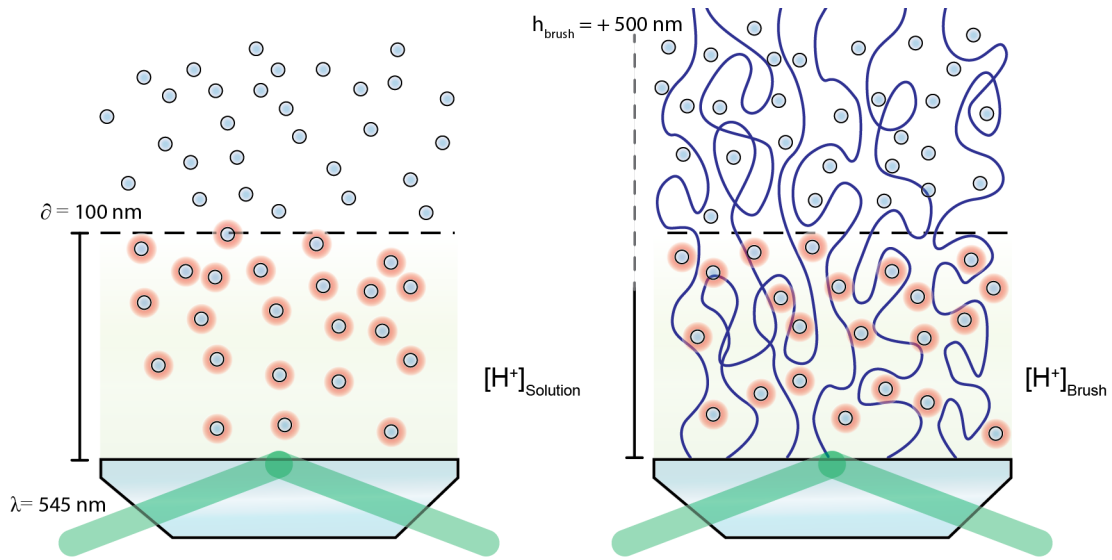

Figure 4.9: TIRF spectroscopy where pH-sensitive fluorophores are excited within the evanescent field of a surface with or without a polyelectrolyte brush.

Carboxynaphtofluorecein (CNF) is a pH responsive fluorophore with a pK_a of 7.6 (Figure 4.9 A),[185] which is similar to the pK_a of the brushes considered in this study making it a suitable probe for detecting the pH within the brushes. The fluorophore is readily excited with a laser of 545 nm, producing an emission peak between 600 to 800 nm, Figure 4.10. The emission properties of the fluorophore vary strongly with response to changes in the pH range 6 to 9, Figure 4.10 C, making CNF a useful tool for detection of changes in the pH within brushes.

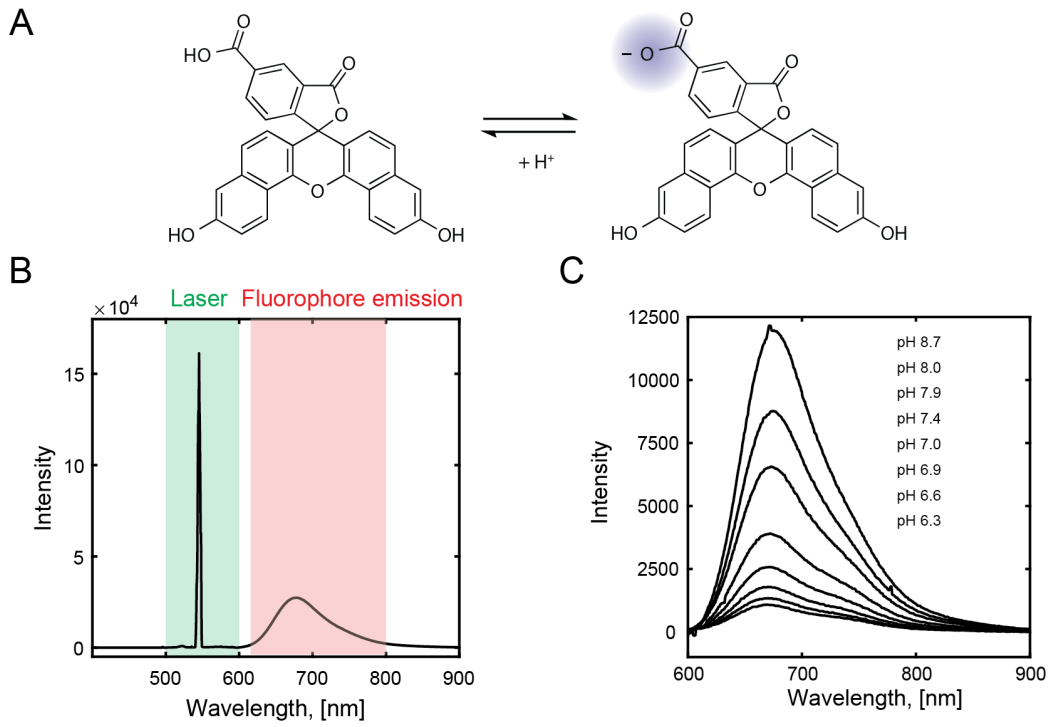

Figure 4.10: (A) The molecular structure of pH-sensitive carboxynaphtofluorescein (CNF). (B) Spectra showing the peak from the 545 nm laser, and the fluorophore emission of CNF. (C) Fluorescence spectra that shows excitation of CNF as function of pH.

The main spectral feature of CNF is a sharp peak centered around 650 nm, with a shoulder peak at higher wavelengths around 710 nm. The analysis of the fluorescence spectra was made using a sum of two Gauss functions representing the peak and the shoulder, analogous to Equation 4.1 and how the IR-RAS spectra was analyzed (Figure 4.6). This resulted in close fits to the experimental spectra at different pH, Figure 4.11 A and B. The integrated area of the peak divided by the area of the shoulder produced a linear trend with respect to pH (R^2>0.99), (Figure 4.11 C), which was used to analyze the pH within the evanescent field of the TIRF set-up.

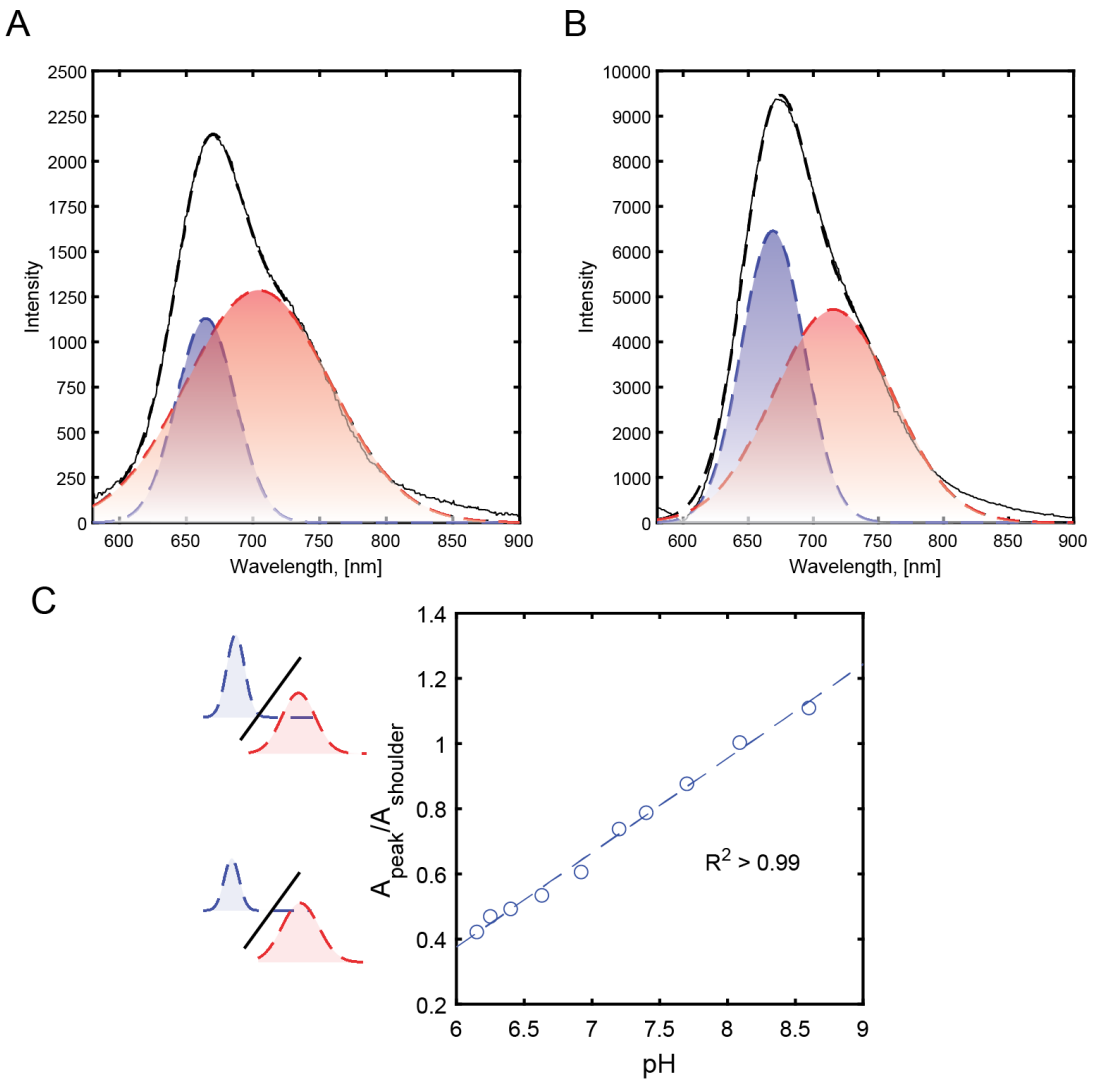

Figure 4.11: Emission spectra of CNF at (A) pH 6.4 and (B) pH 7.4 and (C) calibration curve for pH change of carboxynaphtofluorescein.

The pH could be determined with remarkable accuracy by comparing the peak and shoulder in Figure 4.11. But ideally two spectrally resolved peaks are analyzed. By matching the fluorophore and the laser used, excitation spectra can be produced that generate two separated peaks.[185] This facilitates analysis to determine the pH even further. In general the comparison of spectral features is more reliable compared to methods that compare the relative intensity of the excitation peaks since the intensity may vary strongly between experiments, optics configuration, and light source power.[84]

5

Results and Discussion

The central results of each of the appended papers are summarized. The connections between each of the projects are highlighted to emphasize how the findings in each paper builds on each other.

5.1 Characterization of polyelectrolyte brushes

The switching of pH-responsive brushes was characterized by QCM-D and SPR. Quantitative brush heights in neutral and charged states were obtained by applying the non-interacting particle method.[35, 22]

5.1.1 Interpretation of SPR and QCM-D signals

At high pH PAA becomes charged, attracting water and ions, which gives rise to swelling of the brush, Figure 5.1 A. Conversely, at low pH (below the pK_a of PAA) the brush is neutral, thus contains less water and collapses. The QCM-D signals in Figure 5.1 are simple to interpret: when the charged brush is hydrated, an increased ammount of mass (water and ions) becomes coupled to the surface. This results in a decrease in the frequency signal, which also leads to an increase in the viscoelasticity of the layer that results in higher dissipation. However, the SPR results (Figure 5.1 C) show an unexpected trend, as the signal increases when the brush swells. Intuitively, one would expect the SPR signal to *decrease* upon charging because the monomer concentration becomes lower and is replaced by water, an effect which is expected to decrease the refractive index. Swelling of the brush results in a smaller quantity of polymer at the immediate vicinity of the gold surface where the evanescent field is the strongest, which in theory should contribute further to a decrease in the SPR signal. This is

the case for non-polyelectrolyte stimuli-responsive polymers such as the thermo-responsive PNIPAAM.[22] However, our SPR signal sensorgrams (PAA, PMAA, and PDEA) clearly show the opposite trend. Similar SPR results from switching pH responsive brushes are reported in many other studies,[186, 32] but a satisfactory explanation to why the signal switches in a counter-intuitive way has not been given.

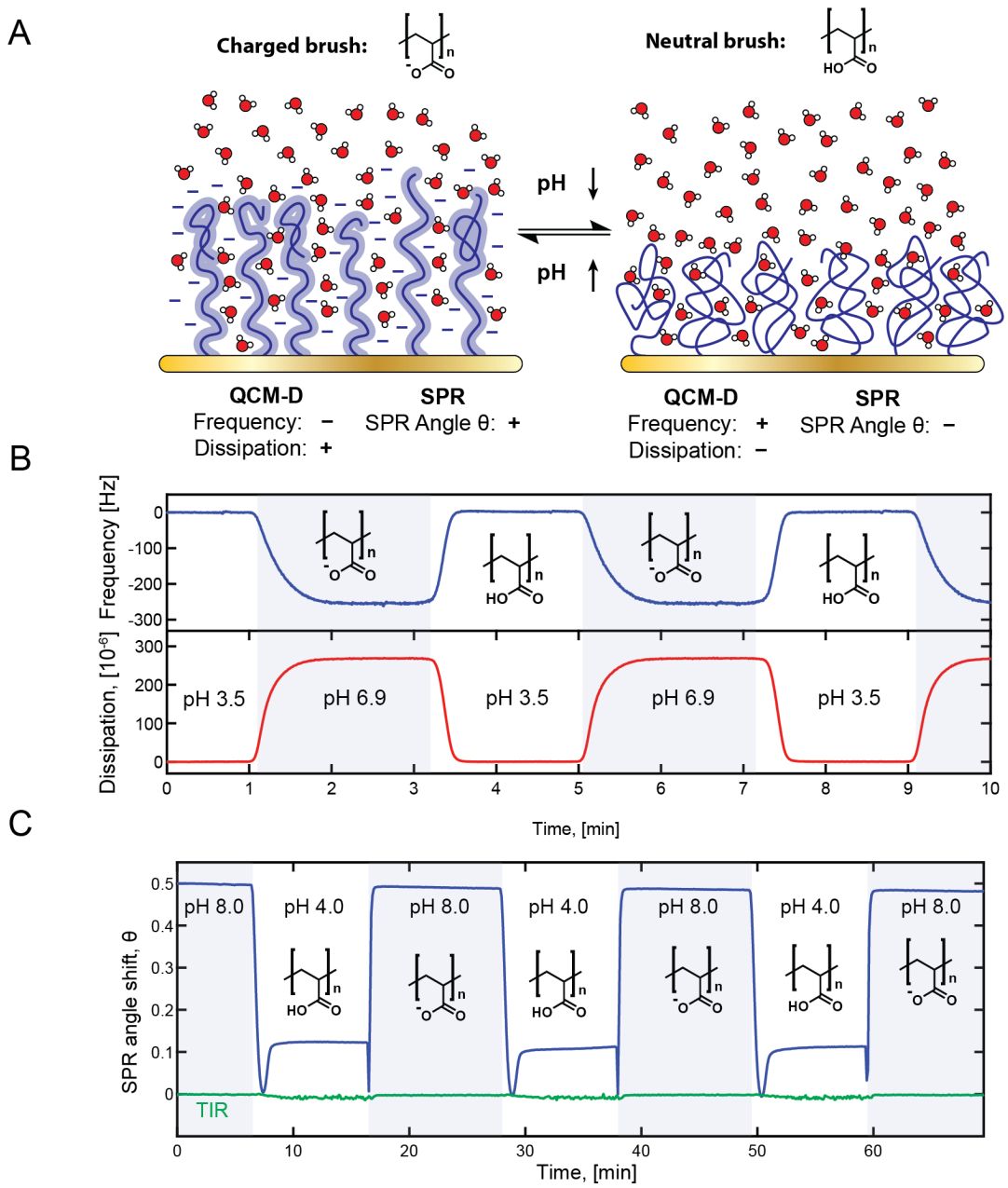

Figure 5.1: (A) Charged and neutral PAA brushes where corresponding signal changes in QCM-D and SPR signal are indicated. (B) QCM-D frequency and dissipation and (C) SPR angle shift of PAA brushes when switching the pH.

The concentration of counter-ions within the brush changes dramatically when the brush charges. If a counterion associates with every charged monomer in the polyelectrolyte brush, the concentration of salt could reach 2 M within the polyelectrolyte brush (based on the dry surface coverage of polyelectrolyte brushes $\approx$ μg$\times$cm^2). However, counterions are unlikely the main explanation for counter-intuitive SPR signal switches because primary counterions for PAA in PBS (Na^+ or K^+), have only a minor refractive index contribution as function of concentration.[187, 188] For cationic polyelectrolyte brush PDEA, the situation is slightly different, its primary counterion (Cl^-) has a significant refractive index as function of concentration. This means that if counter-ion screening is the probable cause of counter-intuitive switches in the SPR signal, then anionic and cationic brushes should display drastically different SPR signal shifts as the pH switches. Yet the trend was observed for all polyelectrolytes, the SPR signal increases with charging.

The anomalous shifts in SPR for pH-responsive brushes was found to occur due to the difference in refractometric index between the charged and neutral polyelectrolytes. PAA displays a large change in $\delta n \times \delta c$ upon change in pH (Figure 5.2) with a difference between neutral and charged of up to 40%. It has been shown for PAA that the $\delta n \times \delta c$ increases almost by a factor of 2 if the degree of charging goes from zero to one.[79] The same effect was observed also for PDEA, confirming that this is a property of both anionic and cationic polyelectrolytes, thus explaining SPR shifts in the "reverse" direction of pH-responsive brushes (Figure 5.1 C).

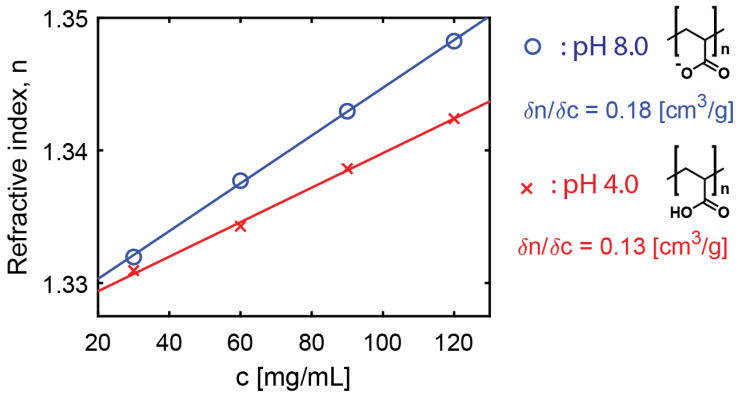

Figure 5.2: Refractive index as a function of concentration, c [mg/mL] for charged (blue) and neutral (red) PAA.

5.1.2 Quantification of polyelectrolyte brush heights

The most common choice of probe to characterize the brush height of non-polyelectrolytes e.g. PEG and PNIPAAM, is bovine serum albumin (BSA),[22, 35] as it has a negligible interaction with these brushes.[22] For probing heights of polyelectrolyte brushes there are reasons to suspect proteins will not work. The first is that proteins are also polyelectrolytes and may bind to charged brushes by electrostatic attraction.[39] Secondly, when neutral, hydrophobic interactions between the brush and the protein may occur.[36] Indeed, I found that BSA bound to both neutral PAA and PDEA. Protein binding to neutral polyelectrolyte brushes is observed not only for BSA but it occurs for proteins in general. Some proteins did not bind to charged polyelectrolytes, displaying non-interacting behavior if the electrostatic repulsion was sufficiently strong. These interactions of proteins and polyelectrolytes are explored further in Chapter 5.4.

Some synthetic polymers with large molecular weights were found to qualify as non-interacting probes. PAA in solution form was used to successfully determine the brush heights of PAA, and PEG was used to determine the brush heights of PDEA brushes (Figure 5.3). Achieving minimal interaction between a synthetic probe and the brush requires striking a balance between high water solubility (to enable high refractive contrast), while avoiding monomers with functional groups that engage in binding. Many polar functional groups that make polymers water soluble also promote hydrogen bonding between the probe and the brush. Also, some polymers displayed a very high affinity towards the brushes with extremely rapid binding, but the interaction was extremely weak between these polymers and useful probes. To make the distinction it was essential to analyze the linearity between the SPR and TIR angle, which showed hysteresis if weak binding did occur.

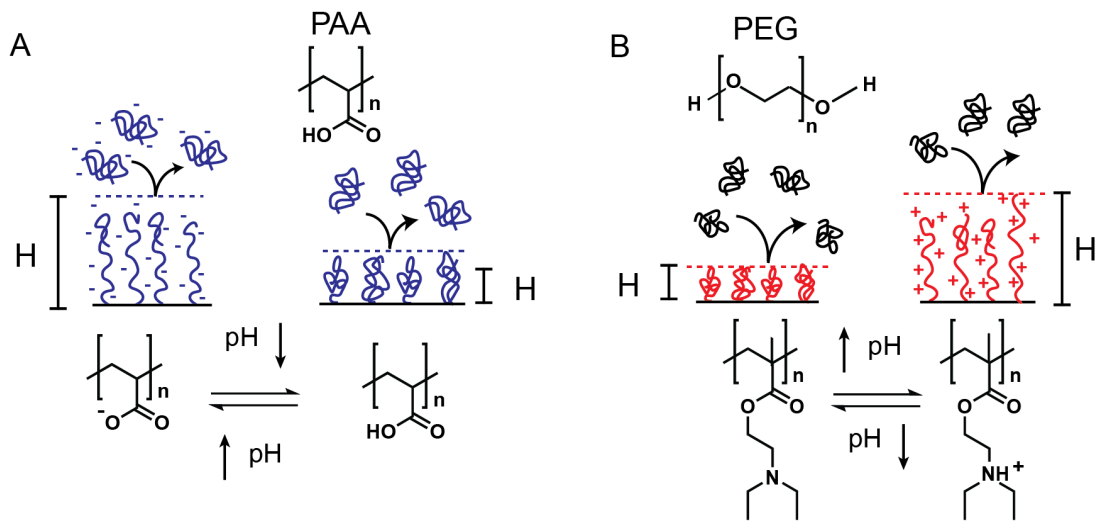

Figure 5.3: Brush height determination of polyelectrolyte brushes using non-interacting probes. (A) PAA used for PAA and (B) PEG used for PDEA.

Many studies that characterize polyelectrolyte brushes strive to confirm theoretical predictions of scaling relationships between the brush height, grafting density, salt concentration etc.[29, 30, 77, 34] The non-interacting probe method provide us with accurate brush heights in both charged and neutral state in solution. However, since PE brushes were prepared by grafting-from we lack information about the molecular weight, M_w, the degree of polymerization, N, and importantly we cannot tie the brush heights to the grafting density, σ. De-grafting of the PE brush and subsequent SEC or MALDI analysis of the de-grafted polymer could have been used, but this was outside of scope of this study. Without these parameters we cannot determine what scaling regime our brushes are in. However, based on the salt concentration, polymerization method, and polyelectrolyte type, we can still make a hypothesis as to which scaling regime our brushes are in.

PAA and PDEA brushes are likely in the salted brush regime (Equation 3.15) when the brushes are charged and when the total ionic strength is physiological concentration, $[C_{salt}] = 0.15$ M.[76] In the salted brush regime salt counter-ions are localized within the brush, as predicted by theoretical models, [74] and as has been observed experimentally.[189] However, with respect to the bulk solution the brush contains a higher amount of ions to satisfy charge neutrality. With either increased or decreased salt concentration the brush will contract

due to osmotic pressure that depletes or enriches ions within the brush. Even though we lack knowledge to prove that the system studied here is in the salted brush regime we can compare to literature cases. For PAA for instance a salt concentration of 0.1 M was found to produce a maximum of brush height as a function of ionic strength.[76, 34]

5.2 Shifts in protonation of brushes by changing salt concentration

Here we show for the first time that changes in salt concentration cause large shifts in the pK_a for brushes, exceeding corresponding shifts for polyelectrolytes in solutions. We demonstrate that failure to account for large shifts in the pK_a of brushes could easily result in erroneous attribution of mechanisms behind protein immobilization.

5.2.1 Detection of shifted pK_a

The pK_a of PMAA brushes was found to shift when varying the salt concentrations of the solution between 510 mM and 1 mM (Figure 5.4). The effect was confirmed using three different characterization techniques SPR (Figure 5.4 A), QCM-D (Figure 5.4 B), and IR-RAS (Figure 5.4 C). In case of SPR and QCM-D the degree of protonation was obtained indirectly through detection of charging and swelling of the brush by refractometric or acoustic readout respectively. The degree of protonation was directly measured by IR-RAS through detection of relative proton dissociation of the carboxylic acid groups. The three methods produce similar results, with some slight deviations as expected since the mechanisms by which the degree of protonation is detected are different. This effect was observed not only for PMAA but also for PAA and PDEA, indicating that this is a property shared among polyelectrolyte brushes. A very recent study (performed simultaneously and independently of this work) shifted the pK_a of PAA by changing the salt concentration, corroborating the results presented here.[34]

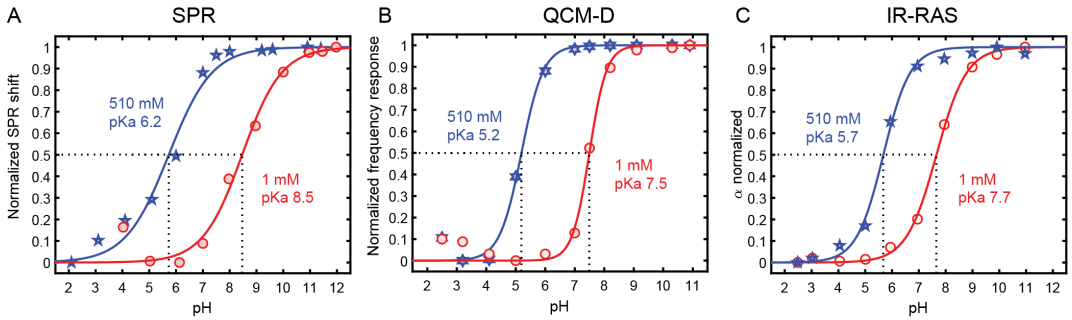

Figure 5.4: Titration of PMAA brushes by (A) SPR, (B) QCM-D, and (C) IR-RAS. Normalized signal which reflects degree of protonation is plotted as function of pH for each technique.

The high sensitivity of the brush pK_a to salt concentration is the result of a very high grafting density that confines polyelectrolytes, giving an extremely high concentration of functional groups. However, it does not explain what the underlying mechanism behind exceptionally large shifts is. Figure 5.5 illustrates three possible mechanisms that explain why, at low salt concentration, the brush remains neutral even when the pH becomes high. The first, (Figure 5.5 A) attributes the preservation of the neutral brush at high pH to monomer-monomer interactions e.g. hydrogen bonding that prevent the acid functional groups of the brush from becoming charged.[36] However this explanation is not likely to be right since changing the salt concentration does not promote, or suppress non-electrostatic bonding to a large extent. Alternatively (Figure 5.5 B) a lack of solvated counterions to screen charges could mean that the brush remains neutral due to the strong energetic electrostatic repulsion penalty associated with charging. This explanation is unlikely because the pK_a shifts gradually as a function of salt concentration and large shifts occur even when the salt concentration is sufficiently high that enough counterions are available to screen charges.[189] The third and final explanation (Figure 5.5 C) is that there is a considerable entropic free energy penalty of counterion confinement. The availability of counterions in the brush, yet large energy penalty for confining these to screen charges, is what keeps the brush neutral at low salt concentrations. Isothermal titration calorimetry of polyelectrolyte have shown that counterion confinement is a significant free energy contribution.[27, 41, 190, 191]

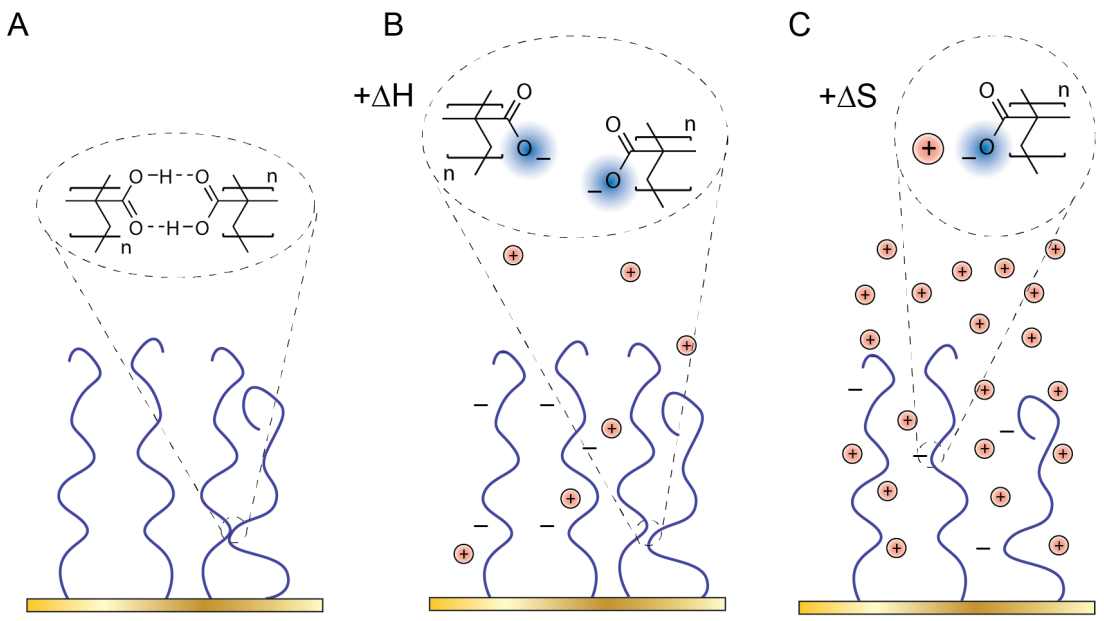

Figure 5.5: Three different proposed for mechanisms that cause brushes to remain neutral at low salt concentration. (A) inter and intrachain hydrogen bonding, (B) electrostatic repulsion between chains, due to lack of counterion screening, or (C) entropic penalty of counterion confinement to charges.

5.2.2 Implications for protein immobilization

If a polyelectrolyte brush is incorrectly assumed to be charged the attraction and repulsion of a charged species will be interpreted as electrostatic interactions. The primary example is a protein with a low pI ~4 (e.g. BSA or GOX) that immobilizes to a polyacidic brush when the pK_a is assumed to be the solution value ~4.5. Despite a net repulsion between the protein and the brush, the protein immobilizes in large quantities at pH 6, pH 7, and even at pH 8, an effect called immobilization on the wrong side of the pI.[19, 39, 38, 41, 42, 43, 44] In many cases where immobilization on the wrong side is observed, the salt concentration is kept very low ~1 mM.[19, 38, 39] Our results show that pH-responsive brushes (PAA, PMAA, and PDEA) are neutral at 1 mM salt concentration. PMAA is neutral with very low degree of charging (α<0.2 until pH ~8) (Figure 5.6). Many previous studies on protein immobilization to polyelectrolyte brushes do not provide a clear investigation into the degree of protonation.[19, 38, 39, 44] This means that protein might have in fact immobilized to neutral brushes, but

the interpretation made at the time was that the brush was charged thus incorrectly suggesting the electrostatic interactions as the underlying mechanism.

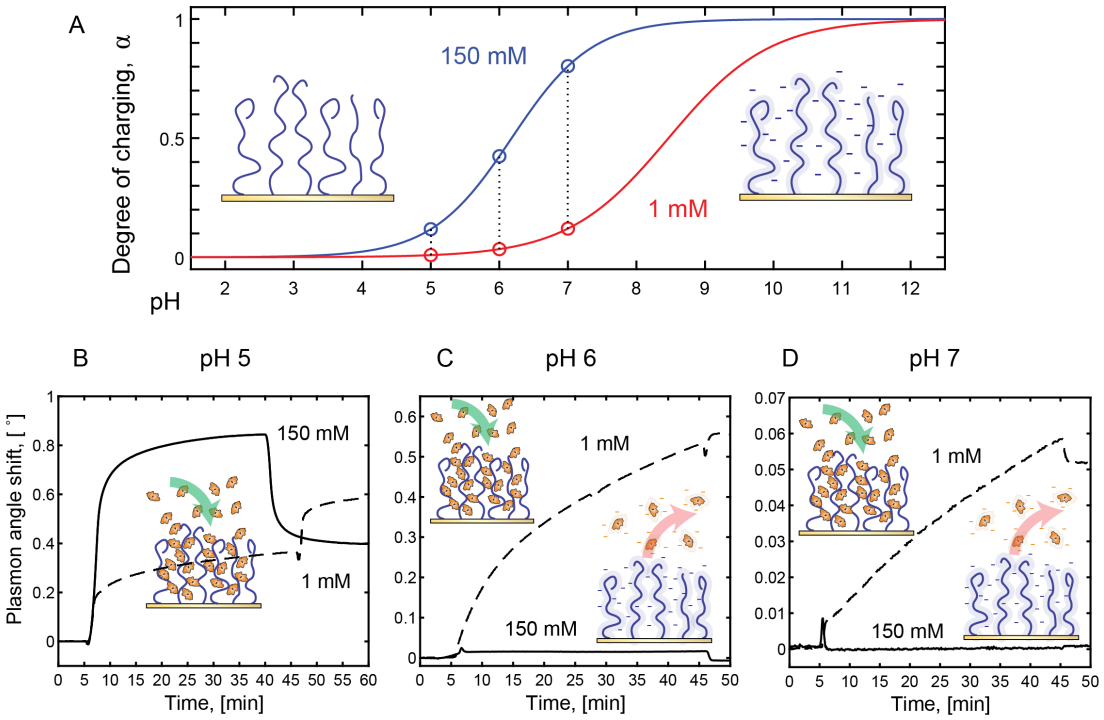

Figure 5.6: (A) Degree of charging (α) of PMAA at very low (1 mM) and physiological (150 mM) salt concentrations where the degree of charging is highlighted for three pH values where protein immobilization was performed. BSA protein immobilization to PMAA brushes at (B) pH 5, (C) pH 6, and (D) pH 7 at high and low salt concentrations.

To prove that the importance of the salt concentration, protein immobilization at 1 mM salt concentration was compared with physiological salt concentration (150 mM), Figure 5.6. Immobilization occured at 1 mM salt concentration for pH: 5, 6, and 7. As demonstrated by previous experiments with similar salt concentrations BSA immobilizes even at pH 7.0,[38] but at this pH the immobilization proceeds at a slower rate and in lower quantity because the pH is so far beyond the pI of the protein that it limits the extent to which the brush and the protein can interact. At physiological salt concentration, we only see immobilization at pH 5 but remarkably there is a complete absence of binding at pH 6 and 7. In summary, BSA only immobilizes to PMAA brushes that are neutral, or at least sufficiently protonated. In Chapter 5.4 I investigate this phenomenon fur-

ther and describe how proteins immobilize to neutral PMAA brushes by forming hydrogen bonds.

5.3 Polymer brushes as soft scaffolds for enzyme catalysis

Polymer brushes can immobilize large quantities of enzymes for efficient biocatalysis.[20, 42, 49, 51, 48, 192] They provide a soft, three-dimensional support where enzymes are immobilized with high retention of activity, in combination with high accessibility of reactants to diffuse to and from the active sites. However, the gain of immobilizing enzymes to brushes has not been systematically compared with alternative methods to clearly elucidate the effect that brushes have on the enzymes. Here we compare polyelectrolyte brushes with monolayers that contain similar functional groups, and with the bulk enzymatic activity as a benchmark. We provide proof of the high utility of polyelectrolyte brushes for enzyme immobilization and catalysis compared to monolayers.

5.3.1 Quantifying enzyme surface coverage to brushes

Glucose oxidase immobilization at pH 6.0 was quantified by SPR scans performed in air, Figure 5.7. An increase in the dry brush height is directly related to mass of immobilized enzymes since the refractive index of proteins on surfaces is 1.5,[193] the same as for brushes[42] and SAMs[194]. The coverage on SAM-modified gold agrees well with a GOX monolayer with reasonably high packing density, ~90 nm^2 per molecule (Figure 5.7).[193] However, the corresponding amount of irreversibly immobilized GOX within PAA and PDEA brushes clearly exceeds monolayer coverage. This proves that brush immobilization accommodate enzymes into a three-dimensional volume. The thickness of the brushes is relevant as this influences the volume of the brush and thus the number of enzymes that can immobilize. This partly explains why it was possible to achieve a higher surface coverage for PDEA than PAA, dry thickness of 42 nm and 26 nm respectively. But even when this is taken into consideration it is evident that PDEA has a higher affinity for GOX than PAA.

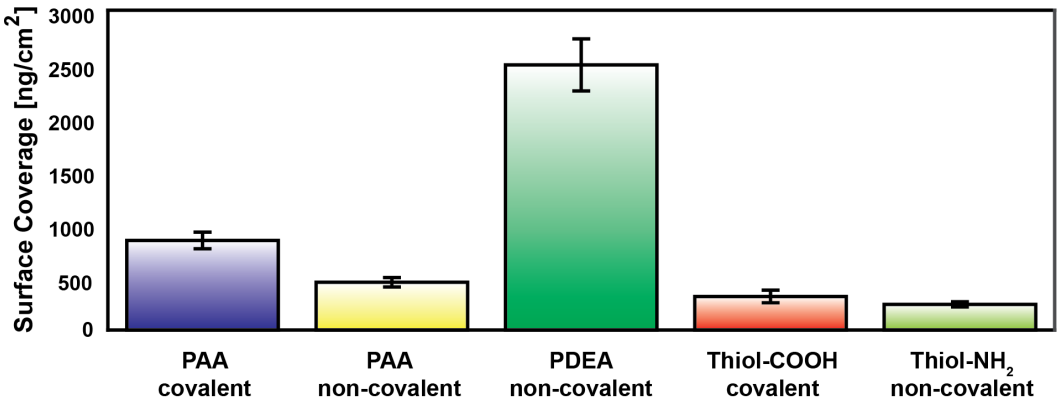

Figure 5.7: Surface coverage of enzymes on brushes and on SAMs achieved by covalent and non-covalent immobilization. (n=5 brushes, n=3 for SAMs). The dry PAA thickness was 27±2 nm and the dry PDEA thickness was 43±4 nm.

Quantification by air scans is advantageous compared to performing scans in liquid. Accurate liquid quantification of enzyme immobilization is difficult because polyelectrolyte brushes hydrate (discussed in Chapter 5.1), and the relative hydration may change as enzymes immobilize. Accurate quantification of bound enzymes is essential to accurately assess the activity per enzyme. Our dry scan methodology offers a simple refractometric way of quantifying enzyme surface coverage, even within brushes.

5.3.2 Activity retention on polyelectrolyte brushes

The activity of GOX immobilized to brushes, SAMs, and in bulk is summarized in Figure 5.8. The initial reaction rate per enzyme allows for a comparison between mechanism of immobilization. Covalent attachement of GOX to PAA, and non-covalent electrostatic attraction to PDEA fully retains the bulk enzyme activity rates. SAMs resulted in significantly lower reaction rates, and interestingly so did non-covalently immobilized GOX to PAA. Preserved activity in brushes has three likely explanations. First, the soft three dimensional structure, minimizing the interaction with the solid support, providing a gentle immobilization of enzymes. Secondly, for covalently bound GOX to PAA there may be a slight fixation of the enzyme by the EDC/NHS treatment, with respect to the significantly lower reaction rates of GOX that was non-covalently immobilized to PAA. Lastly, as shown in Chapter 5.1, polyelectrolyte brushes are highly hydrated which allows

for unhindered transportation of reactants and products to and from the enzyme active site. The activity of GOX in solution measured here is in good agreement with previous studies of GOX.[129, 128, 126] For instance, at the same glucose concentration as in this study, initial rates of 17 s^{-1} have been obtained,[126] similar to our value of 19 s^{-1}.

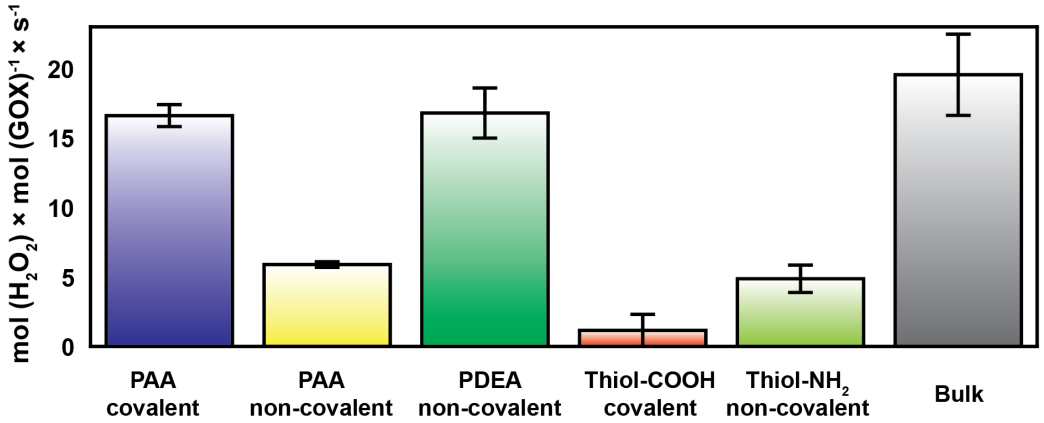

Figure 5.8: GOX initial rate (conversions per second) for different immobilization strategies compared with native bulk activity measured (in PBS pH 6.0 and [Glucose] = 0.01 M and 25 °C). Each measurement was repeated in at least triplicate.

In addition to retention of native GOX activity, it was possible to re-use the surfaces. When non-covalent immobilization was used, as long as the pH was remained fixed to the same solution pH used for immobilization, the enzymes were irreversibly bound to the surfaces. Recovery of enzyme activity upon repeated experiments with the same surface confirmed that reduction in reaction rate is due to enzyme kinetics, not due to inactivation of enzymes. Reduction in rate depletion of reactants was analyzed showing that only 2% of glucose was consumed while 20% of oxygen was consumed at the end of each experiment. It is expected that a gradient of oxygen within the reactant solution develops due to its depletion within the brush by the enzyme reaction. Since only 20% of the oxygen was consumed, lack of reactants is likely not the primary explanation for lowered rate of the reaction over time. Self-poisoning of the products, primarily hydrogen peroxide, is an effect which has been confirmed to occur for GOX, making it a likely cause for the reaction rate reduction. Despite reactant depletion and self-poisoning, the comparison between the brushes, SAMs, and

native GOX still clearly shows that brushes fully preserve GOX activity.

5.4 Generic method for protein capture and release by pH control

Capture of proteins to polyelectrolyte brushes by electrostatic attraction is useful if the intention is to store or use the proteins on the surface.[48] However, removal of protein requires breaking electrostatic attractions, which are relatively strong and may require either extremely large pH changes,[24] high concentrations of salt,[19, 24] or surfactants[55]. This treatment risks denaturing of the proteins, which in turn results in permanent binding of denatured protein to the surface. Contamination by denatured protein risks removing the stimuli-response of the polymer and thus diminishing the capacity between capture and release cycles. Alternatively, electrostatic *repulsion* could be used for protein release. Repulsion of proteins by switching the polyelectrolytes to become highly hydrophilic and charged results in anti-fouling, protein repelling properties of the polyelectrolyte brush, in addition the swelling of the brush due to charging is expected to facilitate the ejection of protein.[18] Here I present a catch-and-release solution that employs release by electrostatic repulsion and which utilizes a non-electrostatic attraction mechanism that is sufficiently strong to hold a significant quantity of protein, but also weak enough to not interfere with pH-induced charging of the brush that triggers release. To begin with, examples of pH induced binding and release of *synthetic polymers* to polyelectrolyte brushes is presented. Following this, I will discuss how the same mechanism for capture and release also apply *for proteins*.

5.4.1 Capture of polymers by hydrogen bonds

In Chapter 5.1, non-interacting probes for polyelectrolyte brushes in neutral and charged states were investigated. If a molecule bound to the polyelectrolyte brush, however weakly, it was discarded as a candidate since it cannot probe the brush height if the molecule binds to the brush. However, in the quest for achieving catch and release of molecules from brushes, the non-interacting probe

candidates that fail the test are interesting. Specifically, a polymer molecule that binds to the neutral brush, but is repelled by the charged brush, is the ideal case for developing a catch and release solution (Figure 5.9).

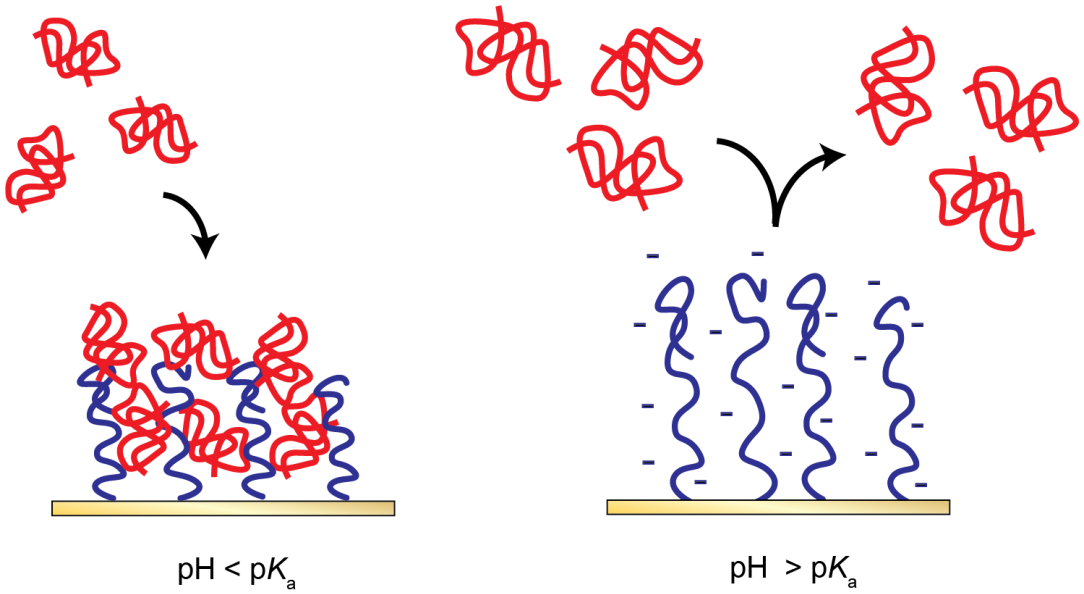

Figure 5.9: Desired properties of a candidate polymer molecule for pH activated catch and release from polyelectrolyte brushes.

PEG was found have a pH dependent interaction with PAA and PMAA brushes, as illustrated in Figure 5.9. PEG displays a weak interaction with neutral PAA and PMAA brushes at low pH, and a large fraction of PEG releases from the brush with rinsing. For small molecular weights of PEG (<2 kDa) almost all bound molecules are rinsed away, but for larger molecular weights (>8 kDa) the binding is stronger and a larger fraction is permanently bound to the neutral brush. The primary interactions between PEG and PMAA are hydrogen bonds (Chapter 3.2.2), which have been extensively studied in polymer solutions.[93] PEG is completely released by even a modest increase in pH, as the brush becomes charged and the hydrogen bonds break (PEG is a neutral polymer so it is not electrostatically repelled from the brush). Thus, polymers that are sufficiently large enough and can form hydrogen bonds can be captured and released as a function of pH.

Capture and release of PEG serves as a proof of concept but our method can be expanded to work with a useful target. PEGylation of proteins is used to

prepare biopharmaceuticals with extended intravenous circulation time.[195] Therefore, we tested PEG conjugation of BSA to see if our polyelectrolyte brushes could be used to capture PEGylated protein (Chapter 4.3). The hypothesis made was that a PEG shell surrounding the BSA would facilitate binding of the protein to the neutral brush in the same way as free PEG coils. PEG-BSA bound to neutral PMAA brushes as predicted, shown in Figure 5.10. But contrary to the expectation, even native BSA bound, meaning that native BSA also possess the functional groups that binds to neutral PMAA. Interestingly, less PEG-BSA bound compared to native BSA. A plausible explanation is that PEG-BSA increases in size to the extent that it is sterically hindered from entering the brush in large quantities (gel electrophoresis showed that at least 10 PEG chains was conjugated to every BSA). However, native BSA is smaller and a more compact molecule which enables it to enter and accumulate within the brush more efficiently.

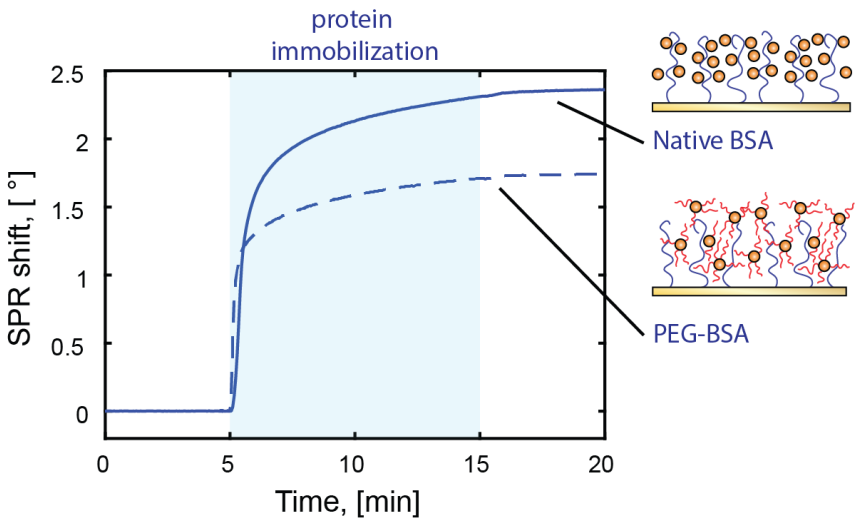

Figure 5.10: SPR sensorgram that compares binding of Native-BSA and PEG functionalized BSA to neutral PMAA.

For proteins, hydrogen bonds with the polymer brush, could be responsible for the immobilization. The specific binding mechanism is more uncertain since the surfaces of proteins display a variety of different amino acids, capable of binding by other mechanisms than forming hydrogen bonds (Chapter 3.2.2), but by electrostatic attraction, and hydrophobic interactions. In addition, if the protein unfolds, the hydrophobic interior of the protein would also interact with

the neutral brush.

In summary, hydrogen bonding polymers like PEG (other confirmed cases are PHEA and PNIPAAM) and proteins immobilize to neutral polyacidic brushes. The equal or larger affinity of proteins to neutral brushes than hydrogen bonding polymers raises the prospect of skipping conjugation of the protein altogether. However, it is crucial to establish that proteins can release equally well as PEG to perform catch and release.

5.4.2 High capacity catch and release of proteins

Release of proteins from polyelectrolyte brushes is more complex than release of synthetic non-ionic purely hydrogen bonding polymers. This is because the release of proteins from the brush is governed not only by the charging of the brush, but also by the changes of the surface charge of the protein. If the pI of the protein is high, charging the brush will at some point result in an opposite charge between the two. Electrostatic attraction between the brush and the protein would suppress the release of protein until the pH>pI of the protein, resulting in net electrostatic repulsion. However, if the pI is relatively low, immediate release is triggered by a small increase in pH. The effect of protein pI was tested with two proteins of different pI; avidin (pI 10.7) and IGG (pI ~7) (Figure 5.11). At pH 5.0 PMAA is completely neutral and a rapid binding event is recorded. At pH 8.0 when PMAA is completely charged avidin immobilizes; this is where the net electrostatic attraction is the highest. But at pH 11.5 the protein is entirely repelled from the brush. For IGG the trend is very different. At pH 5 significant immobilization of the protein is observed, but at pH 6.5 and 8.5 IGG binding to the brush is completely suppressed. Importantly, when a brush is fully loaded with IGG at pH 5.0, then rinsed in buffer solution of pH 8.5, full protein release as a consequence of electrostatic repulsion occurs. The full regeneration of the brush to the state prior to protein immobilization enables multiple catch and release cycles of proteins by this method.

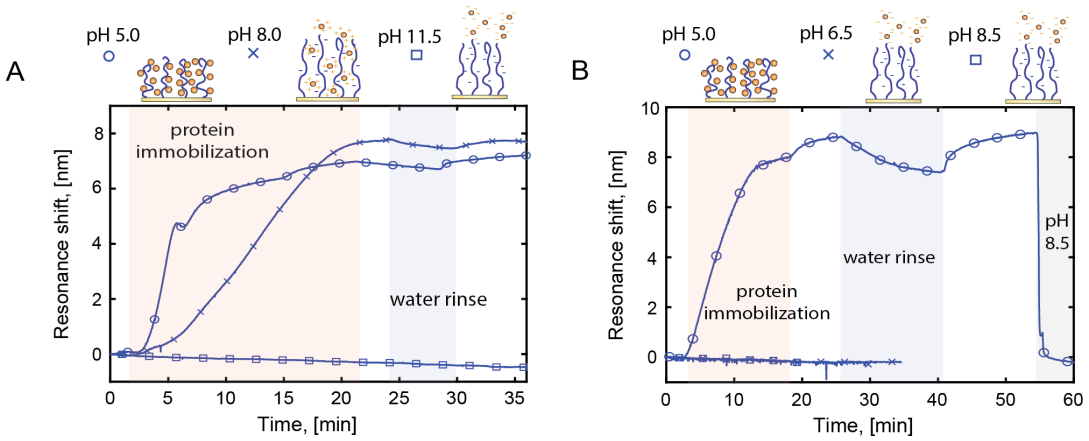

Figure 5.11: Extinction spectroscopy sensorgram of (A) Avidin and (B) IGG binding to PMAA at different pH.

Performing this experiment for many different kinds of proteins clearly demonstrates that immobilization to neutral PMAA occurs *for all* protein (Figure 5.12) in addition to hydrogen bonding polymers, and certain lipids. Nucleic acids and carbohydrates did not immobilize at all, indicating that this could potentially be a method for separation of proteins and certain hydrogen bonding molecules out of complex mixtures. For each protein the amount of immobilized protein was determined by SPR air scans. The quantity of protein that immobilized was mostly within the range of μg/cm^2. The protein structure, investigated by CD, as well as catalytic activity of GOX was shown to be retained after catch and release, indicating that the protein structure and function is preserved making this a gentle but effective method.

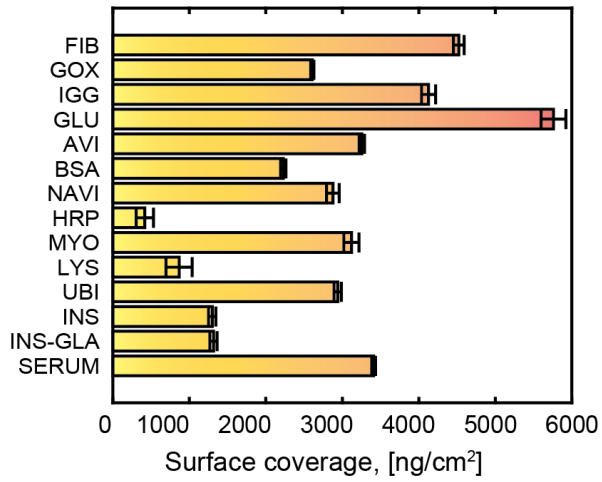

Figure 5.12: High capacity for immobilization of different proteins to PMAA brushes determined by air SPR scan quantification.

In summary, we present a new generic method for catch and release of protein. It operates by changes in pH that triggers the hydrogen bonding capability of the brush (the catch mechanism) when the pH is lowered, and uses electrostatic repulsion as a release mechanism when the pH is increased. Our method is unique compared to conventional protein immobilization by electrostatic attraction and it offers several advantages. First, by hydrogen bond capture is a gentle immobilization mechanism that leads to retention of structure and function. Secondly, the complete reversibility enables surface re-use, enabling multiple capture and release cycles. Third, for release the pH only needs to slightly surpass the pI. Fourth, the quantity per surface area makes this technique appealing for applications requiring high capacity protein handling e.g. protein recovery and purification.

5.5 Electrochemical catch and release of proteins

This chapter presents further development of the generic protein capture and release concept presented in Chapter 5.4. Here, the pH change that triggers capture and release is performed at the interface of the brush by electrochemical reactions rather than changing the pH of the bulk solution. Retaining polyelectrolyte brushes bound to the electrodes has been a great challenge in the past.

By using diazonium surface chemistry we accomplished highly stable polyelectrolyte brushes compatible with electrochemical signals; thus enabling electrochemical capture and release of proteins.

5.5.1 Switch of pH by electrochemical potentials

In a pump-driven fluidic system the pH is changed by pumping different buffers set to the appropriate pH. This is a slow process that relies on fully replacing the fluid in the system before the intended pH is reached. There are several situations where the pH of the system cannot change easily for instance in a biological environment changes in pH will have an impact on health and cell viability. However, the method described in Chapter 5.4 relies on pH changes to achieve capture and release of protein. Therefore, to transfer the method of protein capture and release into pH sensitive environments, there is a need to avoid systemic pH changes while still allowing pH changes within the polymer brushes. Local switching of pH by using electrochemistry is one possible solution since this potentially only changes the pH in the vicinity of the electrode. However, in order to switch pH by electrochemistry the brush needs to be stable to electrochemical potentials. Diazonium salts produce aryl anchors to the gold electrode surface which are electrochemically inert after adhesion. In Figure 5.13, diazonium anchored PMAA polyelectrolyte brushes are switched from high to low pH by oxidation of hydroquinone and from low to high pH by consumption of protons and dissolved oxygen.

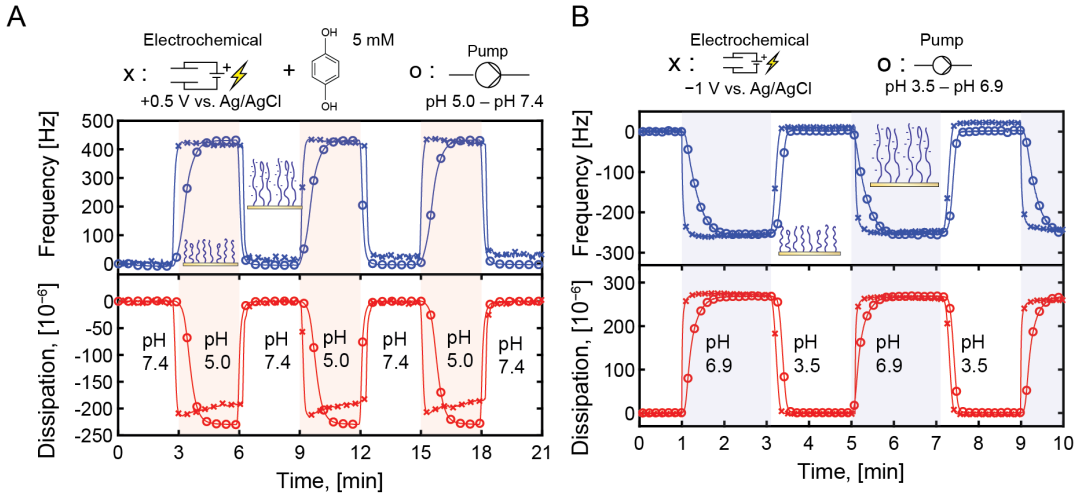

Figure 5.13: In-situ electrochemical QCM-D that compares brush switching by local pH change with application of electrochemical potentials compared to switching the solution pH. In (A) from high pH to low pH and in (B) from low to high pH.

Switching of the polyelectrolyte brush from neutral to acidic pH requires the addition of a reduction agent (Figure 5.13 A). Hydroquinone was oxidised by applying a positive potential, +0.4 V, but switching of the brush was accomplished for even lower magnitude of potentials. Similar to hydroquinone, natural reduction agents such as dopamine and ascorbic acid produced brush collapses too, highlighting that brush switches can be accomplished even with biologically occurring substances (Figure 3.6.2). The opposite brush switching behavior (Figure 5.13 B) from neutral to charged occurs by electrochemical consumption of protons in the presence of dissolved oxygen to form water, Equation 3.6.2.

Surface sensing techniques, such as SPR and QCM-D, detects the gain or loss of material, making these techniques particularly useful for evaluating reversible electrochemical switching of polyelectrolyte brushes. In previous studies using these characterization methods successful electrochemical switching of the brushes did not occur. Unsuccessful switching was most likely because electrochemical reactions that produce a pH change were not used and because of electrochemical instability of the anchor groups of brush to the electrode surface.[58, 57] An alternative method for characterizing electrochemical switches is contact angle. Here the relative wettability of polyelectrolyte brushes was used to indicate electrochemical reversible switching of polyelec-

trolyte brushes.[196, 59] However, this does not prove the absence of brush de-grafting since switchable wettability may persist even after significant loss of polyelectrolyte has occured. In contrast to previous work on electrochemical switching of polyelectrolyte brushes we show for the first time reversible electrochemical switching, by in-situ QCM-D (Figure 5.13) which detects reversible hydration and dehydration alongside extremely sensitive detection of mass uptake and release as a response of the electrochemical signal.

5.5.2 Electrochemical protein catch and release

Building on the results of Chapter 5.4 electrochemical switching of the polyelectrolyte brush to perform electronically induced protein capture and release was applied (Figure 5.14).

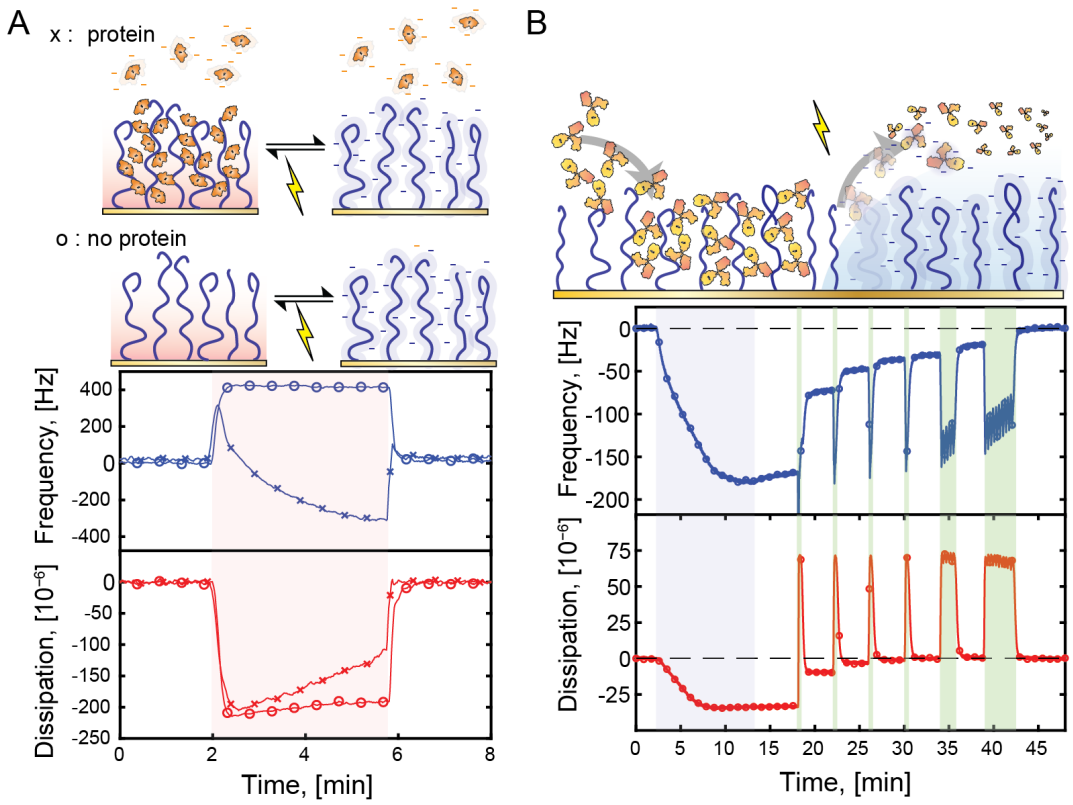

Figure 5.14: Electrochemical catch and release of proteins from PMAA brushes monitored in-situ by QCMD. (A) Protein immobilization on-demand occurs when applying an electrochemical potential in the presence of BSA. (B) Spontaneous immobilization of IGG followed by tunable stepwise electrochemical release.

When a positive potential is applied in a phosphate buffer with pH 7.4 that contains 5 mM hydroquinone in addition to 0.3 g/L BSA, the surface pH rapidly decreases due to oxidation of hydroquinone . This in turn causes spontaneous immobilization of proteins to the neutral brush (crosses in Figure 5.14 A), verified by a control experiment where there was no protein present (circles in Figure 5.10 A). Upon releasing the potential, the pH immediately returns to its initial neutral value, returning the brush to its charged state followed by release of protein due to repulsion. IGG rapidly immobilized reaching equilibrium within 10 minutes when the experiment started in phosphate buffer set to pH 5 (Figure 5.14 B). Gradual release was performed, first by single electrochemical CV scans that removed proteins in small doses, followed by multiple cycles until complete removal of IGG from the PMAA brush was accomplished, that returned the frequency and dissipation signals to the baseline value prior to IGG immobilization introduction.

5.5.3 Dynamic protein biochips

Reversible rearrangement of proteins via mild interactions on surfaces enables electronically controlled protein patterns. This was accomplished using interdigitated gold electrodes (Figure 5.15). Applying electrical signals selectively, only brushes attached to a specific electrode triggered protein release. The gold electrodes were fabricated by colloidal lithography to nanoholes, which enables refractometric confirmation of protein immobilization by the localized plasmonic extinction signal shifts (Figure 5.15 A).[197] Localized release of proteins from electrodes was confirmed by fluorescence microscopy. If the fluorescent proteins are selectively released from an electrode this produces an empty brush. Subsequent immobilization of a protein conjugated to a different color fluorophore produces a high contrast in color when the two electrodes are compared (Figure 5.15 B). The fluorescence signals clearly show that the pH gradient produced is sufficiently local on the micrometer scale to selectively remove proteins from the activated electrode and not to the adjacent passive electrodes.

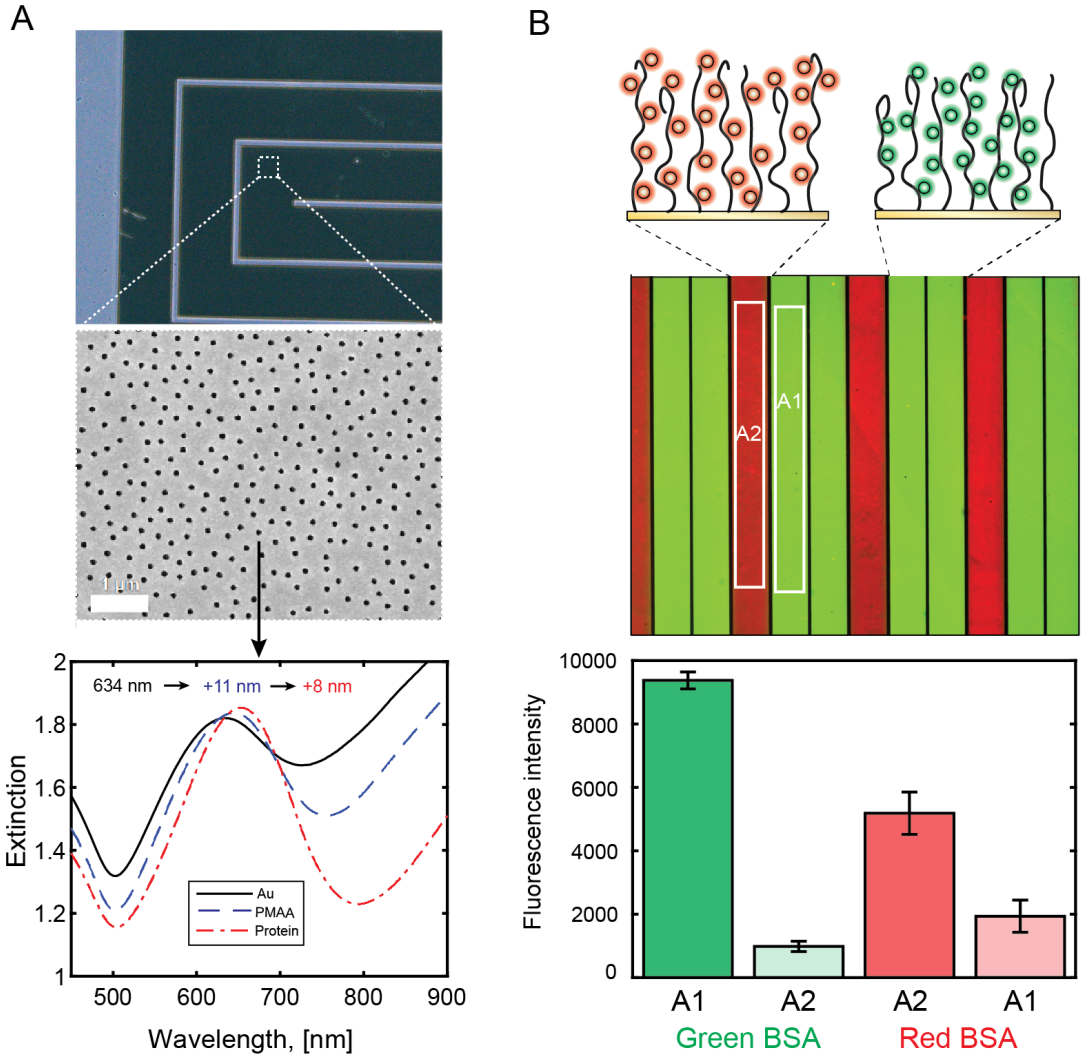

Figure 5.15: Protein capture and release from microelectrodes with a nanostructured surface. (A) Photo of microelectrodes that are 100 μm wide and electron micrograph of nanoholes with a 1 μm scale bar indicated in the figure. The nanostructure produces a resonance peak shift in the extinction spectrum that confirms brush synthesis and protein immobilization on the nanostructured gold. (B) Fluorescence from microelectrode stripes after local release from one electrode followed by a second immobilization step producing protein patterns.

Several methods to produce protein arrays on the micro and nanoscale have been proposed and developed.[52, 10] Our new method for producing patterned protein biochips combines high capacity uptake with highly reversible interactions (see Chapter 5.4). In addition it preserves the protein function and structure, as verified using CD and enzyme activity assays. For bioana-

lytical applications, reversible interactions and retention of protein function are critical for producing dynamic interfaces between between electronics and biological environments. Contrary to our method, many previous solutions form SAMs, or immobilize directly on hard and inflexible surfaces.[52, 198, 199] This greatly limits the capacity for immobilization, decreases the activity of the protein (see Chapter 5.3), and it restricts the applicability of such interfaces. It is also common to utilize irreversible covalent conjugation reactions for patterning.[54] This has limitations as the surface cannot be reset, reconfigured, or adapted to new needs. On the contrary, our solution has the capability to retain the biological function of the biomolecules it immobilizes, it can be reconfigured on-demand by specific electronic signals, and it is re-usable.

5.6 Biocatalytic switching of brushes

We performed switching of polyelectrolyte brushes using a variety of redox species, dopamine, ascorbic acid, and hydroquinone. For substantial pH gradients to occur these redox species needed to be present at relatively high concentrations (5 to 20 mM). However, for the method to be useful in biological environments it preferentially consumes a naturally occurring and abundant substance. Thus, we need to replace hydroquinone, which produced the best electrochemical switches, with some abundant biological molecule that can switch the brush equally well. An alternative strategy is to replace the electrode surface, which alters or expands the electrochemical capability for reactions that produce pH gradients.

Platinum was considered as it is known to have excellent electro-catalytical properties.[200] Diazonium ATRP initiators followed by polymerization of PMAA could be performed with the same protocol as used for gold surfaces, highlighting the possibility to produce PMAA brushes using different substrates with this method.[164] Similar to for gold, platinum surfaces could be used to produce pH gradients. However, we could also produce acidic pH gradients by the consumption of hydrogen peroxide at 5 mM, which was not possible with gold.[147, 201]

$$\mathrm{H_2O_2} \xrightarrow{+1.0\ \mathrm{V}} \mathrm{O_2} + 2\mathrm{H^+} + 2\mathrm{e^-}.$$

Hydrogen peroxide is an interesting example since hydrogen peroxide can be

produced by biocatalysis using abundant substances glucose and oxygen (Scheme 3.8). A modified protocol employing EDC/NHS conjugation was used to create a GOX−PMAA brush where re-hydrolysis of the carboxylic acids restored the pH-response. Complete electrochemically induced switching was observed when exposed to 10 mM glucose and by application of a positive electrochemical potential (Figure 5.16). The exposure of glucose to GOX−PMAA functionalized surface produces a locally elevated hydrogen peroxide within the brush. When a positive potential is applied (+1.0 V and +1.2 V) a switch to acidic conditions occurs where enzymatically produced hydrogen peroxide is consumed to produce protons, analogous to the case where hydrogen peroxide is added to the buffer solution, except now the hydrogen peroxide is produced locally, at the brush interface for rapid electrochemical consumption. The brush returns to basic solution either passively by removal of the pH gradient by the buffer solution, or actively by applying a weakly positive, or negative, potential (+0.05 V and -0.2 V). This results in a rapid return to neutral pH by consumption of protons and oxygen producing primarily water, analogous to Figure 5.13.

The retention of the pH-responsivity of the GOX-PMAA brush indicates that a majority of carboxylic acids remain unchanged. A high concentration of carboxylic acids within the brush means that the brush can still accommodate large quantities of protein, despite that it now contains GOX. Therefore, we can still expect a high surface coverage for other proteins that can be captured by hydrogen bonding, triggered by biocatalytical electrochemical pH gradients. The vast number of enzyme substrate combinations possible that can produce pH gradients indicate the possibility of several other alternatives and combinations that can be used to optimize the switching properties for improved or additional functionalities.

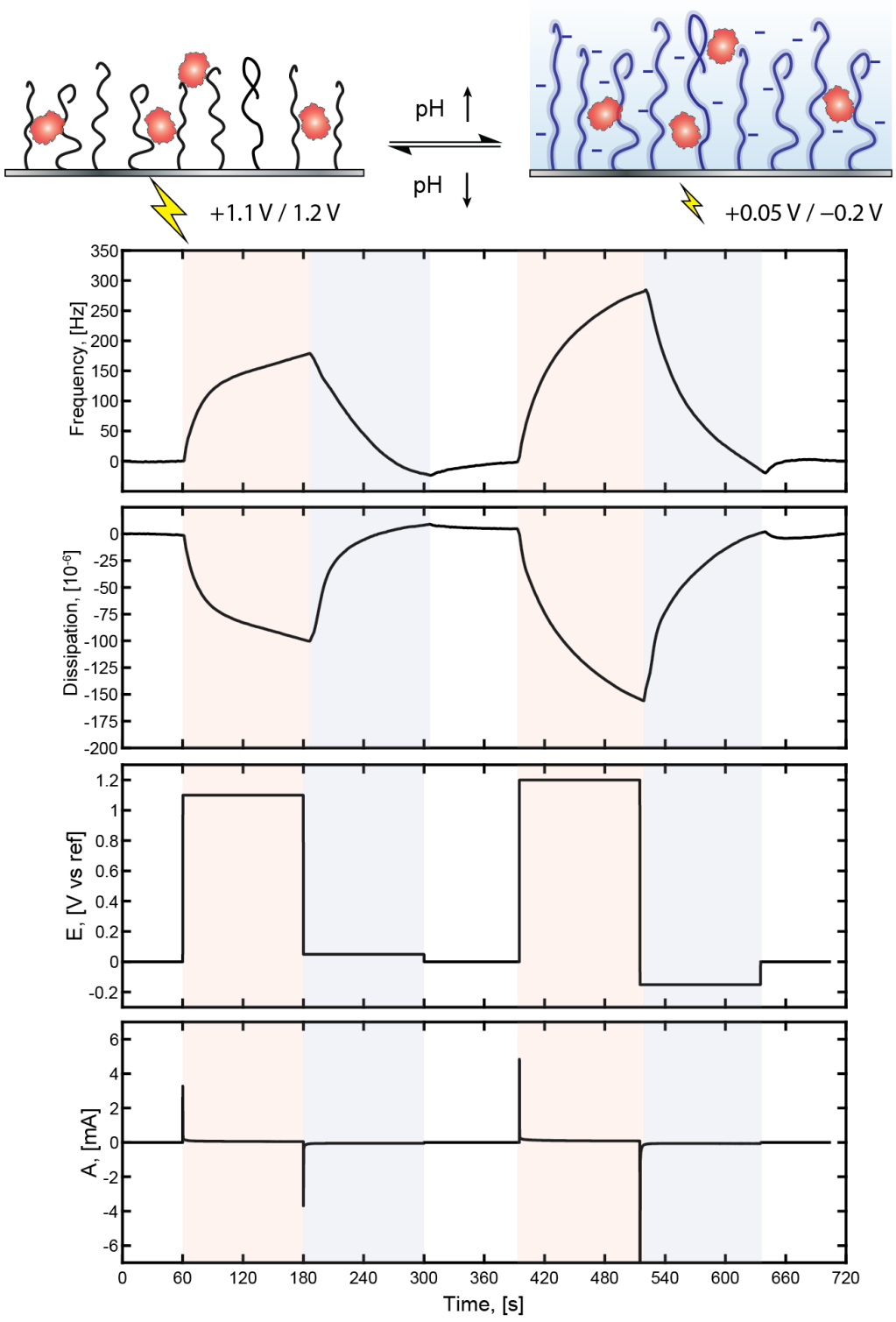

Figure 5.16: In-situ electrochemical QCMD measurement of (A) frequency and (B) dissipation for switching of GOX-PMAA brushes on platinum electrodes in PBS containing 10 mM glucose showing (C) the voltage applied and (D) the corresponding current recording.

The combination of biocatalysis and electrochemistry for switching GOX-PMAA brushes provide a way for producing acidic pH gradients using an abundant, non-toxic, and naturally occurring substances that could be used for holding and releasing proteins in biologically relevant fluids. These results suggests potential use of our protein capture and release system in future bioelectronic interface applications that encompass protein uptake for sampling, protein release for drug delivery and protein repulsion for anti-fouling.

5.6.1 Summary of the concept

The method for electrochemical catch and release of proteins is summarized in Figure 5.17. Proteins hydrogen bond to neutral, weak PMAA brushes. The loaded brush resists spontaneous protein release when exposed to serum. Upon applying an electrochemical signal an interfacial pH gradient is produced, charging the polyelectrolyte brush and inducing protein release. The electrochemically inert aryl anchor prevents de-grafting of the brush upon application of electrochemical potentials.

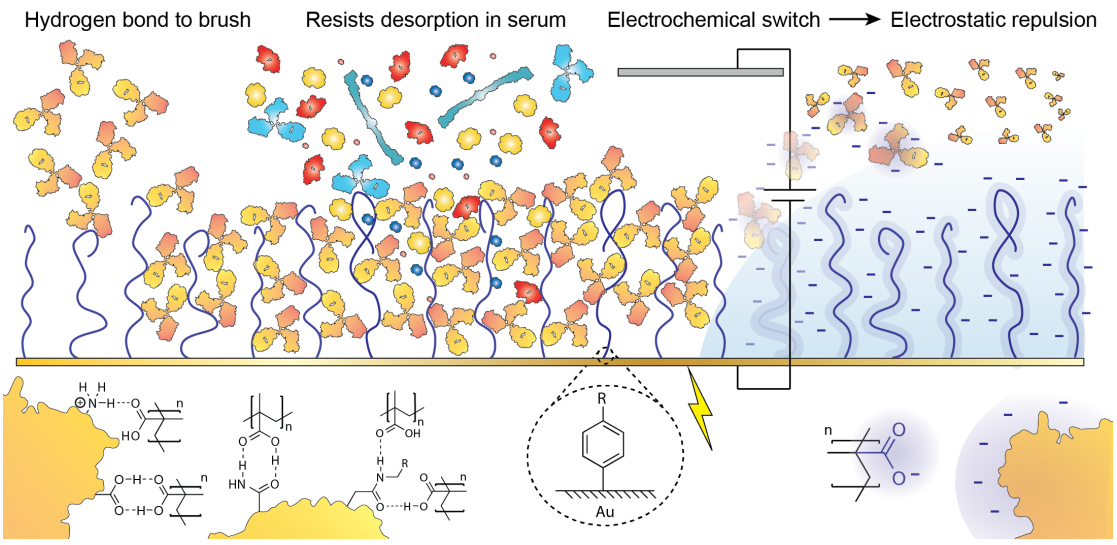

Figure 5.17: Concept for generic capture and electrochemical release of proteins.

As monoclonal antibodies constitute a major class of pharmaceutical and have grown to become an essential tool in life science research they are used as an example in Figure 5.17. The production of antibodies and the downstream pu-

rification processes are extremely expensive and demanding.[202, 203] Therefore any new tool or method that can simplify, reduce the cost of, or improve the purification downstream process is highly desired.

6

Conclusion

In the past polymer brushes were either protein repellent or protein binding. In this thesis I showed how polyelectrolyte brushes can switch between both properties on-demand by electronic signals. Electrochemical capture and release of proteins was enabled by combination of insights. The first insight related to the behavior of polyelectrolyte brushes and in particular their electrostatic and non-electrostatic interactions with proteins. In parallel, I studied the behavior of polyelectrolyte brushes in response to electrochemical gradients. The critical insight was that diazonium salts deposited by mild chemical activation with ascorbic acid produces a strong anchor to the underlying surface, without compromising the electrochemical capability of the underlying electrode. The combination of these results, allowed for the development of polyelectrolyte brush electrodes that switch between an anti-fouling or protein repellent state electronically on-demand.

Polyelectrolyte brushes were characterized for the first time using non-interacting probes. It was shown to be a reliable method for determination of both the charged swollen and neutral collapsed brush height. This is important as it enables improved understanding of the true brush thickness without invasive influence of the probe, while representing a cheap, simple and non-destructive method of characterization. Multiple molecular probes were identified to work for different polyelectrolyte brushes. Proteins, although useful for probing heights of non-polyelectrolyte brushes like PEG, were found to be unsuitable as non-interacting probes of polyelectrolyte brushes due to protein-polyelectrolyte interactions.

The pK_a of polyelectrolyte brushes (basic and acidic) was found to be exceptionally sensitive to changes in the solution salt concentration. Extremely high or low pH was required to fully charge the brush at low salt concentra-

tion, which has implications for the underlying mechanisms behind protein immobilization under these conditions. Brushes were prevented from charging at low salt concentrations due to the high entropic cost of confining counterions within the brush to screen charges. This effect originates from the very dense polymer concentration established within the brush, but which is not unique to brushes. Consequently, strong shifts in pK_a is likely to occur also in other polymer structures with a large concentration of acidic and basic functional groups e.g. hydrogels, layer-by-layer assemblies, and phase separated polyelectrolyte coacervates.

Enzyme activity was fully preserved upon immobilization to polyelectrolyte brushes. The brushes strike a balance between enzyme loading and catalytic activity, superior in both respects to self-assembled monolayer surfaces. Our results suggest that the long and thus more flexible links between the enzyme and surface are important to preserve high activity. However, further work is needed to confirm this for more polymers and other enzymes. Electrostatic attraction of enzymes to polyelectrolyte brushes was shown to constitute a sticky adhesion, retaining all enzymes. Strong adhesion is desirable in biocatalysis to limit leaching of enzymes. However, in applications where the intention is not permanent immobilization, but for subsequent release, an alternative interaction that is easier to break is preferable.

Generic protein uptake and release to PMAA brushes triggered by pH change represent a method for high-capacity capture and release of PMAA to brushes. The pH-responsive interaction between proteins and PMAA brushes was utilized to first bind proteins by hydrogen bonds at low pH below the pK_a of the brush, and to release proteins by electrostatic repulsion by increasing the pH beyond the pI of the protein. Importantly this method resulted in full preservation of protein structure and enzyme activity proving that it is a gentle technique for protein handling. Furthermore, the technique was found to be specific to proteins and synthetic hydrogen bonding polymers, making it a potentially useful technique to capture and purify large quantities of protein from other biological molecules.

pH-induced switching of polyelectrolyte brushes from basic to acidic and reverse could be accomplished using electrochemistry rather than by changing the solution pH. Critical for achieving this was to utilize diazonium surface chemistry to make electrochemically inert polyelectrolyte brushes while preserving

the electrochemical properties of the electrode surface. Electrochemically robust anchoring of polyelectrolyte brushes broadens the scope for applications of polyelectrolyte brushes. One example I explored extensively was the use of polymer brush electrodes for triggering repulsive or attractive interactions with proteins on-demand by electric signals. Electronic control of protein immobilization was used to demonstrate reversible protein patterning on microelectrodes, protein uptake and release by electronic activation, and capture and release of proteins within biological fluids e.g. serum.

The background of this thesis addresses two difficult but important challenges: The realization of synthetic biocatalytic nanoreactors and the development of dynamic biointerfaces that can operate in biological environments. Due to the complexity of these challenges they are to be viewed as open-ended indefinite goals. A nanoreactor could incorporate more functionality with better yield and larger output, and a biointerface can be developed to reach ever finer control and sensitive readout of the living systems it is interfaced with. I am pleased conclude that this thesis contributes with new scientific understanding of polyelectrolyte brushes and with understanding of their potential use in technological applications.

7

Outlook

The Outlook is a summary of interesting directions for future research including some preliminary results, to highlight the potential of new scientific knowledge and technological advances. I will explore the potential of using electrochemical polymer brush electrodes for protein purification and drug delivery. Furthermore, I would like to study the presence of nanobuffering in polyelectrolyte brushes. Lastly, the prospect of using polyelectrolyte brushes as nanoscale scaffolds for enzyme cascade reactions (by bringing different enzymes into close contact in-vitro) is an appealing concept which, if properly tuned, could be used to realize high throughput of complex enzyme reaction pathways.

7.1 Protein purification

Protein pharmaceuticals, primarily monoclonal antibodies (mAbs), are used to treat a wide range of diseases, including cancer, autoimmune, cardiovascular, and infectious.[105, 204, 205, 206] However, the cost of protein production is very high, which limits their widespread use in life-saving therapies.[207] The most cost-intensive part of the production is the downstream purification of proteins by chromatography separation after cell harvest. The current dominant commercial method of mAbs purification is affinity chromatography, which separates mAbs by a highly specific interaction (Figure 7.1). The protein A chromatography resin is very expensive (>50% of downstream processing costs) and requires careful maintenance and cleaning to reduce loss of function, and this treatment generates large volumes of contaminated eluent.[208] The protein capture step by affinity chromatography is often employed as soon as possible after cell harvest, which increases the risk of resin inactivation by non-specific binding.[106] Although significant progress has been made to achieve

some scalability, recent innovations and improvements are arguably incremental.[106, 203] In light of this, our new and unique method comprising an electrochemical capture and release system of proteins provides a new alternative, and powerful method of protein purification.

Four different applications of protein purification are envisioned (Figure 7.1 B-E). The first relates to the high specificity of protein to other biomolecules such as carbohydrates or DNA (Figure 7.1 B). This generic, high-capacity immobilization of proteins could make this a method for early stage capture of proteins out of complex biological solutions. Since our method preferentially immobilizes large proteins there also is a possibility of separation by molecular weight (Figure 7.1 C). Another option is separation by isoelectric point by tuning the electrochemical signal (Figure 7.1 D). The final application uses pH responsive peptide ligands that mimic the hydrogen-bonding properties of carboxylic acids, that improves the selectivity of the interaction to separate a specific protein (Figure 7.1 E). This concept is especially interesting where protein A chromatography is not a viable option, for purifying all kinds of proteins.

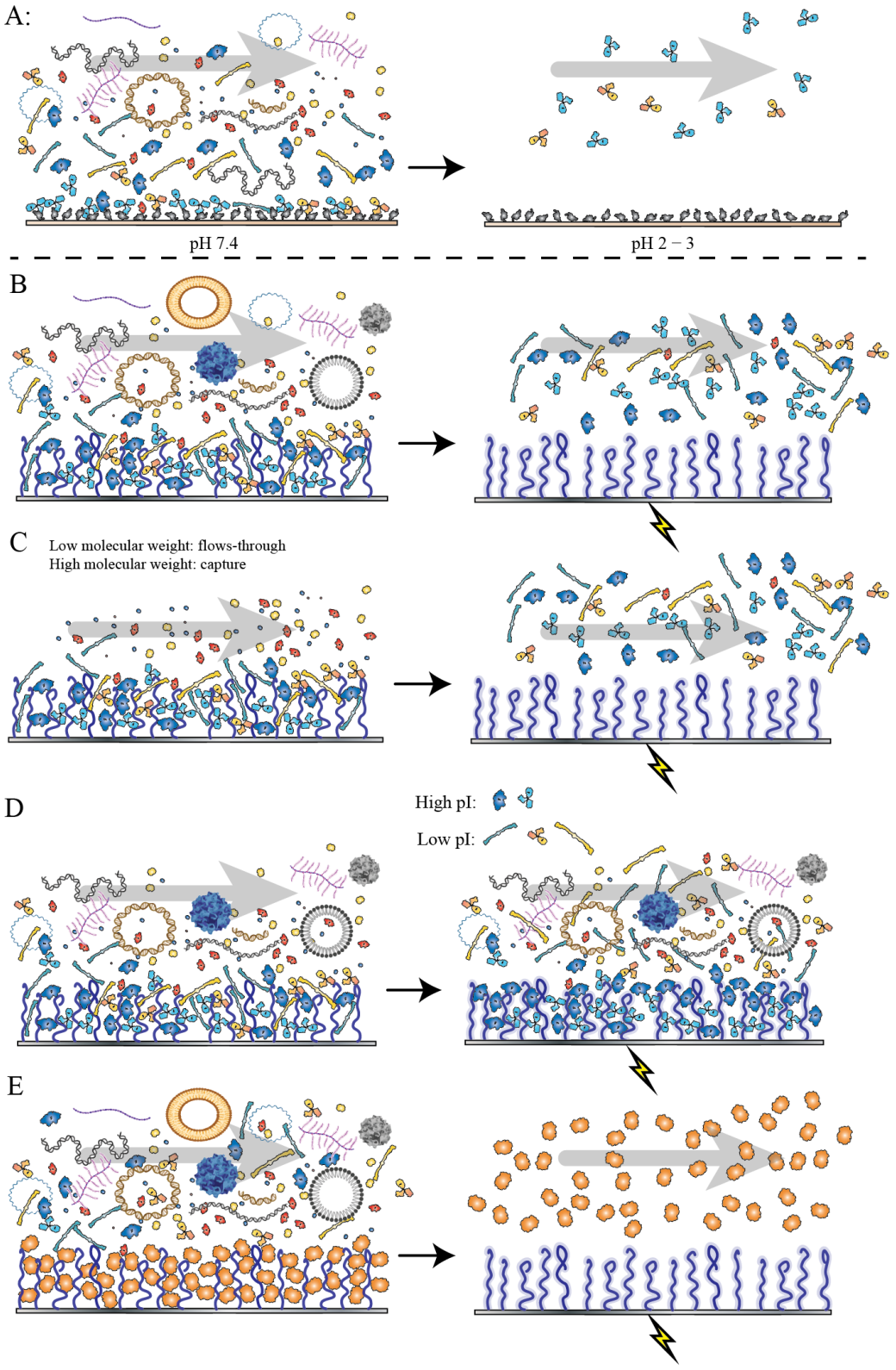

Figure 7.1: Commercial protein A purification of mAbs (blue in figure) from cell culture harvest containing a broad range of contaminant proteins and other biomolecules (A), compared with four potential strategies for electrochemical protein purification (B to E).

In protein purification the release of protein from the stationary phase, often requires harsh conditions. For instance, in protein A chromatography elution occurs at pH $2 - 3$.[106, 208] Passive approaches to pH change require complete replacement of the column liquid, which leads to long exposure to extreme pH values that may denature the protein. Our method actively changes the pH locally on the surface (by electrochemistry), minimizing the exposure to extreme pH, contrary to conventional resins. We utilize polymer brushes which allows exceptional surface coverage capacity compared to monolayers. In contrast to conventional methods the binding capacity of our stationary phase does not rely on containing high internal surface area, potentially removing the need of highly porous solid supports with diffusional contraints. Chromatography columns are routinely regenerated by basic media e.g. sodium hydroxide 0.1 M. This treatment is compatible with our solution too since polyacidic polyelectrolyte brushes become highly non-fouling and completely regenerated from protein at high pH. Furthermore, the cleaning process can even be simplified by increasing the pH electrochemically. Finally, the electrochemical activation that creates local pH gradients on the solid support surface offers unique control of the loading, elution, and cleaning process compared to conventional protein purification.

7.2 Electrochemical protein drug delivery

Implantable electronics are expected to transform medical treatments and realize an unprecedented level of patient specific therapy by providing precise spatial and temporal dosing, and real-time sensory feedback that allows for tracking treatment efficacy.[9] Realization of these devices require dynamic stimuli-responsive materials that can respond to electronic input.[11, 145, 209] However, currently there is a lack of interfaces that can function in biological environments without harmful effects on either the biological system, or to the bioelectronic equipment. A common mitigation strategy is to only produce a highly non-fouling surfaces that communicates with the biological tissue purely by electronic signals.[6] This strategy a clear limitation; biological systems communicate by more than electronic signals. The interchange of chemicals on the nanoscale is essential in the development of future biointerfaces. The polyelectrolyte brush electrodes developed in this thesis could contribute to improved

capabilities in terms of chemical exchange through biointerfaces. The first reason is it combines electronic control of brushes in biological solutions e.g. serum, and it achieves sustained stimuli-response of polyelectrolyte brushes after long exposures. Secondly, the electrodes have the ability to store and release proteins on-demand. This could become a solution to pressing challenges associated with efficient and patient compliant drug-delivery of protein pharmaceuticals.[2, 210] The potential of polymer brush electrodes for use in electronic pills and implants should be viewed in light of the very rapid development of implantable electronics in the recent years.[9] The technology for implanted electronics is well-established.[3] Today what is primarily lacking is the realization of stimuli-responsive biointerfaces that can deliver new functionalities that allow for biochemical exchange.[8]

7.3 Local pH-gradients in brushes: Nanobuffering

Local pH gradients in polyelectrolyte systems, so-called nanobuffering, has wide implications not only for the work presented in this thesis but for the understanding of polyelectrolytes in general.[46] Nanobuffering of the polyelectrolyte brush would complicate characterization of protein-polyelectrolyte interactions since the pH of the solution does not accurately reflect the pH within the brush. This situation would in some sense be analogous to the case of a shifted pK_a of polyelectrolyte brushes as function of the salt concentration. The lack of direct experimental evidence of nanobuffering within polyelectrolyte brushes prevents us from knowing if the effect is really there. However, our preliminary data from TIRF microscopy experiments with pH sensitive fluorophores within PAA brushes detected the presence of nanobuffering. It is manifested by as a deviation from linearity between the pH within the brush compared to the solution pH detected by measurement of CNF fluorescence (Figure 7.2). At high pH (above the pK_a of PAA) brush and solution pH are equal. However, at low salt concentration and at pH 7.5 a new trend in the data is observed (Figure 7.2 A): the pH within the brush is lower than the pH of the solution. Between pH $6 - 7.5$, the brush pH follows a steeper linear trend as a function of solution pH (at most the pH within the brush is displaced by 0.5 units in pH). Interestingly, nanobuffering is strongly influenced by the total salt concentration. At physiological salt concentration the

effect is almost entirely absent (Figure 7.2 B).

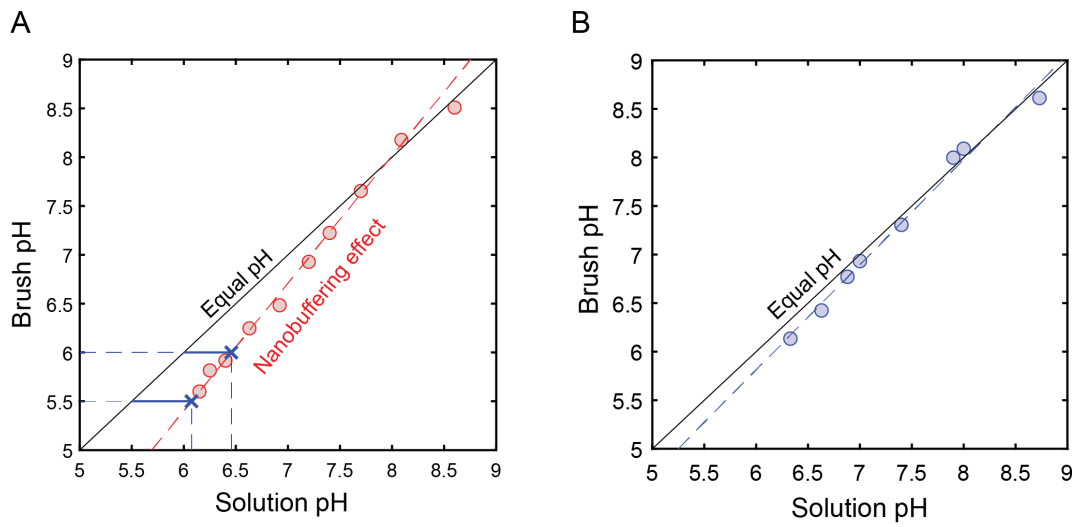

Figure 7.2: Nanobuffering effect observed within PAA brushes where the pH within the brush is compared to the pH of the solution for total salt concentrations of (A) 10 mM and (B) 150 mM.

Our results are the first direct evidence that nanobuffering occurs within polyelectrolyte brushes. In addition to proof of its existence we can also specify the requirements for observing it. However, these results need additional confirmation. A larger range of salt concentration needs to be studied, the grafting density of the polyelectrolyte brush should be varied to determine the importance of the polyeletrolyte crowding effect, and a laser-fluorophore combination that gives separation of the spectral features should be used to determine the solution and polyelectrolyte brush pH.[185]

The presence of nanobuffering at low salt concentrations, but not at physiological salt concentrations, has implications for how interactions between proteins and polyelectrolytes are interpreted.[46, 27] In many cases proteins and polyelectrolytes are characterized in in environments which do not accurately resemble the biological environments. Nanobuffering is a reminder that experimental observations of systems with low salt concentration are not suitable for extrapolation to biological phenomenon. Our results do not disprove the presence of nanobuffering in biological systems, but they show that the displacement of pH in polyelectrolyte brushes is extremely small at physiological salt concentration.

As a final remark I want to emphasize that this thesis contributes with new knowledge of how to displace the pH within polyelectrolyte brushes relative to the solution pH by two different methods: (1) nanobuffering and (2) by electrochemistry. On the one hand, nanobuffering spontaneously displaces the pH at low salt concentrations. On the other hand electrochemical signals actively produces a pH gradient, applicable even at high salt concentrations and in strong buffers. The ability to shift pH in stimuli-responsive materials by different means could become highly useful for applications such as biocatalysis.[82, 99, 46]

7.4 Enzyme cascade reactions in brushes

Controlled compartmentalization of enzymes for performing cascade chain reactions constitute a biomimetic approach for biocatalysis, which could potentially find applications in energy and chemicals industry.[99] A biomimetic approach to catalysis requires non-invasive suspension/immobilization methods of different enzymes that promotes chain reactions between them.[117] Polyelectrolyte brushes are able to immobilize large quantities of enzymes with full retention of enzyme activity, as shown in Chapter 5.3, which makes them well suited as supports for mixtures enzymes that participate in cascade reactions.

We investigated a three enzyme cascade reaction in PDEA brushes by non-covalent immobilization of GOX, GAL, and HRP enzymes (Figure 7.3 A). Spontaneous immobilization of many enzymes into one polyelectrolyte brush risks an uneven stoichiometry of enzymes within the brush. Each enzyme has a different affinity for PDEA, both in terms of the kinetics of binding and the equilibrium binding quantity (Figure 7.3 B). To compensate for its slow binding kinetics and low equilibrium coverage, HRP was immobilized using higher concentration compared to GAL and GOX, which displayed rapid binding kinetics and large equilibrium binding capacities. Simultaneous immobilization of all three enzymes resulted in significant catalytic activity that followed the same reaction pattern of the corresponding mixture of enzymes in a bulk solution.

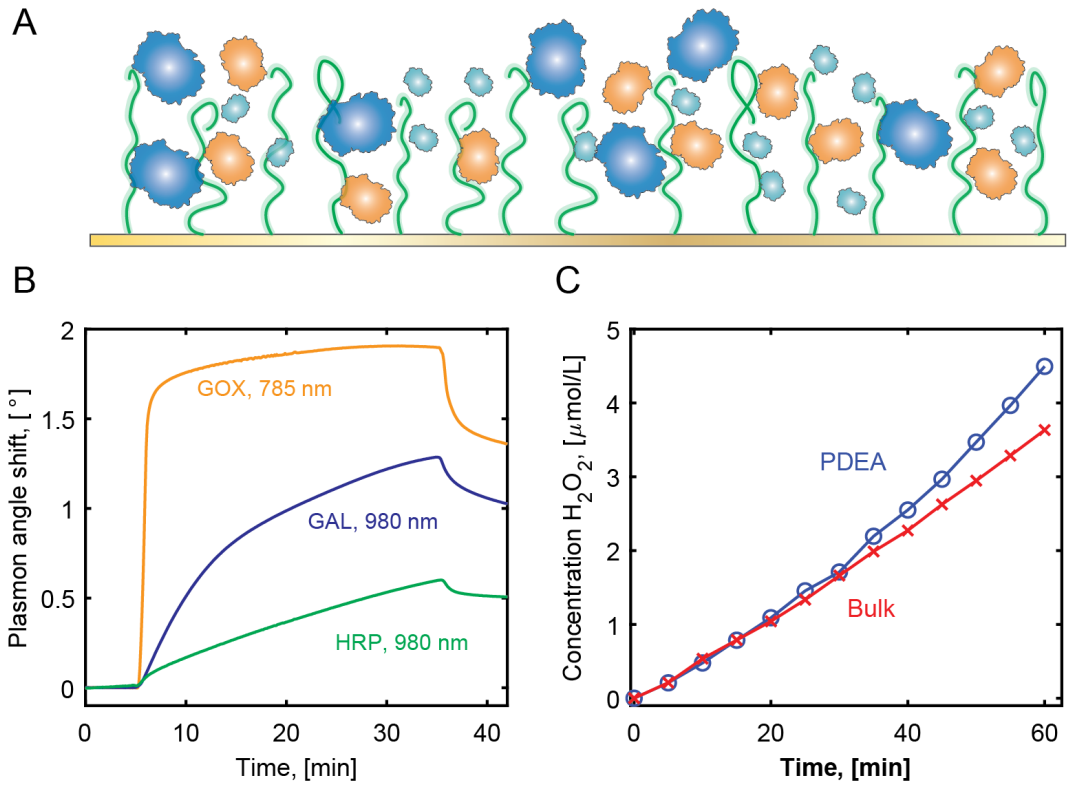

Figure 7.3: (A) Scheme illustrating enzymes immobilized to the polyelectrolyte brush. (B) Immobilization of GOX, GAL, and HRP enzymes to PDEA brushes. (C) Production of hydrogen peroxide H_2O_2 as a function of the enzyme chain reaction studied over time and compared between in solution and in PDEA brushes.

Immobilization of enzymes to polyelectrolyte brushes is appealing since bringing enzymes in close contact within a soft polymer scaffold mimics their native environment.[117] However, there is no guarantee that mixtures of enzymes in brushes do not interfere with each other. Furthermore, the final stoichiometry of enzymes within the brush is unknown. An accurate comparison between enzyme cascade reactions in solution and within brushes require the knowledge of how much enzymes are really present within the brush. Before knowing this a benchmark of the efficiency gain by placing enzymes in brushes cannot be made. One approach is to detect this would be to tag each enzyme with a different fluorophore. Another way to find out is desorption of the enzymes after the experiment and analyze the composition. As a final remark it should be emphasized that the turnover rate of enzymes may differ extremely, which means that equal quantity of all enzymes in the reaction pathway may not be necessary for

high throughput.

An electronic platform for handling enzymes is interesting from a scientific and technological point of view. Enzymes in cells operate in crowded dynamic molecular environments, polyelectrolyte brush electrodes offer the possibility of creating a synthetic environment with similar effects.[211] In cellular environments close proximity of enzymes induce what is called substrate channelling, where reaction intermediates are not in equilibrium with the bulk solution.[212] One way this is achieved is for enzymes to be covalently linked, like in metabolic clusters.[117] However, in many cases it is suspected that enzymes in cells come into close contact and regulate biochemical pathways by other mechanisms, e.g. phase separation of so called biological coacervates.[132] Polyelectrolyte brushes resembles the environment of coacervates which are governed by electrostatic interactions.

The ability of setting well-defined pH gradients could be used to regulate enzyme activity by pH, both by regulating hydration of the brush, and since enzymes activities are in general highly pH dependent.[129] The electronic control could even be used to achieve oscillatory reaction networks, for instance one could have two competing biocatalytic pathways where the dominant pathway is decided by the user. This would be interesting not only for understanding enzymes but also for use in the development of analytical devices and biocatalytic computations.[213] Reversible binding of enzymes to polyelectrolyte brushes by electrostatics or hydrogen bonding could be used to optimize biocatalysis. With spontaneous immobilizing one at the time the polyelectrolyte brush will saturate with whichever enzyme is immobilized first. However, electrochemical control of immobilization can be used to tune the brush enzyme composition. Electrochemical pH gradients can make sure that for each enzyme the brush only fills partially, this can be further improved by coupling to surface sensitive techniques like LSPR and QCMD.

Enzyme reactions in polyelectrolyte brushes could have applications that extend beyond improving catalysis. One possibility is the prospect of boosting the speed and throttle control of enzyme powered micro and nanoswimmers.[214] Catalytic activity on particles with asymmetric shape and chemistry, has been utilized to produce objects that can navigate through complex fluidic environments on the micro and nanoscale. Selective enzyme functionalization of a side

of the particle surface offers one method for achieving phoretic effect. Loading enzymes by physisorption to surfaces may result in distortion and denaturation of the enzymes and the capacity for loading enzymes may be too low to give rise to significant chemical gradients lowering the net propulsion as a result. In one study asymmetric nanoparticles were selectively functionalized with PNIPAAM polymer brushes on one side.[215] However, with this strategy the enzymes were immobilized to the barren side of the nanoparticle, not within the brush. This is unsurprising as PNIPAAM is generally protein repellent. It would be interesting to see if the reverse strategy, where particles equipped with polyelectrolyte brushes, immobilize to the brush in high numbers to achieve efficient propulsion. The potentially high contrast of or enzyme concentration around the particle, but also control over the speed of particles by changing the pH, could create biocatalytically powered nanoswimmers with interesting features. Biocatalytic swimmers with enzyme in brushes has, despite its potential not yet been investigated to the best of my knowledge.

Acknowledgements

To my supervisor Andreas Dahlin. Thank you for your support, what you have taught me and inspired me to do. To my assistant supervisor Annette Larsson, thank you for continuing to be my assistant supervisor since my Master thesis. My choice to return to Chalmers and perform my doctoral thesis studies was in large thanks to inspiring researchers and colleagues like Andreas and Annette.

I want to thank past and current members of the Dahlin group. Without your help and enthusiasm the experiments would not have been possible to perform and this thesis would not have been possible to write.

I want to thank my friends and colleagues at the Division of Applied Chemistry, past classmates, and co-workers from other Divisions and Institutions of Chalmers. I would like to thank my examiner Anders Palmqvist.

I want to thank our German collaborators in particular Petra Uhlmann and Meike Köenig for their support in Paper III of the thesis.

The financial support that allowed me to work as a Ph. D. student provided by Vetenskapsrådet and Knut & Alice Wallenberg stiftelse is important to acknowledge.

I want to thank my friends who always are there for me and cheer me on. I want to thank my family who encourage me so much. Finally I would like to thank Anna for your love and support.

Gustav Ferrand-Drake del Castillo

Bibliography

[1] A. Küchler, J. Adamcik, R. Mezzenga, A. D. Schlüter, and P. Walde, *RSC Advances*, 2015, **5**(55), 44530–44544.

[2] M. W. Tibbitt, J. E. Dahlman, and R. Langer, *Journal of the American Chemical Society*, 2016, **138**(3), 704–717.

[3] R. Farra, N. F. Sheppard, L. McCabe, R. M. Neer, J. M. Anderson, J. T. Santini, M. J. Cima, and R. Langer, *Science Translational Medicine*, 2012, **4**(122).

[4] G. W. Stone, S. G. Ellis, D. A. Cox, J. Hermiller, C. O'Shaughnessy, J. T. Mann, M. Turco, R. Caputo, P. Bergin, J. Greenberg, J. J. Popma, and M. E. Russell, 1 , 2004, **350**(3), 221–231.

[5] H. Ouyang, Z. Liu, N. Li, B. Shi, Y. Zou, F. Xie, Y. Ma, Z. Z. Li, H. Li, Q. Zheng, X. Qu, Y. Fan, Z. L. Wang, H. Zhang, and Z. Z. Li, *Nature Communications*, 2019, **10**(1), 1–10.

[6] J. Sabaté del Río, O. Y. Henry, P. Jolly, and D. E. Ingber, *Nature Nanotechnology*, 2019, **14**(12), 1143–1149.

[7] S. M. Wellman, J. R. Eles, K. A. Ludwig, J. P. Seymour, N. J. Michelson, W. E. McFadden, A. L. Vazquez, and T. D. Kozai, *Advanced Functional Materials*, 2018, **28**(12), 1–38.

[8] M. A. Stuart, W. T. Huck, J. Genzer, M. Muller, C. Ober, M. Stamm, G. B. Sukhorukov, I. Szleifer, V. V. Tsukruk, M. Urban, F. Winnik, S. Zauscher, I. Luzinov, S. Minko, M. Müller, C. Ober, M. Stamm, G. B. Sukhorukov, I. Szleifer, V. V. Tsukruk, M. Urban, F. Winnik, S. Zauscher, I. Luzinov, and S. Minko, *Nat Mater*, 2010, **9**(2), 101–113.

[9] Y. Song, J. Min, and W. Gao, *ACS Nano*, 2019, **13**(11), 12280–12286.

[10] S. J. Todd, D. J. Scurr, J. E. Gough, M. R. Alexander, and R. V. Ulijn, *Langmuir*, 2009, **25**(13), 7533–7539.

[11] E. Katz, J. M. Pingarrón, S. Mailloux, N. Guz, M. Gamella, G. Melman, and A. Melman, *Journal of Physical Chemistry Letters*, 2015, **6**(8), 1340–1347.

[12] P. G. de Gennes, *Macromolecules*, 1980, **13**(5), 1069–1075.

[13] S. T. Milner, 2 , 1991, **251**(4996), 905–914.

[14] D. Chen and Q. Pei, *Chemical Reviews*, 2017, **117**(17), 11239–11268.

[15] A. Hucknall, S. Rangarajan, and A. Chilkoti, *Advanced Materials*, 2009, **21**(23), 2441–2446.

[16] C. Rodriguez-Emmenegger, E. Brynda, T. Riedel, M. Houska, V. Šubr, A. B. Alles, E. Hasan, J. E. Gautrot, and W. T. Huck, *Macromolecular Rapid Communications*, 2011, **32**(13), 952–957.

[17] G. Emilsson, R. L. Schoch, L. Feuz, F. Höök, R. Y. H. Lim, A. B. Dahlin, F. Hook, R. Y. H. Lim, and A. B. Dahlin, *ACS Appl Mater Interfaces*, 2015, **7**(14), 7505–7515.

[18] Y. Higaki, M. Kobayashi, D. Murakami, and A. Takahara, *Polymer Journal*, 2016, **48**(4), 325–331.

[19] A. Kusumo, L. Bombalski, Q. Lin, K. Matyjaszewski, J. W. Schneider, and R. D. Tilton, *Langmuir*, 2007, **23**(8), 4448–4454.

[20] S. P. Cullen, I. C. Mandel, and P. Gopalan, *Langmuir*, 2008, **24**(23), 13701–13709.

[21] J. Dai, Z. Bao, L. Sun, S. U. Hong, G. L. Baker, and M. L. Bruening, *Langmuir*, 2006, **22**(9), 4274–4281.

[22] G. Emilsson, R. L. Schoch, P. Oertle, K. Xiong, R. Y. Lim, and A. B. Dahlin, *Applied Surface Science*, 2016, **396**, 384–392.

[23] M. Dübner, N. D. Spencer, and C. Padeste, *Langmuir*, 2014, **30**(49), 14971–14981.

[24] M. F. Delcroix, S. Laurent, G. L. Huet, and C. C. Dupont-Gillain, *Acta Biomaterialia*, 2015, **11**(1), 68–79.

[25] R. R. Netz and D. Andelman, *Encyclopedia of Electrochemistry*, 2003, **I**.

[26] J. O. Zoppe, N. Cavusoglu Ataman, P. Mocny, J. Wang, J. Moraes, H.-A. A. Klok, N. C. Ataman, P. Mocny, J. Wang, J. Moraes, and H.-A. A. Klok, *Chemical Reviews*, 2017, **117**(3), 1105–1318.

[27] K. Achazi, R. Haag, M. Ballauff, J. Dernedde, J. N. Kizhakkedathu, D. Maysinger, and G. Multhaup, *Angewandte Chemie International Edition*, 2020.

[28] D. Aulich, O. Hoy, I. Luzinov, M. Brucher, R. Hergenroder, E. Bittrich, K. J. Eichhorn, P. Uhlmann, M. Stamm, N. Esser, and K. Hinrichs, *Langmuir*, 2010, **26**(15), 12926–12932.

[29] T. Wu, P. Gong, I. Szleifer, P. Vlček, V. Šubr, and J. Genzer, *Macromolecules*, 2007, **40**(24), 8756–8764.

[30] B. Lego, W. G. Skene, and S. Giasson, *Macromolecules*, 2010, **43**(9), 4384–4393.

[31] M. G. Santonicola, G. W. de Groot, M. Memesa, A. Meszynska, and G. J. Vancso, *Langmuir*, 2010, **26**(22), 17513–17519.

[32] D. Sarkar and P. Somasundaran, *Langmuir*, 2004, **20**(11), 4657–4664.

[33] N. Schüwer and H. A. Klok, *Langmuir*, 2011, **27**(8), 4789–4796.

[34] K. Ehtiati, S. Z. Moghaddam, A. E. Daugaard, and E. Thormann, *Langmuir*, 2020, **36**(9), 2339–2348.

[35] R. L. Schoch and R. Y. Lim, *Langmuir*, 2013, **29**(12), 4068–4076.

[36] R. Arnold, *Journal of Colloid Science*, 1957, **12**(6), 549–556.

[37] J. Zhang, R. Kou, and G. Liu, *Langmuir*, 2017, **33**(27), 6838–6845.

[38] O. Hollmann, T. Gutberlet, and C. Czeslik, *Langmuir*, 2007, **23**(3), 1347–1353.

[39] O. Hollmann and C. Czeslik, *Langmuir*, 2006, **22**(7), 3300–3305.

[40] N. R. Hollingsworth, S. I. Wilkanowicz, and R. G. Larson, *Soft Matter*, 2019, **15**(39), 7838–7851.

[41] C. Yigit, M. Kanduč, M. Ballauff, and J. Dzubiella, *Langmuir : the ACS journal of surfaces and colloids*, 2017, **33**(1), 417–427.

[42] M. Koenig, E. Bittrich, U. König, B. L. Rajeev, M. Müller, K.-J. Eichhorn, S. Thomas, M. Stamm, and P. Uhlmann, *Colloids and Surfaces B: Biointerfaces*, 2016, **146**, 737–745.

[43] E. Bittrich, K. B. Rodenhausen, K.-J. Eichhorn, T. Hofmann, M. Schubert, M. Stamm, and P. Uhlmann, *Biointerphases*, 2010, **5**(4), 159–167.

[44] A. Wittemann, B. Haupt, and M. Ballauff, *Physical Chemistry Chemical Physics*, 2003, **5**, 1671–1677.

[45] P. Anees, Y. Zhao, A. A. Greschner, T. R. Congdon, H. W. de Haan, N. Cottenye, and M. A. Gauthier, 1 , 2019, **13**(2), 1019–1028.

[46] W. Tao, J. Wang, W. J. Parak, O. C. Farokhzad, and J. Shi, *ACS Nano*, 2019, **13**(5), 4876–4882.

[47] M. Hoarau, S. Badieyan, and E. N. G. Marsh, *Organic and Biomolecular Chemistry*, 2017, **15**(45), 9539–9551.

[48] B. Haupt, T. Neumann, A. Wittemann, and M. Ballauff, *Biomacromolecules*, 2005, **6**(2), 948–955.

[49] Y. Fang, W. Xu, X. L. Meng, X. Y. Ye, J. Wu, and Z. K. Xu, *Langmuir*, 2012, **28**(37), 13318–13324.

[50] S. M. Lane, Z. Kuang, J. Yom, S. Arifuzzaman, J. Genzer, B. Farmer, R. Naik, and R. A. Vaia, *Biomacromolecules*, 2011, **12**(5), 1822–1830.

[51] S. P. Cullen, X. Liu, I. C. Mandel, F. J. Himpsel, and P. Gopalan, *Langmuir*, 2008, **24**(3), 913–920.

[52] P. Jonkheijm, D. Weinrich, H. Schröder, C. M. Niemeyer, and H. Waldmann, *Angewandte Chemie - International Edition*, 2008, **47**(50), 9618–9647.

[53] F. Rusmini, Z. Zhong, and J. Feijen, *Biomacromolecules*, 2007, **8**(6), 1775–1789.

[54] R. Dong, S. Krishnan, B. A. Baird, M. Lindau, and C. K. Ober, *Biomacromolecules*, 2007, **8**(10), 3082–3092.

[55] G. Di Palma, A. M. Kotowska, L. R. Hart, D. J. Scurr, F. J. Rawson, S. Tommasone, and P. M. Mendes, *ACS Applied Materials and Interfaces*, 2019, **11**(9), 8937–8944.

[56] G. J. Dunderdale and J. P. A. Fairclough, *Langmuir*, 2013, **29**(11), 3628–3635.

[57] O. V. Borisova, L. Billon, R. P. Richter, E. Reimhult, and O. V. Borisov, *Langmuir*, 2015, **31**(27), 7684–7694.

[58] J. Malmström, M. K. Nieuwoudt, L. T. Strover, A. Hackett, O. Laita, M. A. Brimble, D. E. Williams, and J. Travas-Sejdic, 6 , 2013, **46**(12), 4955–4965.

[59] T. K. Tam, M. Pita, O. Trotsenko, M. Motornov, I. Tokarev, J. Halámek, S. Minko, E. Katz, J. Halamek, S. Minko, and E. Katz, *Langmuir*, 2010, **26**(6), 4506–4513.

[60] M. W. Beulen, M. I. Kastenberg, F. C. Van Veggel, and D. N. Reinhoudt, *Langmuir*, 1998, **14**(26), 7463–7467.

[61] J. Cowie and V. Arrighi, *Polymers: Chemistry and Physics of Modern Materials*, CRC Press, third edit ed., 2007.

[62] P. G. De Gennes, *Scaling Concepts in Polymer Physics*, Cornell University Press, 1979.

[63] W. L. Chen, R. Cordero, H. Tran, and C. K. Ober, *Macromolecules*, 2017, **50**(11), 4089–4113.

[64] S. T. Milner, T. A. Witten, and M. E. Cates, *Epl*, 1988, **5**(5), 413–418.

[65] J. Rühe, M. Ballauff, M. Biesalski, P. Dziezok, F. Gröhn, D. Johannsmann, N. Houbenov, N. Hugenberg, R. Konradi, S. Minko, M. Motornov, R. R. Netz, M. Schmidt, C. Seidel, M. Stamm, T. Stephan, D. Usov, and H. Zhang in *Advances in Polymer Science*, ed. M. Schmidt; Springer, 2004; pp. 79–150.

[66] A. Naji, C. Seidel, and R. R. Netz, *Advances in Polymer Science*, 2006, **198**(1), 149–183.

[67] X. Guo and M. Ballauff, *Physical Review E - Statistical Physics, Plasmas, Fluids, and Related Interdisciplinary Topics*, 2001, **64**(5), 9.

[68] J. Huang, X. Liu, and E. Thormann, *Langmuir*, 2018, **34**(25), 7264–7271.

[69] B. T. Cheesman, J. D. Willott, G. B. Webber, S. Edmondson, and E. J. Wanless, *ACS Macro Letters*, 2012, **1**(10), 1161–1165.

[70] F. Ruggeri, F. Zosel, N. Mutter, M. Rozycka, M. Wojtas, A. Ozyhar, B. Schuler, and M. Krishnan, *Nature Nanotechnology*, 2017, **12**(5), 488–495.

[71] M. Krishnan, *Journal of Chemical Physics*, 2017, **146**(20).

[72] R. R. Netz and D. Andelman, *Physics Reports*, 2003, **380**, 1–95.

[73] M. Biesalski, D. Johannsmann, and J. Rühe, *Journal of Chemical Physics*, 2002, **117**(10), 4988–4994.

[74] M. Ballauff and O. Borisov, *Current Opinion in Colloid & Interface Science*, 2006, **11**(6), 316–323.

[75] E. B. Zhulina, T. M. Birshtein, and O. V. Borisov, *Macromolecules*, 1995, **28**(5), 1491–1499.

[76] P. Gong, T. Wu, J. Genzer, and I. Szleifer, 11 , 2007, **40**(24), 8765–8773.

[77] J. D. Willott, T. J. Murdoch, B. A. Humphreys, S. Edmondson, G. B. Webber, and E. J. Wanless, *Langmuir*, 2014, **30**(7), 1827–1836.

[78] A. Murmiliuk, P. Košovan, M. Janata, K. Procházka, F. Uhlík, and M. Štěpánek, *ACS Macro Letters*, 2018, **7**(10), 1243–1247.

[79] E. P. Currie, A. B. Sieval, M. Avena, H. Zuilhof, E. J. Sudhölter, and M. A. Cohen Stuart, *Langmuir*, 1999, **15**(21), 7116–7118.

[80] S. Zhang, R. Geryak, J. Geldmeier, S. Kim, and V. V. Tsukruk, *Chemical Reviews*, 2017, **117**(20), 12942–13038.

[81] E. B. Zhulina and O. V. Borisov, *Langmuir*, 2011, **27**(17), 10615–10633.

[82] Y. Zhang, Q. Wang, and H. Hess, *ACS Catalysis*, 2017, **7**(3), 2047–2051.

[83] R. Dong, M. Lindau, and C. K. Ober, *Langmuir*, 2009, **25**(8), 4774–4779.

[84] R. V. Klitzing and H. Möhwald, *Langmuir*, 1995, **11**(9), 3554–3559.

[85] R. Barbey, L. Lavanant, D. Paripovic, N. Schuwer, C. Sugnaux, S. Tugulu, and H.-A. Klok, *Chemical Reviews*, 2009, **109**(11), 5437–5527.

[86] W. Jakubowski and K. Matyjaszewski, *Angewandte Chemie - International Edition*, 2006, **45**(27), 4482–4486.

[87] L. Michalek, L. Barner, and C. Barner-Kowollik, *Advanced Materials*, 2018, **30**(21), 1–18.

[88] C. Kang, R. Crockett, and N. D. Spencer, *Polymer Chemistry*, 2016, **7**(2), 302–309.

[89] K. Ohno, T. Morinaga, K. Koh, Y. Tsujii, and T. Fukuda, *Macromolecules*, 2005, **38**(6), 2137–2142.

[90] R. R. Patil, S. Turgman-Cohen, J. Šrogl, D. Kiserow, and J. Genzer, *ACS Macro Letters*, 2015, **4**(2), 251–254.

[91] S. B. Petersen, P. Harald Jonson, P. Fojan, E. I. Petersen, M. T. Neves Petersen, S. Hansen, R. J. Ishak, and E. Hough, *Journal of Biotechnology*, 1998, **66**(1), 11–26.

[92] J. M. Berg, J. L. Tymoczko, and L. Stryer, *Biochemistry, Fifth Edition*, W.H. Freeman, 2002.

[93] V. V. Khutoryanskiy, A. V. Dubolazov, and G. A. Mun in *Hydrogen-Bonded Interpolymer Complexes;* World Scientific, 2009; pp. 1–21.

[94] A. L. Becker, N. Welsch, C. Schneider, and M. Ballauff, *Biomacromolecules*, 2011, **12**(11), 3936–3944.

[95] M. Meot-Ner, *Chemical Reviews*, 2005, **105**(1), 213–284.

[96] K. Takasu, K. Kushiro, K. Hayashi, Y. Iwasaki, S. Inoue, E. Tamechika, and M. Takai, *Sensors and Actuators, B: Chemical*, 2015, **216**, 428–433.

[97] C. Agatemor, M. J. Buettner, R. Ariss, K. Muthiah, C. T. Saeui, and K. J. Yarema, *Nature Reviews Chemistry*, 2019, **3**(10), 605–620.

[98] A. Cornish-Bowden, *Fundamentals of Enzyme Kinetics*, Elsevier, 1979.

[99] K. E. Cassimjee and H. J. Federsel, *RSC Catalysis Series*, 2018, **2018-Janua**(29), 345–362.

[100] L. Li, S. Srivastava, M. Andreev, A. B. Marciel, J. J. De Pablo, and M. V. Tirrell, *Macromolecules*, 2018, **51**(8), 2988–2995.

[101] J. Chapman, A. E. Ismail, and C. Z. Dinu, *Catalysts*, 2018, **8**(6), 20–29.

[102] R. Di Cosimo, J. Mc Auliffe, A. J. Poulose, and G. Bohlmann, *Chemical Society Reviews*, 2013, **42**(15), 6437–6474.

[103] R. A. Sheldon, *Advanced Synthesis and Catalysis*, 2007, **349**(8-9), 1289–1307.

[104] F. H. Arnold, *Angewandte Chemie - International Edition*, 2018, **57**(16), 4143–4148.

[105] P. Chames, M. Van Regenmortel, E. Weiss, and D. Baty, *British Journal of Pharmacology*, 2009, **157**(2), 220–233.

[106] B. Kelley, *Biotechnology Progress*, 2007, **23**(5), 995–1008.

[107] E. D. Carlson, R. Gan, C. E. Hodgman, and M. C. Jewett, *Biotechnology Advances*, 2012, **30**(5), 1185–1194.

[108] G. Rosenblum and B. S. Cooperman, *FEBS Letters*, 2014, **588**(2), 261–268.

[109] C. Mateo, J. M. Palomo, G. Fernandez-Lorente, J. M. Guisan, and R. Fernandez-Lafuente, 5 , 2007, **40**(6), 1451–1463.

[110] M. Hoarau, S. Badieyan, and E. N. G. Marsh, *Organic and Biomolecular Chemistry*, 2017, **15**(45), 9539–9551.

[111] M. Zezzi Do Valle Gomes and A. E. Palmqvist, *New Journal of Chemistry*, 2017, **41**(19), 11391–11397.

[112] N. Carlsson, H. Gustafsson, C. Thörn, L. Olsson, K. Holmberg, and B. Åkerman, *Advances in Colloid and Interface Science*, 2014, **205**, 339–360.

[113] F. Audouin, R. Larragy, M. Fox, B. O'Connor, and A. Heise, *Biomacromolecules*, 2012, **13**(11), 3787–3794.

[114] J. N. Talbert and J. M. Goddard, *Colloids and Surfaces B: Biointerfaces*, 2012, **93**, 8–19.

[115] K. P. Fears, B. Sivaraman, G. L. Powell, Y. Wu, and R. A. Latour, *Langmuir*, 2009, **25**(16), 9319–9327.

[116] K. P. Fears and R. A. Latour, *Langmuir*, 2009, **25**(24), 13926–13933.

[117] A. Küchler, M. Yoshimoto, S. Luginbühl, F. Mavelli, and P. Walde, *Nature Nanotechnology*, 2016, **11**(5), 409–420.

[118] K. K. Dey, X. Zhao, B. M. Tansi, W. J. Méndez-Ortiz, U. M. Córdova-Figueroa, R. Golestanian, and A. Sen, *Nano Letters*, 2015, **15**(12), 8311–8315.

[119] J. M. De Almeida, V. R. Moure, M. Müller-Santos, E. M. De Souza, F. O. Pedrosa, D. A. Mitchell, and N. Krieger, *Scientific Reports*, 2018, **8**(1), 1–11.

[120] A. Chant, C. M. Kraemer-Pecore, R. Watkin, and G. G. Kneale, *Protein Expression and Purification*, 2005, **39**(2), 152–159.

[121] K. Hernandez and R. Fernandez-Lafuente, *Enzyme and Microbial Technology*, 2011, **48**(2), 107–122.

[122] N. S. K. Gunda, M. Singh, L. Norman, K. Kaur, and S. K. Mitra, *Applied Surface Science*, 2014, **305**, 522–530.

[123] J. Lahiri, L. Isaacs, J. Tien, and G. M. Whitesides, 2 , 1999, **71**(4), 777–790.

[124] S. A. Bhakta, T. E. Benavidez, and C. D. Garcia, *Journal of Colloid and Interface Science*, 2014, **430**, 351–356.

[125] Y. Wei, A. A. Thyparambil, Y. Wu, and R. A. Latour, *Langmuir*, 2014, **30**(49), 14849–14858.

[126] Q. H. Gibson, B. E. P. Swoboda, and V. Massey, *J Biol Chem*, 1964, **239**(11), 3927–3934.

[127] C. M. Wong, K. H. Wong, and X. D. Chen, *Applied Microbiology and Biotechnology*, 2008, **78**(6), 927–938.

[128] K. Kleppe, *Biochemistry*, 1966, **5**(1), 139–143.

[129] R. Wilson and A. Turner, 1 , 1992, **7**(3), 165–185.

[130] Z. Y. Jiang, a. C. Woollard, and S. P. Wolff, *FEBS letters*, 1990, **268**(1), 69–71.

[131] H. Fischer, I. Polikarpov, and A. F. Craievich, *Protein Science*, 2009, **13**(10), 2825–2828.

[132] S. F. Banani, H. O. Lee, A. A. Hyman, and M. K. Rosen, *Nature Reviews Molecular Cell Biology*, 2017, **18**(5), 285–298.

[133] H. Raether, *Surface Plasmons*, 1988.

[134] J. Homola, *Chem. Rev.*, 2008, **108**(2), 462–493.

[135] S. a. Maier, *Fundamentals and Applications Plasmonics : Fundamentals and Applications*, Vol. 677, 2004.

[136] A. B. Dahlin, *Advances in Biomedical Spectroscopy*, Vol. 4, IOS Press, Inc., 2012.

[137] B. Liedberg, C. Nylander, and I. Lundström, *Biosensors and Bioelectronics*, 1995, **10**(8).

[138] N. Houbenov, S. Minko, and M. Stamm, *Macromolecules*, 2003, **36**(16), 5897–5901.

[139] L. S. Jung, C. T. Campbell, T. M. Chinowsky, M. N. Mar, and S. S. Yee, *Langmuir*, 1998, **14**(19), 5636–5648.

[140] G. Emilsson, K. Xiong, Y. Sakiyama, B. Malekian, V. Ahlberg Gagnér, R. L. Schoch, R. Y. Lim, and A. B. Dahlin, *Nanoscale*, 2018, **10**(10), 4663–4669.

[141] J. A. De Feijter, J. Benjamins, and F. A. Veer, *Biopolymers*, 1978, **17**(7), 1759–1772.

[142] F. Höök and B. Kasemo in *Piezoelectric Sensors*, Vol. 5; Springer Berlin Heidelberg, 2007; pp. 425–447.

[143] A. J. Bard and L. R. Faulkner, *Electrochemical Methods: Fundamentals and applications*, 2001.

[144] M. Bellare, V. K. Kadambar, P. Bollella, E. Katz, and A. Melman, *ChemElectroChem*, 2020, **7**(1), 59–63.

[145] M. Bellare, V. K. Kadambar, P. Bollella, M. Gamella, E. Katz, and A. Melman, *Electroanalysis*, 2019, **31**(11), 2274–2282.

[146] N. Fomina, C. A. Johnson, A. Maruniak, S. Bahrampour, C. Lang, R. W. Davis, S. Kavusi, and H. Ahmad, *Lab on a Chip*, 2016, **16**(12), 2236–2244.

[147] I. Katsounaros, W. B. Schneider, J. C. Meier, U. Benedikt, P. U. Biedermann, A. A. Auer, and K. J. Mayrhofer, *Physical Chemistry Chemical Physics*, 2012, **14**(20), 7384–7391.

[148] B. K. Chethana and Y. Arthoba Naik, *Analytical Methods*, 2012, **4**(11), 3754–3759.

[149] J. C. Love, L. A. Estroff, J. K. Kriebel, R. G. Nuzzo, and G. M. Whitesides, *Chemical Reviews*, 2005, **105**(4), 1103–1169.

[150] C. A. Widrig, C. Chung, and M. D. Porter, *Journal of Electroanalytical Chemistry*, 1991, **310**(1-2), 335–359.

[151] H. Munakata, D. Oyamatsu, and S. Kuwabata, *Langmuir*, 2004, **20**(23), 10123–10128.

[152] T. Ghaly, B. E. Wildt, and P. C. Searson, *Langmuir*, 2010, **26**(3), 1420–1423.

[153] H. Zhu, J. Yan, and A. Revzin, *Colloids and Surfaces B: Biointerfaces*, 2008, **64**(2), 260–268.

[154] J. A. Howarter and J. P. Youngblood, *Langmuir*, 2006, **22**(26), 11142–11147.

[155] B. Arkles, *Chemtech*, 1977, **7**(12), 766–777.

[156] R. M. Pasternack, S. R. Amy, and Y. J. Chabal, *Langmuir*, 2008, **24**(22), 12963–12971.

[157] E. T. Vandenberg, L. Bertilsson, B. Liedberg, K. Uvdal, R. Erlandsson, H. Elwing, and I. Lundström, *Journal of Colloid And Interface Science*, 1991, **147**(1), 103–118.

[158] M. Zhu, M. Z. Lerum, and W. Chen, *Langmuir*, 2012, **28**(1), 416–423.

[159] F. Zhang, K. Sautter, A. M. Larsen, D. A. Findley, R. C. Davis, H. Samha, and M. R. Linford, *Langmuir*, 2010, **26**(18), 14648–14654.

[160] A. R. Yadav, R. Sriram, J. A. Carter, and B. L. Miller, *Materials Science and Engineering C*, 2014, **35**(1), 283–290.

[161] T.-J. Lee, L.-K. Chau, and C.-J. Huang, 6 , 2020, **36**(21), 5935–5943.

[162] Y. Ko and J. Genzer, *Macromolecules*, 2019, **52**(16), 6192–6200.

[163] C. J. Galvin, E. D. Bain, A. Henke, and J. Genzer, *Macromolecules*, 2015, **48**(16), 5677–5687.

[164] J. Pinson and F. Podvorica, *Chemical Society Reviews*, 2005, **34**(5), 429–439.

[165] S. Mahouche-Chergui, S. Gam-Derouich, C. Mangeney, and M. M. Chehimi, *Chemical Society Reviews*, 2011, **40**(7), 4143–4166.

[166] T. Matrab, M. M. Chehimi, C. Perruchot, A. Adenier, A. Guillez, M. Save, B. Charleux, E. Cabet-Deliry, and J. Pinson, *Langmuir*, 2005, **21**(10), 4686–4694.

[167] A. Mesnage, M. A. Magied, P. Simon, N. Herlin-Boime, P. Jégou, G. Deniau, and S. Palacin, *Journal of Materials Science*, 2011, **46**(19), 6332–6338.

[168] V. Mévellec, S. Roussel, L. Tessier, J. Chancolon, M. Mayne-L'Hermite, G. Deniau, P. Viel, and S. Palacin, *Chemistry of Materials*, 2007, **19**(25), 6323–6330.

[169] J. E. Friis, G. Subbiahdoss, G. Gerved, A. H. Holm, O. Santos, A. B. Blichfeld, S. Z. Moghaddam, E. Thormann, K. Daasbjerg, J. Iruthayaraj, and R. L. Meyer, *Progress in Organic Coatings*, 2019, **136**(October 2018), 105196.

[170] M. Kongsfelt, J. Vinther, K. Malmos, M. Ceccato, K. Torbensen, C. S. Knudsen, K. V. Gothelf, S. U. Pedersen, and K. Daasbjerg, *Journal of the American Chemical Society*, 2011, **133**(11), 3788–3791.

[171] G. T. Hermanson, *Bioconjugate Techniques*, Elsevier, 2013.

[172] X. Liu, K. G. Neoh, L. Cen, and E. T. Kang, *Biosensors and Bioelectronics*, 2004, **19**(8), 823–834.

[173] D. Pallarola, N. Queralto, F. Battaglini, and O. Azzaroni, *Physical chemistry chemical physics : PCCP*, 2010, **12**(28), 8071–8083.

[174] C. Gay, J. Collins, and J. M. Gebicki, *Analytical biochemistry*, 1999, **273**(2), 149–155.

[175] H. Bäumler and R. Georgieva, *Biomacromolecules*, 2010, **11**(6), 1480–1487.

[176] J. C. Myland and K. B. Oldham, *Analytical Chemistry*, 2000, **72**(17), 3972–3980.

[177] J. Ruhe, M. Ballauff, M. Biesalski, P. Dziezok, F. Gröhn, D. Johannsmann, N. Houbenov, N. Hugenberg, R. Konradi, S. Minko, MichailMotornov, R. R. Netz, M. Schmidt, C. Seidel, M. Stamm, T. Stephan, D. Usov, and H. Zhang in *Advances in Polymer Science*, ed. M. Schmidt, Vol. 165; Springer, 2004; chapter 79, pp. 79–150.

[178] B. L. Frey and R. M. Corn, *Analytical Chemistry*, 1996, **68**(18), 3187–3193.

[179] F. Hoffmann, 9 , 1983, **3**(2-3), 107.

[180] S. Gam-Derouich, M. N. Nguyen, A. Madani, N. Maouche, P. Lang, C. Perruchot, and M. M. Chehimi, *Surface and Interface Analysis*, 2010, **42**(6-7), 1050–1056.

[181] R. Dong, M. Lindau, and C. K. Ober, *Langmuir*, 2009, **25**(8), 4774–4779.

[182] M. Koenig, U. König, K. J. Eichhorn, M. Müller, M. Stamm, and P. Uhlmann, *Frontiers in Chemistry*, 2019, **7**(MAR), 1–8.

[183] S. Beychok, 12 , 1966, **154**(3754), 1288–1299.

[184] S. Kelly and N. Price, *Current Protein & Peptide Science*, 2005, **1**(4), 349–384.

[185] A. Song, S. Parus, and R. Kopelman, *Analytical Chemistry*, 1997, **69**(5), 863–867.

[186] P. Akkahat, W. Mekboonsonglarp, S. Kiatkamjornwong, and V. P. Hoven, *Langmuir*, 2012, **28**(11), 5302–5311.

[187] S. Nizamov, V. Scherbahn, and V. M. Mirsky, *Analytical Chemistry*, 2017, **89**(7), 3873–3878.

[188] X. Wang, G. Liu, and G. Zhang, *Langmuir*, 2011, **27**(16), 9895–9901.

[189] Y. Tran, P. Auroy, L.-T. Lee, and M. Stamm, 12 , 1999, **60**(6), 6984–6990.

[190] J. Yang, Z. Hua, T. Wang, B. Wu, G. Liu, and G. Zhang, *Langmuir*, 2015, **31**(22), 6078–6084.

[191] K. Henzler, B. Haupt, K. Lauterbach, A. Wittemann, O. Borisov, and M. Ballauff, *Journal of the American Chemical Society*, 2010, **132**(9), 3159–3163.

[192] F. J. Xu, Q. J. Cai, Y. L. Li, E. T. Kang, and K. G. Neoh, *Biomacromolecules*, 2005, **6**(2), 1012–1020.

[193] J. Vörös, *Biophysical Journal*, 2004, **87**(1), 553–561.

[194] B. L. Frey, C. E. Jordan, R. M. Corn, and S. Komguth, *Analytical Chemistry*, 1995, **67**(24), 4452–4457.

[195] S. N. Alconcel, A. S. Baas, and H. D. Maynard, *Polymer Chemistry*, 2011, **2**(7), 1442–1448.

[196] E. Spruijt, E. Y. Choi, and W. T. Huck, *Langmuir*, 2008, **24**(19), 11253–11260.

[197] K. Xiong, G. Emilsson, and A. B. Dahlin, *Analyst*, 2016, **141**(12), 3803–3810.

[198] J. F. Young, H. D. Nguyen, L. Yang, J. Huskens, P. Jonkheijm, and L. Brunsveld, *ChemBioChem*, 2010, **11**(2), 180–183.

[199] D. Wasserberg, C. Nicosia, E. E. Tromp, V. Subramaniam, J. Huskens, and P. Jonkheijm, *Journal of the American Chemical Society*, 2013, **135**(8), 3104–3111.

[200] S. C. Perry, D. Pangotra, L. Vieira, L. I. Csepei, V. Sieber, L. Wang, C. Ponce de León, and F. C. Walsh, *Nature Reviews Chemistry*, 2019, **3**(7), 442–458.

[201] A. M. Gómez-Marín, A. Boronat, and J. M. Feliu, *Russian Journal of Electrochemistry*, 2017, **53**(9), 1029–1041.

[202] A. C. A. Roque, A. S. Pina, A. M. Azevedo, R. Aires-Barros, A. Jungbauer, G. Di Profio, J. Y. Heng, J. Haigh, and M. Ottens, *Biotechnology Journal*, 2020, **15**(8), 1–8.

[203] U. Gottschalk, *Biotechnology Progress*, 2008, **24**(3), 496–503.

[204] A. C. Chan and P. J. Carter, *Nature Reviews Immunology*, 2010, **10**(5), 301–316.

[205] L. M. Weiner, R. Surana, and S. Wang, 5 , 2010, **10**(5), 317–327.

[206] BioPlan Associates Inc. 17th Annual Report and Survey of Biopharmaceutical Manufacturing Technical report, 2020.

[207] Wellcome IAVI, *Expanding access to monoclonal products: A global call to action*, 2020.

[208] M. C. Flickinger, *Downstream Industrial Biotechnology: Recovery and Purification*, John Wiley & Sons, Incorporated, 2013.

[209] M. Bellare, V. K. Kadambar, P. Bollella, E. Katz, and A. Melman, *Chemical Communications*, 2019, **55**(54), 7856–7859.

[210] S. Mitragotri, P. A. Burke, and R. Langer, *Nature Reviews Drug Discovery*, 2014, **13**(9), 655–672.

[211] G. A. Ellis, W. P. Klein, G. Lasarte-Aragonés, M. Thakur, S. A. Walper, and I. L. Medintz, *ACS Catalysis*, 2019, **9**(12), 10812–10869.

[212] I. Wheeldon, S. D. Minteer, S. Banta, S. C. Barton, P. Atanassov, and M. Sigman, *Nature Chemistry*, 2016, **8**(4), 299–309.

[213] D. Molinnus, A. Poghossian, M. Keusgen, E. Katz, and M. J. Schöning, *Electroanalysis*, 2017, **29**(8), 1840–1849.

[214] M. Fernández-Medina, M. A. Ramos-Docampo, O. Hovorka, V. Salgueiriño, and B. Städler, *Advanced Functional Materials*, 2020, **30**(12), 1–17.

[215] Y. Ji, X. Lin, Z. Wu, Y. Wu, W. Gao, and Q. He, *Angewandte Chemie - International Edition*, 2019, **58**(35), 12200–12205.